UNIVERSITY OF CALIFORNIA

Los Angeles

Molecular Mechanisms Regulating Epithelial Barrier Function and Inflammatory Response

A dissertation submitted in partial satisfaction of the
requirements for the degree Doctor of Philosophy
in Oral Biology

by

Shebli Mehrazarin

2016

ABSTRACT OF THE DISSERTATION

Molecular Mechanisms Regulating

Epithelial Barrier Function and Inflammatory Response

by

Shebli Mehrazarin

Doctor of Philosophy in Oral Biology

University of California, Los Angeles, 2016

Professor No-Hee Park, Co-Chair

Professor Mo Kang, Co-Chair

The long-term goal of this study is to develop mode of treatment for inflammation in the oral cavity. To this end, we sought to investigate both (1) the mechanism regulating the integrity of the mucosal barrier, as well as (2) the epigenetic mechanisms by which inflammatory response is elicited and regulated. Epithelial tissue serves as an important barrier against infection. In response to physical injury or infection, this tissue undergoes significant phenotypic changes for eliciting its barrier function. For example, epithelial cells, major components of epithelial tissue,

upregulate the expression of TGF-β when the tissue is encountered by inflammation or injury in the human oral cavity. TGF-β induces cellular proliferation and differentiation, and also initiates a reversible process known as epithelial-mesenchymal transition (EMT) for wound healing processes. During EMT, epithelial cells exhibit phenotypic changes, loss of cell-cell adhesion, enhanced migratory capacity, and disruption of epithelial integrity. We have demonstrated that transcription factors Grainyhead-like 2 (GRHL2) and p63 regulate epithelial proliferation and differentiation, and may regulate EMT in human keratinocytes. Thus, to explore the molecular mechanism of TGF-β-dependent EMT, we investigated the effects of p63 and Grainyhead-like 2 (GRHL2) modulation on epithelial plasticity. We found that TGF-β leads to downregulation of GRHL2 and p63 expression, and facilitation of EMT molecular phenotype. Knockdown of all p63 isoforms by transfection of p63 Si-RNA was sufficient to induce EMT phenotype in normal human keratinocytes (NHK), and EMT in NHK accompanied loss of GHRL2 and miR-200 family gene expression, both of which play crucial roles in determining epithelial phenotype. Modulation of GRHL2 in NHK also led to congruent changes in p63 expression. Lastly, conditional knockout of GRHL2 resulted in significant phenotypic changes affecting the epithelial barrier and led to enhanced *Porphyromonas gingvalis (P.g.*) bacterial load within the bloodstream. These findings indicate that GRHL2 and p63 play an important role in inhibiting TGF-β-dependent EMT in epithelial cells, and that loss of GRHL2 expression induces phenotypic changes altering epithelial barrier function and facilitates accumulation of *P.g.* bacteria in the bloodstream. These bacteria are known to release lipoglycan endotoxin lipopolysaccharide (LPS) that triggers the expression of pro-inflammatory cytokines. Although previous literature has identified an association between dynamic demethylation of distinct histone marks and cytokine transcriptional activation, the role of histone lysine demethylases in

the epigenetic regulation of inflammatory response is not well understood. Thus, to explore the epigenetic regulation of *P.g.* lipopolysaccharide (*P.g.* LPS) induced inflammatory response, we discovered a novel histone lysine demethylase KDM3C that regulates pro-inflammatory cytokine induction and inflammatory response. We found that *P.g.* LPS culture led to KDM3C upregulation and enrichment on the promoter regions of several inflammatory cytokines, driving their transcriptional activation by demethylating H3K9me2. Overexpression of histone methyltransferase G9a maintained the H3K9me2 repressive mark and prevented inflammatory cytokine induction. Knockout of KDM3C also prevented induction of inflammatory signaling molecules, including pro-inflammatory cytokines, by *P.g.* LPS. These findings indicate that KDM3C plays an important functional role in the epigenetic regulation of inflammatory response. Collectively, these data demonstrate the effect that injury or infection in the oral cavity can have on epithelial integrity and resistance against pathogenic bacteria, and the epigenetic mechanisms that trigger the inflammatory response to these bacteria. As a result, we have identified the potential of KDM3C as novel anti-inflammatory therapeutic target, and our understanding of the mechanisms regulating epithelial barrier function and inflammatory response will be useful in the management and treatment of inflammatory diseases affecting oral tissues.

The dissertation of Shebli Mehrazarin is approved.

Cun-Yu Wang

Yousang Gwack

No-Hee Park, Committee Co-Chair

Mo Kang, Committee Co-Chair

University of California, Los Angeles

2016

TABLE OF CONTENTS

LIST OF FIGURES AND TABLES

ACKNOWLEDGEMENTS

I would like to sincerely thank the incredible faculty, colleagues, and family that served as my support throughout the course of my graduate studies.

I am indebted to Dr. Mo Kang and Dr. No-Hee Park for their never-ending mentorship and guidance during both the completion of my doctorate degree and my application for both T90 and F30 fellowship awards. Dr. Kang and Dr. Park taught me to always work hard, push myself to my limit, and above all else to have integrity and self-respect. For this, I am eternally grateful.

I would also like to thank Dr. Cun-Yu Wang and Dr. Yousang Gwack for their insight and guidance during the completion of my dissertation project. Dr. Wang and Dr. Gwack provided invaluable feedback that helped strengthen my project, and I am grateful for their willingness to serve on my committee and for their support.

I would like to thank Dr. David Wong for his guidance and support in applying for and securing T90 and F30 fellowships and funding for my graduate program.

I would also like to thank Dr. Reuben Kim and Dr. Ki-Hyuk Shin for their mentorship and support, and I would like to thank the incredible colleagues that I have had the opportunity to work with these past few years. Without their support, I would not have been able to complete my doctorate degree. In particular, I would like to thank Dr. Wei Chen, Dr. Sol Kim, Dr. Bo Yu, Dr. Saaket Varma, Abdullah Alshaikh, Terresa Kim, Cindy Lee, Chris Chun, Paul Yang, and Sonia Kim for taking time out of their own busy schedules to teach, help, and support me in my research endeavors.

Lastly, I would like to thank my incredible wife, Saman Karimi, my loving parents Reza and Gilda, and my brother Shayan for their support and encouragement during this challenging journey. Your love and support has not gone unnoticed, and was critical to all of my success.

BIOGRAPHICAL SKETCH

NAME	POSITION TITLE
Mehrazarin, Shebli	PhD Candidate in Oral Biology

EDUCATION/TRAINING

INSTITUTION AND LOCATION	DEGREE	MM/YY	FIELD OF STUDY
University of California, Los Angeles	B.S	03/08	Biochemistry
University of California, Los Angeles	D.D.S.	06/12	Dentistry
University of California, Los Angeles	Ph.D		Oral Biology

A. Positions and Honors

Positions and Employment

2006-2008	Research Assistant, UCLA School of Dentistry
2008-Present	Program Instructor, HHMI Pipeline Program for Dentists-Scientists, UCLA School of Dentistry
2010-2011	Lecturer, Basic Dental Principles Course, UCLA School of Dentistry
2012-Present	Graduate Student Researcher, Division of Oral Biology & Medicine, UCLA School of Dentistry

Academic and Professional Honors

2008	Regents Graduate Stipend - Division of Oral Biology & Medicine, UCLA School of Dentistry
2009	Johnathon Ship Junior Investigator Award in Oral Research, International Association of Dental Research
2011	Dean's Leadership Institute Scholar, UCLA School of Dentistry
2012	Robert C. Caldwell Research Award, UCLA School of Dentistry
2015	Journal of Endodontics Award, Journal of Endodontics

B. Publications

1. **Mehrazarin S**, Alshaikh A, Varma S, Chen W, Chun C, Shin K-H, Kim RH, Park N-H, Kang MK (2016). Histone lysine demethylase KDM3C epigenetically regulates pro-inflammatory cytokine induction and systemic inflammatory response. Manuscript in preparation.

2. Chen W, Yi JK, Shimane T, **Mehrazarin S,** Lin Y-L, Shin K-H, Kim RH, Park N-H, Kang MK. (2016) Grainyhead-like 2 (GRHL2) regulates epithelial plasticity for oral carcinogenesis. *Carcinogenesis*, accepted for publication.

3. **Mehrazarin S***, Chen W*, Oh J, Liu ZX, Kang KL, Yi JK, Kim RH, Shin K-H, Park N-H, and Kang MK. (2015) p63 gene is regulated by Grainyhead-Like 2 (GRHL2) through reciprocal feedback and determines epithelial phenotype in human keratinocytes. *J. Biol. Chem.,* **290:**19999-20008.

4. Kang MK, **Mehrazarin S**, Park N-H. (2015) Oral Mucosal Stem Cells: Identification, Characterization, and Clinical and Disease Implications. *Stem Cell Bio & Tis. Eng. Dent. Sci.,* **1:**307-18.

5. Yi JK*, **Mehrazarin S***, Oh JE, Bhalla A, Oo J, Chen W, Lee M, Kim RH, Shin K-H, Park N-H, Kang MK. (2014) Osteo-/Odontogenic Differentiation of Induced Mesenchymal Stem Cells Generated through Epithelial-mesenchyme Transition of Cultured Human Keratinocytes. *J. Endod.*, **40:**1796-801.

6. Kim RH, Williams D, Bae S, Lee RS, Oh JE, **Mehrazarin S**, Kim T, Shin KH, Park NH, Kang MK (2012). Camphorquinone inhibits odontogenic differentiation of dental pulp cells and triggers release of inflammatory cytokines. *J. Endod*., **39**:57-61.

7. Kim RH, **Mehrazarin S**, Kang MK. (2012) Therapeutic Potential of Mesenchymal Stem Cells for Oral and Systemic Diseases. *Dent. Clin. North Am.,* **56**:651-75.

8. **Mehrazarin S**, Oh JE, Chung CL, Chen W, Kim RH, Shi S, Park NH, Kang MK. (2011) Impaired odontogenic differentiation of senescent dental mesenchymal stem cells is associated with loss of Bmi-1 expression. *J. Endod*., **37**:662-666.

9. Kim RH, Kim R, Liebermann M, Shin K-H, **Mehrazarin S**, Park N-H, and Kang MK. (2010) Bmi-1 extends the lifespan of normal human oral keratinocytes by deregulating the TGF-β signaling pathway. *Exp. Cell Res.,* **316**:2600-2608.

***Co-first author**

C. Research Support

Completed Research Support

F30 DE024005 (PI: Shebli Mehrazarin, D.D.S.) 01/01/14 – 12/31/15
NIH/NIDCR
"Role of GRHL2 in Oral Carcinogenesis"
The objective of this study is to investigate the role of GRHL2 in oral carcinogenesis, and investigate the effect of oral cancer-associated GRHL2 dysregulation on epigenetic regulation of keratinocyte proliferation.
Role: Principle Investigator

T32 DE007296-12 (PI: David Wong, D.M.D., D.M.Sc) 01/01/09 - 12/31/13
NIH/NIDCR
UCLA Fundamental Clinical Research Training Grant
The objective of this training program is to provide a rigorous training environment for clinician (DDS/DMD,MD), basic (PhD) and baccalaureate scientists to enable them to pursue academic careers in oral health research.
Role: Doctoral Trainee

1 INTRODUCTION

1.1 Specific Aims

Infection of pulpal and periodontal tissues in the oral cavity, if left untreated, leads to gross alveolar bone and tooth loss, abscess formation, sinus infection and bacteremia (Wilson, 1995; Dahlen, 2000; Kinney *et al.,* 2007). Chronic infection and inflammation in these tissues have also been associated with several systemic diseases, including cardiovascular diseases and diabetes (Buhlin *et al.,* 2003; Faria-Almeida *et al.,* 2006). Infectious bacteria affecting these tissues often spread and are characterized as endodontic-periodontic or periodontic-endodontic lesions, in which bacteria spread from pulpal tissues to periodontal ligament and surrounding gingival tissues, and vice versa. Over 80 million patients are diagnosed or seek treatment for pulpal or periodontal infections in the United States annually (American Dental Association, 2007; Eke *et al.,* 2012), and although treatment options exist, pathogens causing chronic infection, such as *Porphyromonas gingivalis* (*P.g.*)*,* often continue to persist despite active treatment (Johnson *et al.,* 2008). Although phenotypic alterations in the epithelial barrier may account affect persistent infection in oral tissues, the mechanisms behind this phenomenon is not well understood.

Epithelial plasticity is the ability of epithelial cells to alter their cellular phenotype and is tightly regulated by a process known as epithelial-mesenchymal transition (EMT). During EMT, epithelial cells undergo molecular and morphological changes towards fibroblast phenotype, and exhibit loss of cell-cell adhesion and increased cell motility (Banyard and Bielenberg, 2015). Transcription factors Grainyhead-like 2 (GRHL2) and p63 have independently been shown to regulate epithelial proliferation and differentiation, and based on our preliminary data, may play an important role in regulating EMT in human keratinocytes (Truong *et al.,* 2006; Chen *et al.,* 2012; Xiang *et al.,* 2012). Transforming growth factor beta (TGF-β) is known to be critical for

initiation of EMT, and is also highly expressed in epithelial cells when epithelial tissue is encountered by inflammation or injury in the human oral cavity (Steinsvoll *et al.*, 1999; Xu *et al*., 2009; Mize *et al*., 2015). Thus, we were interested in investigating whether GRHL2 and p63 regulate EMT in a TGF-β-dependent manner, and whether this EMT mechanism alters the epithelial barrier and its ability to protect against oral bacteria, such as *Porphyromonas gingivalis* (*P.g.*).

Several gram-negative oral bacteria are known to be responsible for the initiation and propagation of pulpal and periodontal infection and inflammatory response. Many of these bacteria, including *P.g.,* secrete lipoglycan endotoxins known as lipopolysaccharides (LPS) (Kabanov & Prokhorenko, 2010). Binding of LPS to Toll-like receptors (TLRs) are known to initiate downstream signaling pathways leading to transcriptional activation and secretion of pro-inflammatory cytokines, including several interleukins (ILs), that drive $CD4^+$ T cell differentiation and recruitment of inflammatory cells to the site of pathogenesis (Buer & Balling, 2003; McAleer & Vella, 2008). Although previous literature has identified an association between dynamic demethylation of histone marks and cytokine transcriptional activation (Saccani & Natoli, 2002), the role of histone lysine demethylases in the epigenetic regulation of inflammatory response is not well understood. Our preliminary data indicated that histone lysine demethylase KDM3C was upregulated in dental pulpal stromal cells (DPSC), immortalized monocytic cell line THP-1, and bone marrow macrophages cultured with *P.g.* LPS, and activated IL-6 induction by demethylating lysine 9 residues on histone 3 (H3K9). Thus, we were interested in whether KDM3C plays a functional role in epigenetically regulating *P.g.* LPS-mediated inflammation in oral tissues infected with *P.g.* bacteria.

In the current study, we proposed a hypothesis that during injury or inflammation of oral

epithelial tissues, upregulation of TGF-β expression in human keratinocytes result in downregulated expression of GRHL2 and p63, initiation of EMT, altered epithelial phenotype and inability of epithelial barrier to protect against *P.g.* bacteria. We also hypothesized that secretion of bacterial endotoxin LPS from these bacteria induce expression of KDM3C, leading to epigenetic activation of pro-inflammatory signaling pathways and inflammatory response (**Figure 1-1**). In order to test these hypotheses, we proposed the following Specific Aims:

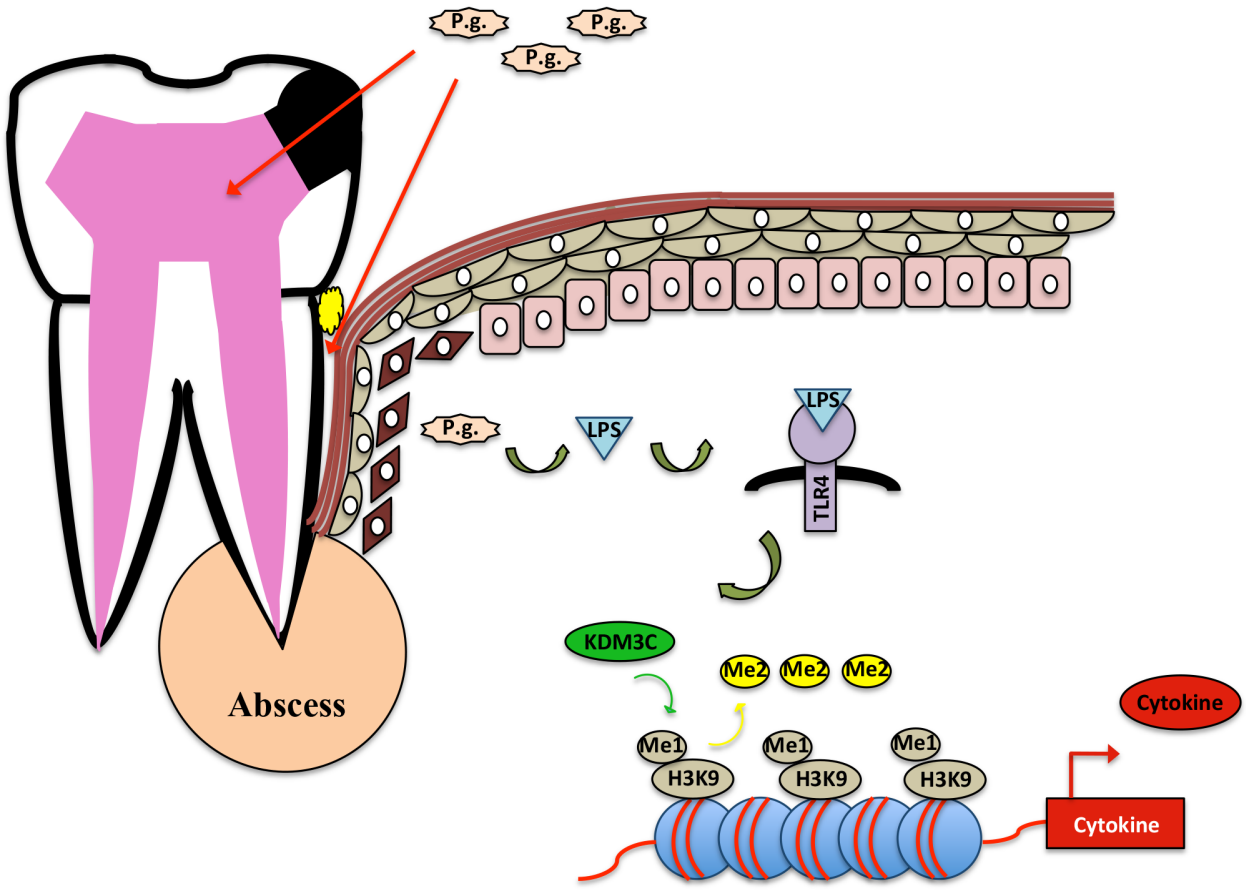

Figure 1-1. Proposed model of EMT-mediated alteration of epithelial barrier and epigenetic mechanisms regulating inflammatory cytokine induction.

Specific Aim 1 – To investigate the molecular mechanism of TGF-β-dependent EMT. NHEK were transiently transfected with siRNA targeting p63 (Si-p63). Onset of EMT was assessed by altered cellular morphology and expression of EMT markers, including fibronectin (FN), E-Cadherin (E-Cad), and ZEB proteins. Stemness was assessed by change in expression of cell surface markers, e.g., CD44, CD73, CD90, and CD105. Expression of p63 and GRHL2 were assessed in Si-p63/NHEK. Effect of TGF-β-dependent EMT induction on p63 and GRHL2 expression was evaluated. ChIP assay was performed to assess both enrichment of p63 on miR-200 family genes and enrichment of GRHL2 on p63 promoter. Luciferase activity was measured to assess GRHL2 and p63 reciprocal feedback and regulation of promoter activity. Tongues of Wt or GRHL2 KO mice administered *P.g.* bacteria by oral inoculation were stained with toluidine blue to assess extent of phenotypic alteration of epithelial barrier. Whole blood was collected, genomic DNA was extracted, and conventional PCR was used to assess bacterial load of *P.g.* in whole blood.

Specific Aim 2 – To investigate the functional role of KDM3C in the epigenetic regulation bacterial endotoxin mediated inflammatory response. Dental pulp stromal cells (DPSCs), human monocytic cell line THP-1, and bone marrow macrophages were cultured with *P.g.* LPS in time-dependent manner and screened for differential expression of KDMs by qRT-PCR. Transient knockdown of KDM3C using Si-RNA was used to assess its functional role in cytokine induction. ChIP-Seq experiments were performed to assess global binding of KDM3C to inflammatory cytokine gene targets upon exposure to *P.g.* LPS. For *in vivo* study, both KDM3C knockout (KO) mice and mice administered with *in vivo*-specific Si-RNA targeting KDM3C were intravenously exposed to *P.g.* LPS. Inflammatory cytokine induction in these mice was assessed by qRT-PCR, ELISA, and cytokine antibody array.

1.2 Epithelial-Mesenchymal Transition

1.2.1 *Definition of Epithelial-Mesenchymal Transition*

Epithelial-Mesenchymal Transition (EMT) is a process by which epithelial cells exhibit morphologic and molecular changes consistent with mesenchymal phenotype and is involved in tissue and organ development and repair (Hay & Zuk, 1995) (**Figure 1-2)**. Alteration in epithelial phenotype was first noted as "epithelial-mesenchymal transformation" (Hay, 1995), as the process was initially thought to be unidirectional. Subsequent study has established the reversibility of epithelial transition and the existence of a complementary phenomenon referred to as Mesenchymal-Epithelial Transition (MET), which serves an important role in many processes, including cancer metastasis (Yao *et al.,* 2011).

1.2.2 Characterization of EMT

EMT is characterized by downregulation of notable epithelial markers, loss of cell-cell adhesion and acquisition of fibroblast-like phenotype, mesenchymal marker expression, increased motility and invasiveness, and apoptotic resistance (Banyard and Bielenberg, 2015). Among the epithelial markers downregulated, E-Cadherin is the most critical for the loss of epithelial phenotype and transition towards mesenchymal phenotype. E-Cadherin is a glycoprotein belonging to the Cadherin family of calcium-dependent cell-cell adhesion molecules and plays an important role in maintenance of epithelial integrity (van Roy and Berx, 2008). Loss of E-Cadherin and epithelial cell-cell adhesion plays an important role in facilitating the enhanced motility, migratory capacity and invasiveness associated with EMT (Grille *et al.,* 2003; Moreno-Bueno *et al.,* 2009). Cytokeratins, in particular K5 and K14, are intermediate filament proteins that play a distinct but similarly important role in regulating epithelial cell proliferation and differentiation and are important epithelial markers (Alam *et al.,* 2011). K5 and K14 are located in the epithelial

basal layer and are important for maintaining cell shape (Moll *et al.,* 1982). Downregulated expression of these cytokeratins compromises epithelial differentiation and ultimately facilitates mesenchymal transition.

In addition to loss of epithelial marker expression, cell adhesion and integrity, EMT is also characterized by the acquisition of several mesenchymal markers, *e.g.* Fibronectin, N-Cadherin, Snail, and ZEB-1. Fibronectin is a stromal extracellular matrix protein that binds to integrin receptors and has been shown to facilitate EMT by activating MAP/ERK signaling (Park and Schwarzbauer, 2014). N-Cadherin also belongs to the cadherin family of calcium-dependent cell-cell adhesion molecules and has been shown to promote EMT-associated motility and invasion independent of E-Cadherin loss (Hazan *et al.,* 1997; Niemen *et al.,* 1999). Snail is a zinc-finger transcription factor that promotes EMT and mesenchymal phenotype by binding to the E-box region of E-Cadherin and repressing its transcription (Batlle *et al.,* 2000; Barrallo-Gimeno & Nieto MA, 2005). Similar to Snail, Zinc finger E-box binding homeobox 1 (ZEB-1) promotes EMT by binding to E-box regions on E-Cadherin and repressing E-Cadherin expression (Postigo & Dean, 2000; Liu *et al.,* 2008). These mesenchymal markers help promote mesenchymal transition, and in particular enhanced migratory and invasive capacity, through unique mechanisms and are thus vital for EMT.

1.2.3 Role of EMT in Disease and Development

EMT is known to play a prominent role in both human development and diseases processes. In particular, EMT has been found to play an integral role in embryonic development and maintenance of normal epithelial tissues. In particular, EMT has been found to regulate neural crest, cardiovascular, and mesoderm development through transcriptional regulation by EMT

markers Snail, Slug, and Twist1 (Carver *et al,* 2001; Nieto, 2002; Soo *et al.,* 2002; Yang & Weinberg, 2008). EMT has also been shown to play an important role in oral palatogenesis. During development of the oral palate, palatal shelves grow towards the palatal midline, ultimately resulting in medial epithelial seam development. These epithelial cells undergo EMT shortly after fusion and complete oral palatogenesis by growing towards the mesenchymal palatal region, and EMT has been shown to be critical for successful palate formation (Fitchett & Hay, 1989; Hay & Griffith 1992). Wound healing and re-epithelialization are also known to be facilitated by EMT. Movement and closure of epithelial sheets is a hallmark feature of wound healing, and is induced by EMT in response to inflammatory cytokines (Chen *et al.,* 1995; Yan *et al.,* 2010). In particular, tumor necrosis factor alpha (TNF-α) has been shown to activate bone morphogenetic protein-2 (BMP-2) and receptor BMPR1A, ultimately resulting in EMT in human keratinocytes and enhanced migratory capacity necessary for epithelial sheets to move and close epithelial wounds (Yan *et al.,* 2010).

In addition to its developmental roles in palatogenesis and wound healing, EMT has also been heavily implicated in the promotion and facilitation of cancer metastasis. Metastasis is a process by which tumorigenic cells travel to other sites in the body through the blood stream and reattach at a secondary site, thereby accounting for the "spread" of many cancers (Tsai and Yang, 2013). EMT has been implicated in tumor initiation, as EMT marker Twist1 has been shown to promote malignancy driven by Her2 and H-ras by inhibiting tumor suppressor protein p53 (Ansieau *et al.,* 2008; Morel *et al.,* 2012). In order to enter the vasculature, many tumorigenic epithelial cells rely on the loss of cell-cell adhesion and enhanced migratory and invasive capacity characteristic of EMT. The transition from immotile epithelial cell to motile mesenchymal-like tumor cell facilitates the dissemination of these cells and the first several steps of cancer metastasis, namely

local invasion, intravasation, systemic transport, and extravasation (Tsai and Yang, 2013). Upon reaching and colonizing secondary tissues, these mesenchymal-like tumor cells undergo morphological and molecular reversal towards epithelial phenotype, either by reversal of EMT phenotype or by undergoing MET, allowing proliferation and spread of tumorgenic cells in these distant tissues. Thus, complete characterization and understanding of EMT and MET processes, and in particular their role in metastasis, continues to be of great interest. Undoubtedly, EMT plays an important role in not only cancer metastasis, but in embryogenesis and wound healing as well, and may provide in further insight into the importance of epithelial plasticity in epithelial barrier function and protection against pathogens.

1.2.4 Molecular Regulation of EMT

Transforming growth factor beta (TGF-β) is known to play an important role in triggering EMT in cultured normal human keratinocytes (NHK) (Xu *et al*., 2009). Our previous study demonstrated that overexpression of the ΔNp63 isoform of p63, a transcription factor that regulates epithelial phenotype and keratinocyte proliferation, induces EMT in NHK in a TGF-β dependent manner (Oh *et al*., 2011). These cells exhibited morphological and molecular changes consistent with EMT, and also acquired multipotency and other stemness characteristics, such as enhanced expression of reprograming factors Lin28 and Nanog (Oh *et al*., 2011).

In addition to p63, Grainyhead-like 2 (GRHL2), a novel transcription factor involved with epithelial morphogenesis, cell proliferation, and differentiation, has also been found to play an important role in the regulation of EMT (Chen *et al.,* 2012; Xiang *et al.,* 2012). GRHL2 has been found to transcriptionally regulate broad spectrum of target genes including the human telomerase (hTERT) gene, proliferating cell nuclear antigen (PCNA), and epidermal

differentiation complex (EDC) genes and has been found to promote epithelial cell proliferation and inhibit keratinocyte differentiation in NHK (Chen *et al.,* 2010b, Chen *et al.,* 2012). GRHL2 has recently been found to negatively regulate EMT by upregulating microRNA 200 (miR-200) family genes, namely miR-200b and miR-200c (Cieply *et al.,* 2012). Upregulation of miR-200b/miR-200c has been shown to suppress ZEB1 signaling, there by inhibiting EMT by preventing E-Cadherin transcriptional repression (Korpal *et al.,* 2008; Wellner *et al.,* 2009). Further, a reciprocal feedback loop between ZEB1 and GRHL2 has been shown to exist, thereby indicating that EMT is a tightly regulated process (Cieply *et al.,* 2013). Clearly, GRHL2 is a determinant of epithelial phenotype through transcriptional network of its target genes. The interaction between p63 and GRHL2 and its implications in EMT and epithelial plasticity has not been investigated, and will be the focus of this study.

1.3 Epithelial Barrier Maintenance

1.3.1 Wound Healing

Epithelial wound healing is a highly regulated process that includes changes in cellular motility, proliferation, and inflammatory response. During wound healing, epithelial cells utilize actinomyosin fibers to migrate towards the wound site, allowing cell-to-cell interaction and wound closure (Bement *et al.,* 1993). During this time, epithelial cells undergo enhanced cellular proliferation (Todaro *et al.,* 1965) and secrete growth factors, *e.g.,* fibroblast growth factor (FGF) and platelet-derived growth factor (PDGF) (Werner *et al.,* 1992). However, it is the inflammatory response to wound healing that has the largest impact on the rate and efficiency of wound repair, as well as on cutaneous scar formation.

In response to injury and trauma, an inflammatory response is mounted to aid in wound healing and to prevent infection. Polymorphonuclear cells are recruited to the wound site to clear bacterial pathogens and secrete pro-inflammatory cytokines, *e.g.,* IL-1α, IL-1β, IL-6, and TNF-α, with macrophages aiding in cytokine secretion later in the wound healing process (Hubner *et al.,* 1996; Grellner *et al*., 2000). This pro-inflammatory cytokine release promotes keratinocyte and fibroblast cell proliferation, regulates extracellular matrix (ECM) protein metabolism, and mediates the body's immune response to wound formation (Werner *et al.,* 2003).

1.3.2 Impact of Deregulated Cytokine Release on Wound Healing

Deregulation of pro-inflammatory cytokine release may impose detrimental effects on wound healing. Wound induced in IL-6-deficient mice exhibited delayed reepithelialization and wound healing as well as impaired granulation tissue formation (Gallucci *et al.,* 2000). Excessive IL-6 cytokine expression in adult tissues results in significant cutaneous scarring (Liechty *et al.,* 2000). Human fetal tissues with reduced IL-6 expression exhibit minimal scarring during wound healing (Schrementi *et al.,* 2008); similar relationship between TGF-β and scar formation has been observed during wound healing.

Oral mucosa is composed of highly regenerative stratified epithelium and submucosal connective tissue, which demonstrate accelerated epithelial turnover and scarless wound healing, when compared epidermal and other epithelial tissues (Chen *et al.,* 2010a). This improved wound healing is attributed to enhanced growth factor secretion as well as increased amount, potency, and proliferation capacity of oral keratinocyte stem cells (OKSCs) (Chen *et al.,* 2010a). Differences in inflammatory response and pro-inflammatory cytokine secretion have also been associated with improved oral mucosal healing, and are thought to be responsible for the

minimal scar formation exhibited by oral mucosa.

When compared to skin wound healing, oral mucosal wound repair involves an much milder inflammatory response, with reduced concentration of neutrophils, macrophages, T cells, and other inflammatory cells, as well as suppressed angiogenesis and no change in VEGF expression (Szpaderska *et al.,* 2003; Szpaderska *et al.,* 2005; Mak *et al.,* 2009). Although activated by the wound healing process, expression level of inflammatory cytokines, *e.g.,* IL-1α, IL-1β, IL-6, and TNF-α, as well as TGF-β, at the oral mucosal wound site are lower than those of skin (Spaderska *et al.,* 2005; Schrementi *et al.,* 2008). Oral mucosal wounds undergo complete reepithelialization after one day, and the wound closes after 3 days; this is in contrast to 40% reepitelialization at one day and wound closure after 5 days in skin wound (Spaderska *et al.,* 2003; Spaderska *et al.,* 2005). Reduced inflammatory cell recruitment, pro-inflammatory cytokine release, and enhanced rates of reepithelialization and wound closure account for the minimal scar formation in mucosal wound healing, indicating that oral mucosal wound repair involves a more simple and efficient mechanism than that of skin.

1.3.3 Effect of Chronic inflammation on Epithelial Maintenance

Although oral epithelial tissues are known to exhibit rapid and scarless wound healing, they are also susceptible to chronic inflammatory disease due to the interruption of epithelial coverage around the teeth. Chronic periodontitis is the most common oral inflammatory disease and affects up to 15% of the adult population worldwide (Preshaw et al., 2012). It is characterized by inflammation of surrounding gingival tissues, deepening of the periodontal pocket, and destruction of periodontal ligament fibers and alveolar bone (Teng *et al.,* 2000; Tunkel *et al.,* 2002; Preshaw et al., 2012). This persistent alveolar bone loss leads to gingival recession and

further deepening of periodontal pocket depth, ultimately resulting in tooth loss (Heitz-Mayfield *et al.,* 2002). In addition to osteoclastogenesis and alveolar bone loss, chronic periodontitis also results in compromised epithelial integrity and internalization of many oral bacteria, including *Porphyromonas gingivalis, Fusobacterium nucleatum,* and *Treponema denticola,* within buccal and gingival epithelial cells (Teng *et al.,* 2000; Rudney *et al.,* 2005; Colombo *et al.,* 2007; Groeger *et al.,* 2010). Management of periodontitis involves physical debridement of plaque that accumulates along surface of the root adjacent to periodontal tissues and elimination of infectious bacteria. Periodontal infection can also lead to the spread of infection to adjacent tissues, such as dental pulp, by means of accessory canals and the apical foramen, and management of this inflammatory disease is important to ensure both retention of natural dentition and prevent rampant destruction of oral tissues (Zehnder *et al.,* 2002).

Chronic periodontitis is associated with the upregulation of and secretion of several notable inflammatory cytokines and growth factors by macrophages, gingival epithelial cells and gingival fibroblasts (Leask & Abraham, 2006; Cetinkaya *et al.,* 2013). In particular, transforming growth factor beta (TGF-β) is highly expressed in surgically removed inflamed tissues from chronic periodontitis patients (Steinsvoll *et al.*, 1999; Mize *et al*., 2015), and is responsible for activation and upregulation of connective tissue growth factor (CTGF) (Gurkan *et al.,* 2006). During chronic periodontitis, TGF-β and CTGF promote tissue degradation and enhanced osteoclastogenesis and bone destruction by activating macrophage colony stimulating factor and RANK ligand (Jagels & Hugli, 2000; Nozawa *et al.,* 2009; Jun & Lau, 2011). As described previously, TGF-β also plays an important role in mediating EMT in cultured normal human keratinocytes (NHK) (Xu *et al*., 2009), and is critical for activation of EMT phenotype. EMT involves the loss of cell-cell adhesion mediated by E-Cadherin and β-Catenin, which are critical

for epithelial integrity (Tian *et al*., 2011). Since TGF-β is highly expressed during chronic periodontitis and is also critical for the initiation of EMT, it is possible EMT is initiated in oral epithelial cells during chronic inflammation, leading to loss of epithelial integrity and barrier function and enhanced bacterial infiltration in gingival and periradicular tissues. Ultimately, the role of EMT and compromised epithelial barrier function on oral bacterial infiltration is not well understood, and will be a major focus of this study.

1.4 Mechanisms of Bacterial Endotoxin Induced Inflammation

1.4.1 Role of Porphypromonas gingivalis in Inflammation

Gram-negative anaerobic bacterium *Porphyromonas gingivalis* (*P.g.*) is known to trigger oral inflammation in both periodontal and pulpal tissues (Nair, 2004), and to play an important role in endodontic-periodontal lesion development (Fujii *et al.,* 2014). Over 47% of Americans, or nearly 65 million adults, present symptoms of periodontitis (Eke *et al.,* 2012) and chronic periodontitis has been shown to lead to gross alveolar bone and tooth loss (Wilson, 1995; Kinney *et al.,* 2007) and potentially aggravate of cardiovascular diseases and diabetes (Buhlin *et al.,* 2003; Faria-Almeida *et al.,* 2006). Similarly, over 15 million root canals are performed annually in order to alleviate pulpal and periradicular inflammation (American Dental Association, 2007), which if left untreated could lead to periradicular abscess formation, alveolar bone destruction, sinus infection and bacteremia (Dahlen, 2000). *P.g.* play a critical role in these periodontal and endodontic inflammatory disease processes by secreting lipoglycan endotoxins known as lipopolysaccharides (LPS).

1.4.2 Molecular Mechanisms of Endotoxin-Dependent Cytokine Induction

Gram-negative bacteria utilize LPS, which reside on the outer layer of their cell membrane, to confer toxicity and to protect the bacteria from phagocytosis and degradation (Kabanov & Prokhorenko, 2010). LPS are structurally conserved, consisting of a hydrophobic lipid A, which is responsible for endotoxicity, as well as hydrophilic core and O-antigenic polysaccharide chains (Maeshima & Fernandez, 2013). The O-antigenic polysaccharide side chain consists of a repeating oligosaccharide unit, and accounts for the distinct LPS serotypes that exist both physiologically and commercially (Whitfield *et al.,* 1992). The lipid A molecule binds to Toll-like receptor 4 (TLR4) and triggers a signaling cascade that ultimately results in the transcription of several pro-inflammatory cytokines and inflammatory response (Kawai & Akira, 2010).

Toll-like receptors (TLRs) are a class of pattern recognition receptors (PRRs) that recognize several distinct pathogen-associated molecular pattern (PAMP) molecules (Netea *et al.,* 2004). The ten distinct TLRs recognize lipopeptides, glycolipids, lipoteichoic acid, profilin, and double stranded RNA, among other PAMPs, from fungi, viruses, and bacteria (Akira *et al.,* 2006; Uematsu *et al.,* 2006). During gram-negative bacterial infection, LPS binding protein (LBP) removes LPS from the bacterial membrane and presents it to CD14, which carries LPS to the Toll-like receptor 4 (TLR4) and MD-2 complex (Maeshima & Fernandez, 2013). Binding of LPS to the TLR4-MD-2 complex activates either Toll-IL-1R domain-containing adapter protein (MAL/TIRAP) or myeloid differentiation primary response gene 88 (MyD88) signaling, resulting in activation of interleukin 1 receptor association kinase 2 (IRAK2), protein kinase R (PKR), nuclear factor–kappa B (NF-κB) and mitogen-activated protein kinase (MAPK) signaling, ultimately resulting in transcriptional activation of inflammatory response, dendritic cell maturation, chemotaxis and T-cell differentiation (Buer & Balling, 2003). In particular, these

downstream signaling molecules lead to the transcriptional activation of several important inflammatory cytokines, including IL-1β, IL-6, IL-8, and TNF-α (Rossol *et al.,* 2011; He *et al.,* 2013). Since these signaling pathways are involved in the regulation of distinct downstream targets, including those not involved in inflammation (Chang *et al.,* 2001; Ngo *et al.,* 2011), identification and characterization of epigenetic regulators of *P.g.* LPS and TLR-mediated pro-inflammatory cytokine gene targets may be important for the identification of a novel and potent anti-inflammatory therapeutic target, and will be an important focus of this study.

1.5 Epigenetic Modifications

1.5.1 Definition of Epigenetics

Epigenetic regulation involves alteration of gene expression that does not affect the nucleotide sequence. Epigenetic mechanisms have been implicated in cancer, psychiatric diseases, developmental abnormalities, and other molecular processes (Boulle *et al.,* 2012; Ohnishi *et al.,* 2014; Bai *et al.,* 2014). Epigenetic modifications primarily involve DNA methylation or histone modification, and are regulated by a wide range of epigenetic modification-specific enzymes (Copeland *et al.,* 2010). DNA methyltransferases (DNMT1/3a/3b) are known to methylate the 5-position of cytosines in GC rich regions, referred to as CpG islands, on gene promoters in order to prevent transcription and silence gene expression (Bestor *et al.,* 1988; Okano *et al.,* 1998; Jones and Takai, 2001). Histone modifications are post-translational modifications to histone proteins that are critical for transcriptional repression or activation. These modifications include lysine and arginine methylation and acetylation, serine and threonine phosphorylation, and lysine ubiquitylation and sumoylation, occur on distinct sites on histones H2A, H2B, H3 and H4 and are carried out by distinct epigenetic enzymes (Peterson & Laniel, 2004). Histone modification

enzymes modify distinct histone residues and are thus site specific, as is their effect on gene expression. Whereas histone acetylation generally results in transcriptional activation (Peterson & Laniel, 2004), methylation of lysine 4 on histone 3 (H3K4), H3K36, and H3K79 results in transcriptional activation (Wang *et al.,* 2001; Krogan *et al.,* 2003; Sawado *et al.,* 2008), and methylation of H3K9, H3K27, and H4K20 results in transcriptional repression (Tachibana *et al.,* 2001; Cao *et al.,* 2002; Nishioka *et al.,* 2002). Thus, histone modifications are important epigenetic alterations that are critical for tightly controlled transcriptional regulation.

1.5.2 Role of Histone Methylation/Demethylation on Disease & Development

Histone lysine demethylases (KDMs) have been shown to play an important role in transcriptional regulation as well as gene silencing and activation (Tsukuda *et al.,* 2006; Fodor *et al.,* 2006; Bjorkman *et al.,* 2011; Hubner *et al.,* 2011), and many of these KDMs are known to play a role in disease and developmental processes. For instance, KDM6B is known to promote neural differentiation (Jepsen *et al.,* 2007), KDM4B and KDM6B have been shown to facilitate osteogenic differentiation in human mesenchymal stem cells (MSCs) (Ye *et al.,* 2012), and several KDMs, including KDM2B, KDM4C, KDM5B and KDM6A, have been implicated in cancer development (Yang *et al.,* 2000; van Haaften *et al.,* 2009; Hayami *et al.,* 2010; He *et al.,* 2011).

Among these, KDM3C, or alternatively JMJD1C, of the KDM3/JMJD1 family of histone demethylases has been shown to drive transcriptional activation by demethylating mono- and di-methylated lysine 9 residues on histone 3 (H3K9me1 & H3K9me2) (Kim *et al.,* 2010; Peeken *et al.,* 2013). KDM3C has previously been shown to be a potential tumor suppressor (Wolf *et al.,* 2007), repress neural differentiation of human embryonic stem cells (Wang *et al.,* 2014), to play

a critical role in steroidogenesis (Kim *et al.,* 2010; Kuroki *et al.,* 2013), and has been implicated in leukemia maintenance (Sroczynska *et al.,* 2014). In contrast to KDMs, histone methyltransferase (HMTase) G9a has been shown to mono-/di-methylate H3K9, recruiting heterochromatin protein 1 (HP1) to bind to and stabilize methylated H3K9 (Tachibana *et al.,* 2005; El-Gazzar *et al.,* 2008). G9a also recruits DNA methyltransferase 3a/b (DNMT3a/b) to methylate DNA CpG islands upstream of the transcription start site (TSS) and silence gene expression.

Despite one study demonstrating that KDM6B is upregulated in monocytes undergoing terminal differentiation towards macrophage lineage (De Santa *et al.,* 2007), the role of KDMs, and KDM3C in particular, in epigenetically mediating inflammatory response is not well understood. There is no information regarding downstream targets in inflammatory pathways or evidence of functional role of KDM3C in regulating pro-inflammatory cytokine expression. Thus we were very interested in the role of KDMs, and KDM3C in particular, in the epigenetic regulation of inflammation and potential as novel anti-inflammatory therapeutic targets in the management and treatment of inflammatory oral diseases. The underlying epigenetic mechanisms regulating inflammatory response will be explored extensively in this study.

2 MATERIALS AND METHODS

2.1 Cells and cell culture

Primary NHEK cultures were prepared from discarded foreskin epidermal tissues and grown in EpiLife medium supplemented with growth factors (Invitrogen, Carlsbad, CA), as described elsewhere (Kang *et al.,* 2000). Normal human oral keratinocytes (NHOK) isolated from separated keratinizing oral epithelial tissues were prepared similar to NHEK. NHEK were serially subcultured and passed at 70% confluence until they reached replicative senescence. Replication kinetics were recorded as described previously (Kang *et al.,* 2000). Normal human oral fibroblasts (NHOF) were obtained from discarded gingival connective tissue and cultured in Dulbecco's modified Eagle's medium (DMEM) (Invitrogen), supplemented with 10% fetal bovine serum (FBS) (Invitrogen). Bone marrow mesenchymal stromal cells (BM-MSCs) and dental pulp stem cells (DPSCs) were cultured in α-MEM medium (Invitrogen) supplemented with 10% FBS (Invitrogen), and 5 mg/mL gentamicin sulfate (Gemini Bio-Products, West Sacramento, CA). SCC4 and SCC9 cancer cell lines were cultured in DMEM/F12 (Invitrogen) and supplemented with 10% FBS and 0.4 pg/ml hydrocortisone, as described elsewhere (Kang *et al.,* 1998). Immortalized keratinocyte cell line HaCaT cells were grown in EpiLife medium supplemented with growth factors (Invitrogen). THP-1 cells were cultured in Roswell Park Memorial Institute medium (RPMI) (Invitrogen) supplemented with 10% fetal bovine serum (Invitrogen), and 5 μg/mL gentamicin sulfate (Gemini Bio-Products), and terminally differentiated towards macrophage lineage by 24 hour treatment with 100 ng/mL phorbol 12-myristate 13-acetate (PMA) (Sigma, St Louis, MO). Bone marrow monocytes were isolated from femurs of wild type and KDM3C knockout mice and negatively selected using EasySep mouse monocyte enrichment kit (StemCell Technologies, Vancouver, BC, Canada). Bone marrow

monocytes were cultured in RPMI growth medium (Invitrogen) supplemented with 10% fetal bovine serum (Invitrogen), 5 μg/mL gentamicin sulfate (Gemini Bio-Products), and 40 ng/ml M-CSF (R&D Systems, Minneapolis, MN) for 5 days to facilitate terminal macrophage differentiation. DPSC, THP-1, and bone marrow macrophages were further cultured with 1 μg/mL *P.g.* LPS (Invivogen, San Diego, CA) for 0, 1, 2, 4, 8, 12, or 24 hours prior to being harvested. DPSC and THP-1 were also cultured with 1 μM BIX-01294 (diazepin-quinazolin-amine derivative) (Sigma) for 24 hours to inhibit G9a enzymatic activity. DPSC were infected with retroviral vectors expressing full-length G9a (pMSCV-G9a) or empty vector (pMSCV-EV) as described elsewhere (Kang & Park, 2007), and selected with 50 mg/ml Hygromycin B (Sigma) for 14 days prior to being cultured with *P.g.* LPS for 24 hours. Cells were maintained at 37°C at 5% CO_2 in a humidified chamber.

2.2 Retroviral vector construction and transduction of cells

We constructed retroviral vectors expressing human wild-type ΔNp63α, ΔNp63β, and ΔNp63γ. Full-length cDNAs of ΔNp63 were cloned from the cDNA library obtained from primary human keratinocytes by PCR amplification. ΔNp63α, ΔNp63β, and ΔNp63γ cDNAs were subcloned into pLXSN retroviral expression vector (Clontech, Mountainview, CA) at XhoI/BamHI restriction sites, and isoforms were confirmed by sequencing. Retroviral construction and infection were performed as described elsewhere (Kang & Park, 2007), and the infected cells were selected with 200 μg/ml G418 (Sigma, St. Louis, MO). G418-resistant cells were continually maintained by serial subculture as outlined above.

2.3 Transwell Migration Assay

Transwell chambers with polycarbonate membranes were used to measure cell migration (Corning Inc., Corning, NY), according to previously described methods (Giannelli *et al.,* 1997). NHEK/LXSN, NHEK/ΔNp63α, NHEK/ΔNp63β, and NHEK/ΔNp63γ cells were cultured in EpiLife (Invitrogen) and seeded in the upper chamber of the transwell. Cells were allowed to migrate for 24 hours, and the transwell was washed with 1x phosphate-buffered saline (PBS) and fixed in 10% formalin for 10 min. Cells were then stained with 1% crystal violet dissolved in 10% formalin for a duration of 1 hour. Non-migratory cells were removed from the chamber and transwells were photographed.

2.4 Immunofluorescence Staining

Cells were fixed for 15 minutes in 3.7% formaldehyde prior to permeabilization with 0.25% Triton X-100 for 10 minutes. Cells were then blocked in 10% normal goat serum for 1 hour. Antibodies against p63 (A4A), E-Cad, β-catenin, Zinc Finger E-Box Binding Homeobox 1 (ZEB1) (Santa Cruz Biotech, Santa Cruz, CA), GRHL2 (Abnova, Taipei City, Taiwan), and anti-FN (Sigma) were used as primary antibodies, and Alex Fluor 488 IgG (Invitrogen) was used as secondary antibody. Cells were counterstained with DAPI, and Olympus BH2-RFCA fluorescence microscope was used to obtain images.

2.5 siRNA Transient Transfection

NHEK were transfected with non-specific, scrambled siRNA (Si-SCR) or siRNA targeting human p63 (Si-p63), and DPSC were transfected with non-specific Si-RNA or Si-RNA targeting human KDM3C, at a concentration of 10 nM using Lipofectamine reagents (Invitrogen)

according to the manufacture's instructions. NHEK were transfected with Si-p63 once every 3 days over the course of 9 days. NHEK growth medium was replaced with mesenchymal growth medium (α-MEM medium/10% FBS, 5 mg/mL gentamicin sulfate) upon morphological transition to mesenchymal phenotype. DPSC were cultured with *P.g.* LPS 24 hours post-transfection, and harvested 48 hours post-transfection.

2.6 Western Blotting

Whole cell extracts or protein lysates from 100 mg ground liver tissue were isolated from the cultured cells, fractionated by sodium dodecylsulfate polyacrylamide gel electrophoresis, and transferred to Immobilon membrane (Millipore, Billerica, MA). Antibodies against p63 (A4A), p63 (H129), E-Cad, K14, ZEB1, N-Cad, KDM3C, HP-1, DNMT3a/b, IL-6, TNF-α, GAPDH (Santa Cruz Biotech), GRHL2 (Abnova), FN, Snail (Sigma), G9a (Millipore, Chicago, IL), H3K9me1, and H3K9me2 (Abcam, Cambridge, MA), were used. Chemiluminescence signal was detected by using the HyGLO Chemiluminescent HRP antibody detection reagent (Denville Scientific, South Plainfield, NJ).

2.7 Real-time qRT-PCR

Total RNA was extracted from cultured cells by using RNeasy Plus Mini kit (Qiagen, Valencia, CA). Reverse transcription (RT) was performed with 5 μg RNA by using the method described elsewhere (Kang *et al.,* 2004). qRT-PCR was performed for the relative mRNA expression of TAp63, ΔNp63, GRHL2, KDM2A, KDM2B, KDM3A, KDM3B, KDM3C, KDM4A, KDM4B, KDM4C, KDM4D, KDM5A, KDM5B, KDM5C, KDM5D, KDM6A, KDM6B, IL-6, IL-33, MAPK14, STAT3, and PIK3R1, relative microRNA expression of miR-200a, miR-200b, miR-

200c, miR-141, miR-429, and enrichment of GRHL2, H3K4me3, H3K27me3, KDM3C, G9a, H3K9me1 and H3K9me2 in triplicates for each sample with LC480 SYBR Green I master (Roche, Basel, Switzerland) using LightCycler 480 (Roche). Second derivative Cq value was calculated after running a total of 50 cycles in order to compare relative change in mRNA and microRNA expression. The primer sequences and the PCR conditions will be available on request.

2.8 F-Actin Staining / Stress Fiber Formation

Cells were fixed for 10 minutes in 3.7% formaldehyde prior to permeabilization with 0.1% Triton X-100 for 5 minutes. Cells were stained with Alexa Fluor 594 Phalloidin (Invitrogen) for 20 minutes at room temperature. Cells were counterstained with DAPI, and Olympus BH2-RFCA fluorescence microscope was used to obtain images.

2.9 Lentiviral vector construction and knockdown of endogenous GRHL2

Lentiviral vector expressing short hairpin RNA (shRNA) against GRHL2 (Sh-GRHL2) and control vector expressing enhanced green fluorescence protein (EGFP) were constructed as described earlier (Kang *et al.,* 2009). Endogenous GRHL2 was knocked down with Sh-GRHL2. All lentiviral vectors used allow identification of infected cells by GFP fluorescent signal under epifluorescence microscope.

2.10 Dual-Luciferase Reporter Assay

Promoter regions of GRHL2 and p63 were cloned into pGL3B-Luc reporter plasmid (Promega, Madison, WI) expressing firefly luciferase. The promoter-luciferase constructs were transfected

into SCC4 or SCC9 using Lipofectin Reagent (Invitrogen), along with pRL-SV40 containing *Renilla* luciferase cDNA under the control of SV40 enhancer/promoter. After 48 hours post-transfection, cells were collected and the lysates were prepared using Dual Luciferase Reporter Assay System (Promega). Firefly and *Renilla* luciferase activities were measured using a luminometer (Turner Designs, Sunnyvale, CA). *Renilla* luciferase activity was used to control for the varied transfected efficiency. The gene promoter activity, reflected by the firefly luciferase activity, was determined as the mean of at least triplicates per experiment.

2.11 Chromatin Immunoprecipitation (ChIP) / ChIP-qPCR Assay

ChIP assay was performed as described previously (Chen *et al.,* 2012). Nuclear proteins were cross-linked to DNA by adding 10% formaldehyde for 10 minutes, and 0.15 M glycine was used to stop cross-linking. The cells were then collected in ice-cold phosphate-buffered saline (PBS) supplemented with a protease inhibitor mixture and lysed in buffer (1% SDS, 10mM EDTA, protease inhibitors, 50mM Tris-HCl, pH 8.1). Genomic DNA was sonicated to produce DNA fragments 300–1000 bp in length. Cellular lysates were diluted 1:10 in ChIP dilution buffer (0.01% SDS, 1.1% Triton X-100, 1.2mM EDTA, 16.7mM NaCl, protease inhibitors, 16.7mM Tris-HCl, pH 8.1). Chromatin solutions were incubated with 4 μg p63, GRHL2, H3K4me3, H3K27me3, KDM3C, G9a, H3K9me1 or H3K9me2 primary antibody (or 1 μl of mouse IgG) overnight at 4°C with rotation. Immunocomplexes were precipitated with 30 μl of protein G-agarose slurry (Upstate Biotechnology, Lake Placid, NY, USA) and eluted in 500 μl of buffer (1% SDS, 100mM $NaHCO_3$). Precipitated DNA was recovered by phenol extraction and used for PCR amplification to check the enrichment of p63, GRHL2, H3K4me3, H3K27me3, KDM3C, G9a, H3K9me1, or H3K9me2 in gene promoter regions. qPCR was performed with the purified

DNA using LightCycler 480 (Roche). Semi-quantitative PCR was also performed, and samples pulled down with IgG were included as the negative control. qPCR readout was normalized relative to the amount of amplification from input.

2.12 Generation of Knockout Mice Models

GRHL2 conditional knockout (KO) mice were established by crossing K14/Cre/ERT mice with GRHL2/LoxP mice. GRHL2 knockout was induced by daily intraperitoneal injection of 20mg/mL Tamoxifen for one week. Genotyping was performed using primer sequences against LoxP: F- 5'CCAACCTTCCCTTTCCATTC-3", R- 5"AGAGGACTTGAGGTCGGAG-3" and Cre: F – 5"-GTTCGCAAGAACCTGATGGAC-3", R- 5"CTGGCAATTTCGGCTAT ACG-3". Tissue specificity of GRHL2 knockout was assessed by semi-quantitative PCR in skin, tongue, gingiva, stomach, and small intestine of wildtype and KO mice. GRHL2 KO mice were administered $1x10^9$ *P.g.* bacteria by oral inoculation every other day for 6 weeks, or had ligatures placed around 2^{nd} molars for 3 weeks, and harvested. Tongues from wildtype and KO mice were collected and stained with 1% toluidine blue to assess epithelial barrier damage. Whole blood was collected, and genomic DNA was extracted to assess *P.g.* bacterial load in blood by semi-quantitative PCR. Heterozygous KDM3C mice were obtained from RIKEN BRC, courtesy of Dr. Makoto Tachibana, and crossed to breed KDM3C knockout (KO) mice. Genotyping was performed and KDM3C wild-type and mutant alleles were identified using wild type primers 2C-144121-F- 5"-AGTCCCCGCACTCAGGAGGCTGCTG-3" and 2C-144790-R- 5"-ATATACACTATGATAC AGGAACAGC-3" and mutant primers IN-60F- 5"-CGCCTTCTT GACGAGTTCTTCTGAGGGG-3" and 2C-144790-R- 5"-ATATACACTATGATACAGGAAC AGC-3".

Table 2-1. Human primer sequences used for real time qRT-PCR.

Genes	Forward (5'-3')	Reverse (5'-3')
TAp63	TTGAGATTAGCATGGACTGTA	GTTCTGAATCTGCTGGTCCAT
ΔNp63	GGAAAACAATGCCCAGACTC	CTGCTGGTCCATGCTGTTC
GRHL2	GGACAGCACATACAGCGAGA	AGCCCCAACTGAAGCACTC
KDM2A	CGGATAGTTGAGAAAGCCAAGATCCG	CTCTTTGGTGGGCCTCTGTAGC
KDM2B	GTTAGTGGTAGTGGTGTTTTGG	AGCAGATGTGGTGTGTGGTC
KDM3A	ACCTGCAGTTATTCTTCAGC	TAATGCCAGTCCTATGCCAT
KDM3B	TGTTCCCTGGGGACTCCTCT	GGGCACTACAGTACAGCTGG
KDM3C	TTTGTTGAAGCTATTGACTG	CACTTTAACAAAAGCAAGCC
KDM4A	CCTCACTGCGCTGTCTGTAT	CCAGTCGAAGTGAAGCACAT
KDM4B	CGGGTTCTATCTTTGTTTCTCTCACCC	AAGGAAGCCTCTGGAACACCT
KDM4C	GGCATAGGTGACAGGGTGTGTC	CGGGGACCAAACTCTGGAAACCCG
KDM4D	CGGGATCTGCACAGATTATCCACCCG	AGTTTCTGAGGAGGGCGACCA
KDM5A	GTTTCTTAAGGTGGCAAGTC	TCTTTTGTACTGTTCCCTAC
KDM5B	AGCTTTCTCAGAATGTTGGC	GCAGAGTCTGGGAATTCACA
KDM5C	GGGTTTCTAAAGTGTAGATCT	CCACACATCTGAGCTTTAGT
KDM5D	ATCTCCTCACCTCTCCAAAG	TTGTCTCTAGGCGTGGCCGT
KDM6A	CGTCCGAGTGTCAACCAACTGGACG	TGAGAGTCCTGGAGTAGGAGCAG
KDM6B	CTCAACTTGGGCCTCTTCTC	GCCTGTCAGATCCCAGTTCT
IL-6	AAATTCGGTACATCCTCGAC	CAGGAACTGGATCAGGACTT

Table 2-2. Mouse primer sequences used for real time qRT-PCR.

Genes	Forward (5'-3')	Reverse (5'-3')
KDM3C	GAGGACTTCAAGGCC	AATTAGGTGTCTTCC
IL-6	GAGGATACCACTCCCAACAGACC	AAGTGCATCATCGTTGTTCATACA
IL-33	CAATCAGGCGACGGTGTGGATGG	TCCGGAGGCGAGACGTCACC
MAPK14	GCATCGTGTGGCAGTTAAGA	GTCCTTTTGGCGTGAATGAT
STAT3	CTTGTCTACCTCTACCCCGACAT	GATCCATGTCAAACGTGAGCG
PIK3R1	CTTGTCCGGGAGAGCAGTAAGCA	TTGTTGGCTACAGTAGTGGGCTTGG

Table 2-3. MicroRNA primer sequences used for qRT-PCR.

Genes	Sequence (5'-3')
miR-200a	CATCTTACCGGACAGTGCTGGA
miR-200b	TAATACTGCCTGGTAATGATGA
miR-200c	CGTCTTACCCAGCAGTGTTTGG
miR-141	TAACACTGTCTGGTAAAGATGG
miR-429	TAATACTGTCTGGTAAAACCGT

Table 2-4. Human ChIP PCR primer sequences.

Genes	Forward (5'-3')	Reverse (5'-3')
p63	GGTGGAAGTTGATGGATTGG	CTTCTGGCTCCAGGATTTTG
miR-200a	TGGGCCTGTGTGCAGTCTCA	TGTGGAAGCCCAGGGAAGA
miR-200b	CCCACTCCGACCTAGTCCTC	ACTCGCTGGGAAGCTCAGTA
miR-200c	CTGCTTGGACTGCAACCTGG	ACCTTGGGTCAGGCAGCTTC
miR-141	AAGCCCCTCGTCTTGAGCTG	CCAACCCCAAGCTCAAGGTC
miR-429	GGGGCTGCAGGGAACCTTTG	GTGCTGCGGGGCTGTGAA
IL-6 (TSS)	AATTCCCTGGGCATCTTCTT	GAATTCTGCAGCATCACCAG
IL-6 (1kb)	GCAAAGAAACCGATTGTGAAG	CCAGTCTCCAGAGACCCAGA
IL-6 (1.5kb)	AATGAAACCATCCAGCCATC	TCGTGCATAACATTTCAGGAC
IL-6 (2.2kb)	TGGACTAATTATCTAAAACAAGAGACC	CCAATCATTTTCCCTCAAAA
IL-33	CGGAGCTTGAAGTGAGCTG	ATTTTGTCCCCCTGGCTGGCTTAT
MAPK14	CTCCCAAAGTGCTGGGATTA	GAGCACCTGCTCACCTGAA
STAT3	GGCAGCCAGTGGAAGAATAG	CCAATTCCTCTTGGCTAAATG
PIK3R1	AATCCCCGAATGTTGAGAAA	GTGCCACACTTTTAAACCATCA

2.13 Interpapillary Endotoxin Inoculation

C57BL/6 mice were injected with 10 mg/ml *P.g.* LPS (Invivogen) between first and second molars. Whole blood was collected by cardiac puncture 24 hours post-injection, and placed in blood collection tubes (Fisher Scientific, Houston, TX) and diluted in PBS. Harvested blood was diluted over Lympholyte cell separation media (Cedarlane Labs, Burlington, NC) and centrifuged at room temperature for 20 minutes at 800g. The Lympholyte layer was separated, diluted in PBS, and centrifuged for 10 minutes at 800g to collect peripheral blood mononuclear cell (PBMC) pellet. Interpapillary tissues were also collected, and change in KDM3C and IL-6 mRNA expression in PBMCs and interpapillary tissues was assessed by qRT-PCR.

2.14 In Vivo Si-RNA Administration

KDM3C *in vivo* Si-RNA and scrambled *in* vivo Si-RNA were prepared using Invivofectamine

2.0 reagent and complexation buffer (Life Technologies, Grand Island, NY) and dialyzed using Float-A- Lyzer G2 cassette (Spectrum Laboratories, Rancho Dominguez, CA). Prepared Si-RNA were intravenously administered to C57BL/6 mice at a concentration of 7 mg/kg, followed by intravenous administration of 250 ug/kg *P.g.* LPS 24 hours later. C57BL/6 mice were sacrificed 3 hours post-*P.g.* LPS injection, and tissues and blood were harvested.

2.15 Enzyme Linked Immunosorbent Assay

Blood collected by cardiac puncture was centrifuged at 200g for 10 minutes, and serum was collected for ELISA assay using IL-6 ELISA Max Standard kit (Biolegend, San Diego, CA). Protein standards and serum IL-6 protein were measured at 450 nm, and a standard curve was established to determine IL-6 protein levels in serum samples. Additionally, serum from whole blood was used to perform mouse cytokine antibody array (RayBiotech, Norcross, GA) to assess whole blood serum secretion of 97 unique pro-inflammatory cytokines, as per the manufactures instructions. ImageJ software was used to quantitate cytokine array data.

2.16 High Throughput Sequencing & Data Extraction

DNA precipitate "libraries" were prepared from the IP samples obtained above by enzymatic repair of the ends and ligation of the adapter sequences, as described elsewhere (Barski *et al.,* 2007). High throughput sequencing was performed with Illumina Genome Analyzer IIx Sequencer located at the UCLA Genome Sequencing Center (Los Angeles, CA). Sequence tags were mapped to the human genome using the Illumina Genome Analyzer Pipeline. Output data in browser extensible data (BED) format was viewed with UCSC Genome Browser, allowing for alignment of multiple datasets in reference to the human genome. In doing so, we compared the

peak locations representing KDM3C binding between untreated and *P.g.* LPS treated THP-1 cells. Processed data was also ran through Ingenuity Pathway Analysis (IPA) software to identify unique inflammatory signaling targets bound by KDM3C between untreated and *P.g.* LPS treated THP-1, and those targets that are shared. DNA binding motif sequences were generated for those targets bound by KDM3C.

3 MOLECULAR REGULATION OF EPITHELIAL PLASTICITY BY p63 AND GRAINYHEAD-LIKE 2 (GRHL2) RECIPROCAL FEEDBACK

3.1 Overexpression of ΔNp63α in NHEK yields EMT morphology and phenotype

NHEK were infected with retroviruses containing empty vector LXSN or those expressing ΔNp63α, ΔNp63β, or ΔNp63γ isoforms. Among the transduced cells, cells expressing ΔNp63α and ΔNp63β isoforms showed morphological changes indicative of EMT, *e.g.*, elongated, flattened, and spindle-like morphology (**Figure 3-1A, left panel**). However, we observed that in NHEK expressing ΔNp63β isoforms, few mesenchymal-like cells were formed and were not able to be maintained in culture. Transwell migration assay also showed enhanced cellular motility, a hallmark of EMT (Xu *et al.,* 2009) in NHEK/ΔNp63α, while NHEK/ΔNp63β, NHEK/ΔNp63γ, and NHEK/LXSN showed limited transwell migration (**Figure 3-1A, right panel**).

To further confirm the molecular phenotype of EMT, we detected the level of EMT markers by Western blotting in NHEK infected with various ΔNp63 isoforms. Cells infected with ΔNp63α, ΔNp63β, and ΔNp63γ were harvested at two different population doubling (PD) levels at 24 and PD28; EMT phenotype occurred between these two PD levels (**Figure 3-1C**). We used both pan-p63 antibody (p63 A4A) and ΔNp63α-specific antibody (p63 H129) to assess protein expression of ΔNp63 isoforms. We observed specific bands corresponding to the α, β, and γ isoforms of ΔNp63 that were distinctly visible at 60, 50, and 40 kDa, respectively (**Figure 3-1B, C**). We also noted that high molecular weight p63 band denoted with asterisk (*) disappeared with occurrence of EMT only in the culture infected with LXSN-ΔNp63α at PD28, concomitant with appearance of the EMT phenotype. We also found that only prolonged

subculture of NHEK/ΔNp63α led to reduced protein expression of epithelial markers E-Cad and K14 and increased expression of mesenchymal marker FN (**Figure 3-1B, C**). Prolonged subculture of NHEK/ΔNp63α also led to downregulation of GRHL2, a transcriptional regulator and EMT-inhibitor that regulates epithelial proliferation and differentiation (Chen *et al.,* 2012). Loss of E-Cad and enhanced FN expression in NHEK/ΔNp63α cells were also confirmed *in situ* (**Figure 3-2**). In this particular culture, both cell types exhibiting the mesenchymal or epithelial phenotype were visible; those cells with the mesenchymal morphology also demonstrated enhanced FN and reduced E-Cad signal. Collectively, these data indicate that ectopic expression of ΔNp63α, but not ΔNp63β and ΔNp63γ, in NHEK triggers the EMT phenotype.

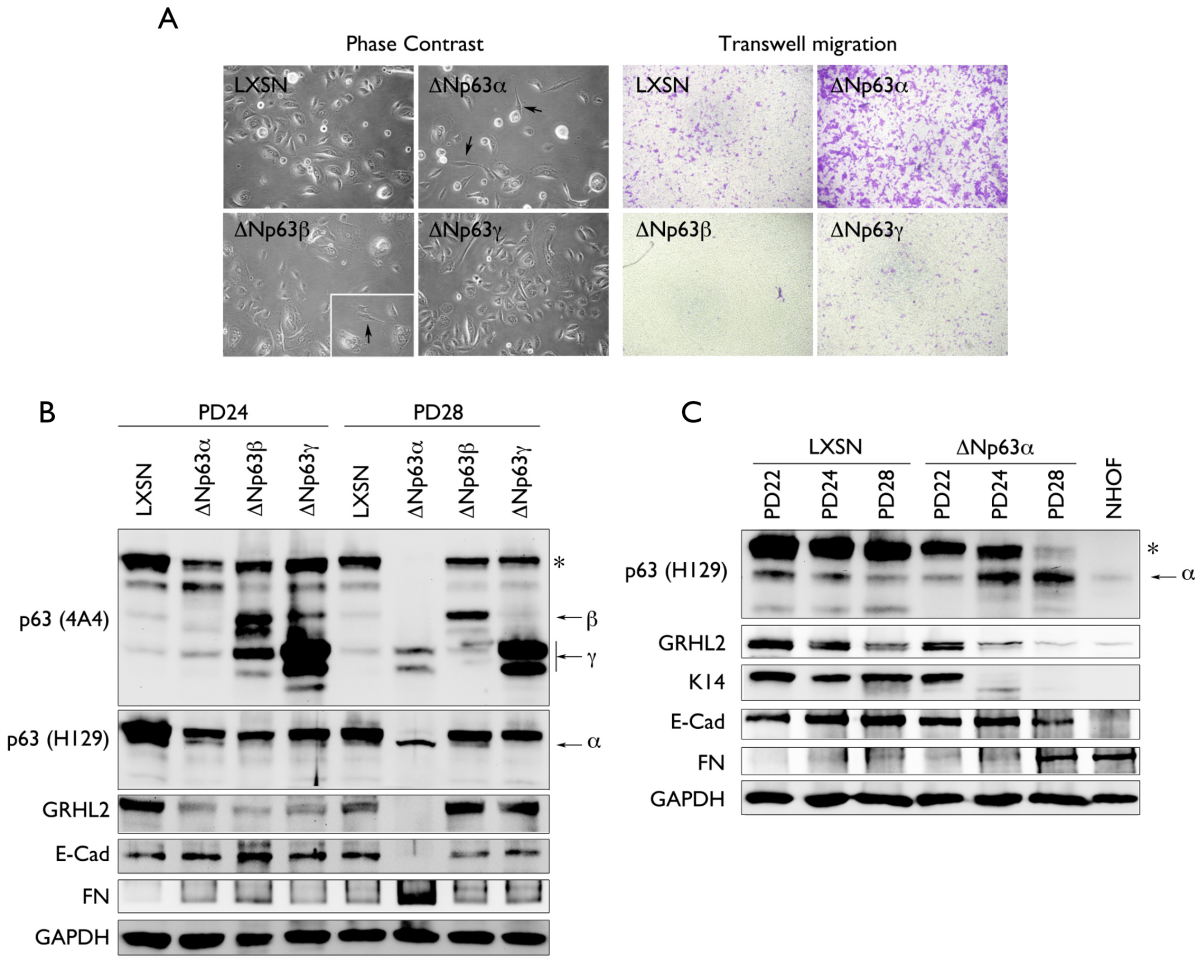

Figure 3-1. Overexpression of ΔNp63α in NHEK yields EMT phenotype.

(**A**) NHEK were stably transduced using retroviruses containing an empty vector (LXSN), or ΔNp63 isoforms α, β, or γ. Morphological changes were observed in cells after stable infection of ΔNp63 isoforms by phase contrast. Change in cell motility was assessed by transwell migration assay. (**B**) NHEK stably transduced using retroviruses containing an empty vector (LXSN), or ΔNp63 isoforms α, β, or γ were serially subcultured and assessed for change in protein expression of ΔNp63α, ΔNp63β, and ΔNp63γ isoforms, GRHL2, E-Cad and FN at two different population doubling levels (PD 24 and PD28) by Western blotting. Asterisk (*) indicates high molecular weight band of p63. (**C**) NHEK stably transduced using retroviruses containing an empty vector (LXSN), or ΔNp63α isoforms at PD 22, PD24 and PD28 were assessed for change in protein expression of ΔNp63α (using ΔNp63α specific antibody H129), GRHL2, K14, E-Cad and FN. NHOF was used as a negative control. GAPDH was using as a loading control. Asterisk (*) indicates high molecular weight band of p63.

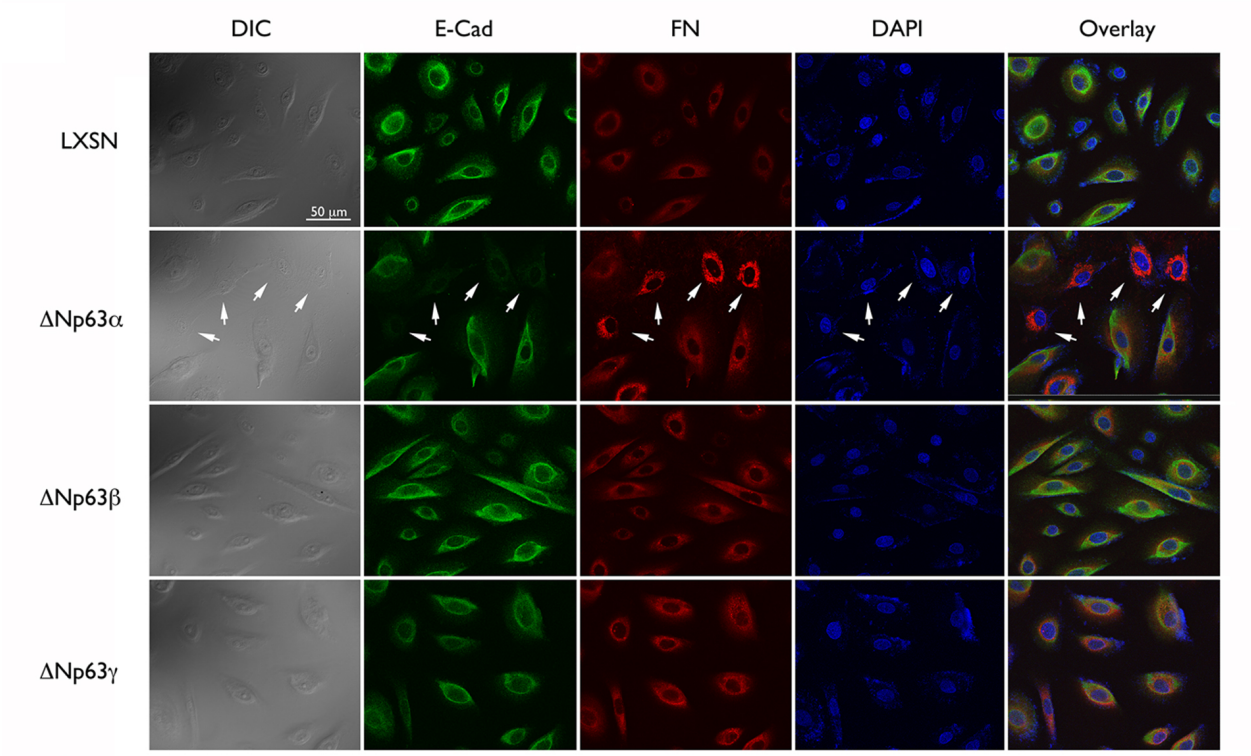

Figure 3-2. Overexpression of ΔNp63α in NHEK results in EMT molecular profile.

Changes in the expression of E-Cad and FN were assessed in NHEK transduced with ΔNp63α, ΔNp63β, or ΔNp63γ by means of fluorescence microscopy. Arrow indicates the NHEK/ΔNp63α cells exhibiting EMT phenotype.

3.2 Knockdown of all p63 isoforms in NHEK by transient transfection of siRNA results in EMT phenotype

Since EMT occurrence by ΔNp63α overexpression was accompanied by loss of the major p63 band (denoted with an asterisk in **Figures 3-1B, C**), we asked whether the loss of all p63 isoforms would lead to EMT. NHEK were transiently transfected with the control, scrambled siRNA (Si-SCR) or siRNA targeting p63 (Si-p63). In order to assess phenotypic and morphological changes upon p63 knockdown, we examined the changes in protein expression of p63, E-Cad, and FN after 3, 6, and 10 days post-transfection with Si-SCR or Si-p63. After 10 days post-transfection, NHEK/Si-p63 cells exhibited complete loss of p63 and E-Cad protein expression, whereas FN expression was notably enhanced (**Figure 3-3A**). These cells also exhibited mesenchymal cell morphology after 17 days when compared to NHEK/Si-SCR (**Figure 3-3B**).

We confirmed successful knockdown of p63 by qRT-PCR (**Figure 3-3C**). In the control cells (Si-SCR), the levels of ΔNp63 and GRHL2 were substantially higher than those in NHOF; upon Si-p63 transfection, p63 was almost completely knocked down to the level similar to those of NHOF. TAp63 expression level was negligible in all tested samples. Concomitantly, we found that GRHL2 level was also drastically reduced by p63 knockdown, indicating a link between p63 and GRHL2 in epithelial phenotype.

We also determined mesenchymal cell surface markers (*e.g.*, CD44, CD73, CD90, and CD105) in NHEK/Si-p63 cells with EMT phenotype. For comparison, we included BM-MSCs, DPSCs, and parental NHEK. The NHEK/Si-p63 cells with EMT phenotype showed elevated CD44, CD90, and CD105 expression compared with the parental NHEK, while the level of

CD73 was reduced, consistent with other MSC cell types (**Figure 3-4**), further supporting EMT in cells after loss of p63 expression.

EMT is a process by which epithelial cells lose the cell-to-cell contact adhesion and associated protein expression and exhibit mesenchymal phenotype, including stress fiber formation and migration (Xu *et al.,* 2009). As additional evidence of EMT, the NHEK/Si-p63 cells demonstrated stress fiber formation with organized F-actin (**Figure 3-3D**). We also performed fluorescence microscopy to determine changes in the EMT marker expression upon p63 knockdown in NHEK. NHEK/Si-p63 cells showed loss of p63 and GRHL2 expression, reduced expression of E-Cad and β-catenin, and enhanced expression of ZEB1 and FN (**Figure 3-3E**). We used NHEK treated with 5 ng/ml TGF-β for 10 days as a positive control for EMT, which similarly showed reduced GRHL2, p63, K14 and β-catenin expression and enhanced FN expression by immunofluorescence staining (**Figure 3-5**). Collectively, these data indicate that knockdown of all p63 isoforms in NHEK led to EMT.

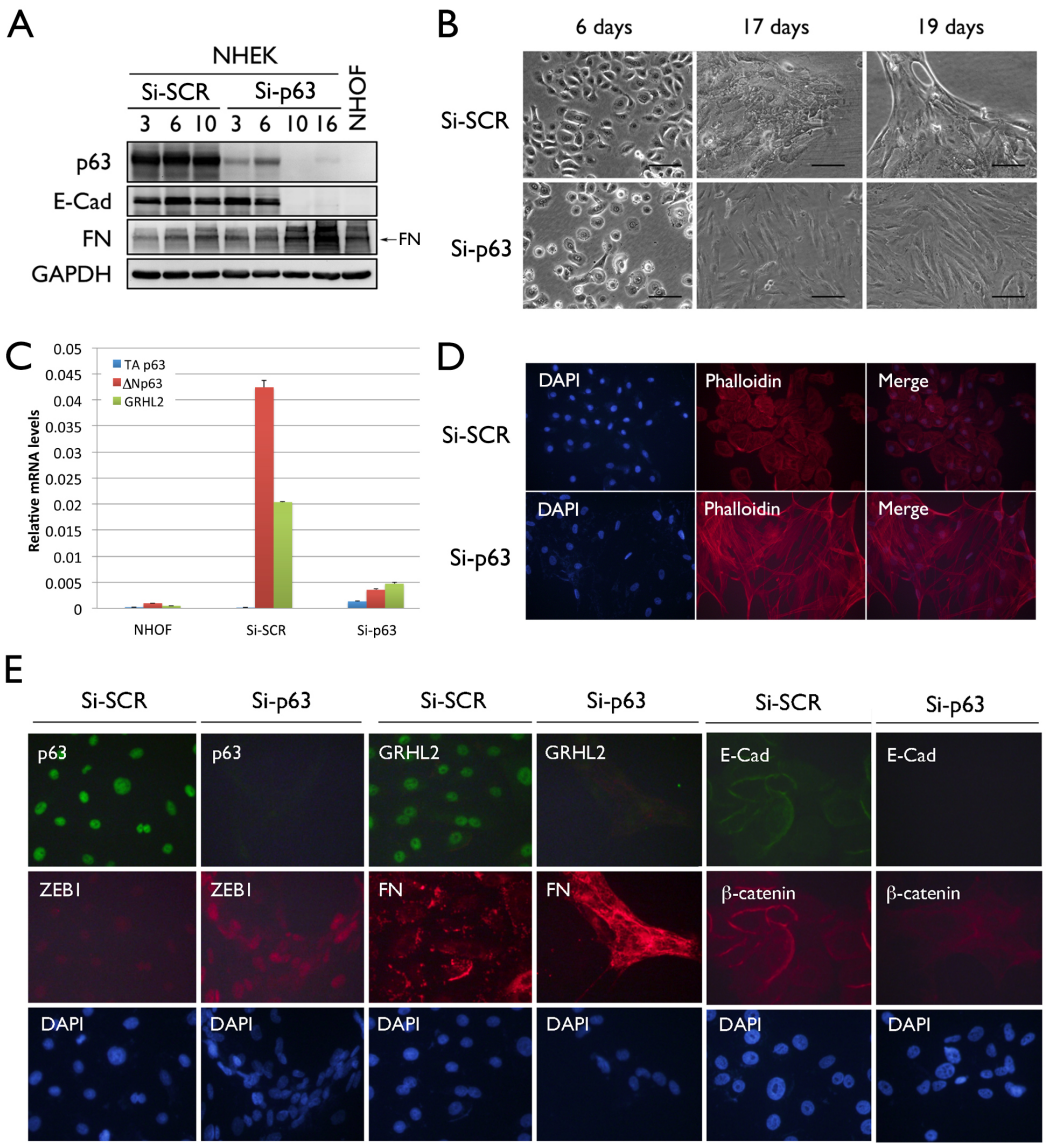

Figure 3-3. Knockdown of p63 in NHEK by transient transfection with p63 si-RNA (Si-p63) results in EMT phenotype.

(**A**) Western blotting was performed using whole cell lysates of NHEK transiently transfected using scramble siRNA (Si-SCR) and NHEK transiently transfected using siRNA targeting p63 (Si-p63) to confirm loss of p63 and E-Cad protein expression, and enhanced FN expression (arrow) consistent with EMT. NHOF was used as a positive control for mesenchymal phenotype. GAPDH was used as a loading control. (**B**) Morphological changes were observed in Si-SCR and Si-p63 transfected NHEK to determine onset of EMT phenotype. (**C**) Relative mRNA expression of TAp63, Δ Np63, and GRHL2 was assessed in NHOF, and NHEK transiently transfected using Si-SCR or Si-p63 by qRT-PCR. (**D**) Stress fiber formation in NHEK/Si-SCR and NHEK/Si-p63 was determined by F-actin staining using Alexa Fluor 594 Phalloidin. (**E**) Changes in p63, GRHL2, ZEB1, FN, E-Cad and β-catenin expression were determined in NHEK/Si-SCR and NHEK/Si-p63 by immunoflourescent staining.

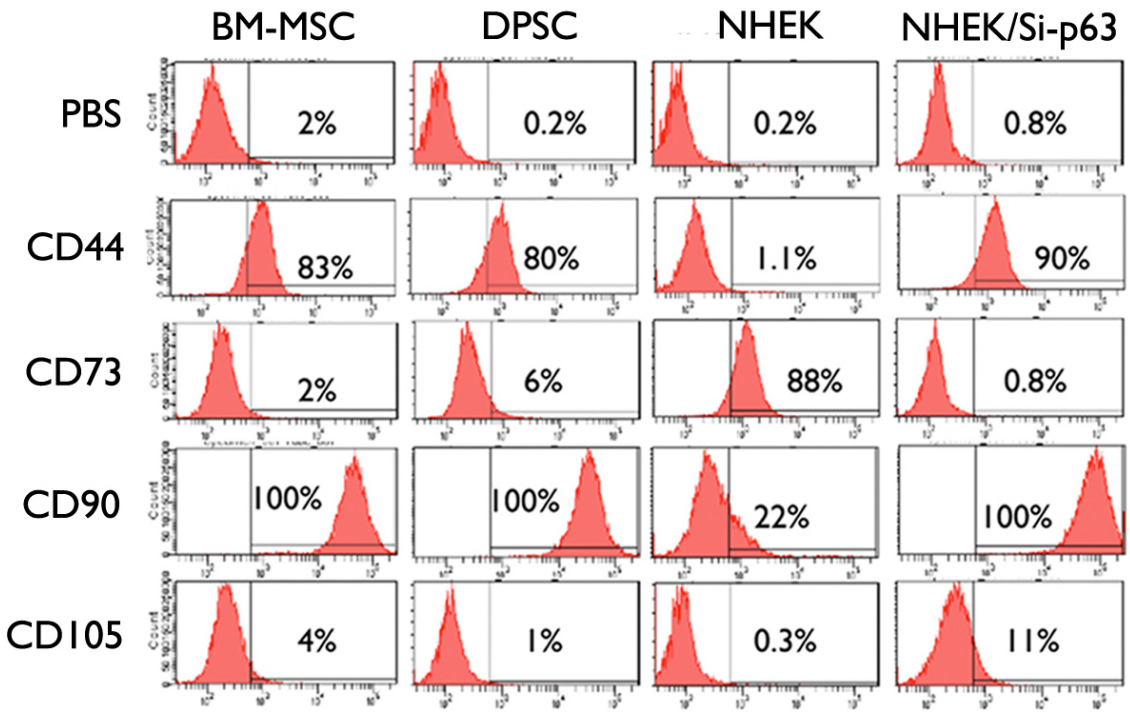

Figure 3-4. Modulation of p63 results in acquisition of stem-like molecular profile in NHEK.

Flow cytometry was performed to assess change in expression of stem cell-associated cell surface markers CD44, CD73, CD90, and CD105 in Parental NHEK, early and late passage Si-p63 (PD 42 and PD 59, respectively). BM-MSC and DPSC were used as positive controls.

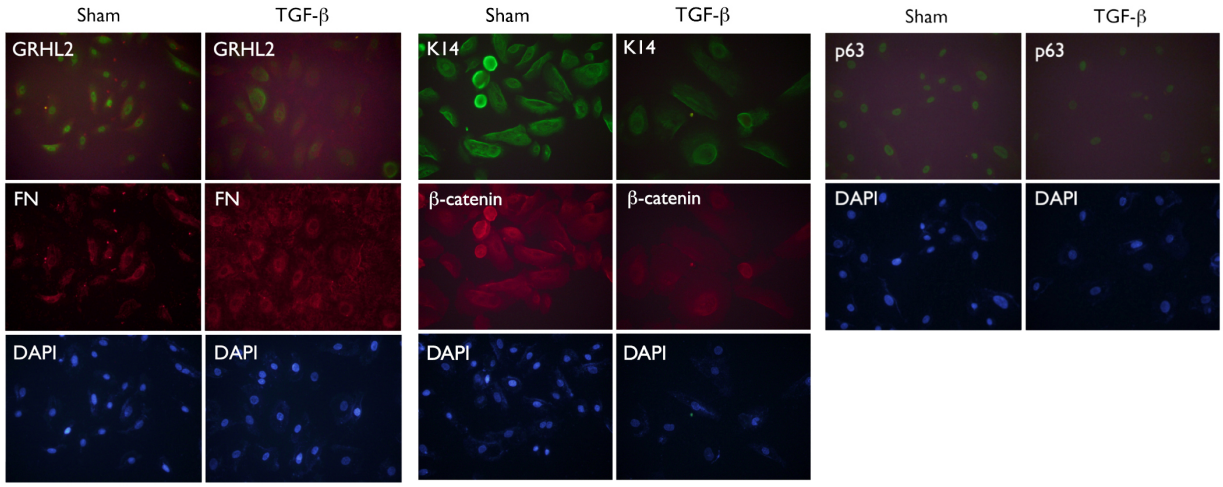

Figure 3-5. TGF-β induces EMT phenotype in NHEK.

NHEK were cultured in 5 ng/mL TGF-β for 10 days and expression of GRHL2, p63, FN, K14, and β-catenin were assessed by immunofluorescent staining. Cells were counterstained using DAPI.

3.3 Knockdown of p63 in NHEK results in loss of GRHL2 and miR-200 family gene expression

Having demonstrated that p63 modulation regulates EMT in NHEK, we sought to understand the mechanisms underlying the p63-associated EMT. In both NHEK/ΔNp63α and NHEK/Si-p63 cells, EMT occurred with enhanced expression of ZEB1 and N-Cad, which are linked with mesenchymal and stem characteristics (Gandarillas & Watt, 1997) (**Figure 3-6A**). We also found that both NHEK/ΔNp63α and NHEK/Si-p63 exhibiting EMT phenotype lost GRHL2 and E-Cad expression. Since GRHL2 is a direct upstream regulator of E-Cad (Varma *et al.,* 2012), our data suggest that p63 modulation could lead to EMT through loss of GRHL2.

Recent studies showed that GRHL2 suppressed EMT by upregulating miR-200 family genes (Cieply *et al*., 2012), which then downregulate ZEB1 (Korpal *et al.,* 2008). In the current study, acquisition of EMT phenotype in NHEK/ΔNp63α and NHEK/Si-p63 resulted in strong downregulation of miR-200a, miR-200b, miR-200c, miR-141, and miR-429 microRNA expression (**Figure 3-6B**). To test whether p63 directly binds to and regulates the gene expression of miR-200 family genes, we performed ChIP assay; NHEK/ Δ Np63 α and NHEK/Si-p63 with EMT phenotype showed loss of p63 enrichment on the promoter regions of the miR-200a, miR-200b, miR-200c, and miR-429 loci, compared to those of parental NHEK (**Figure 3-6C**). No change in p63 enrichment on miR-141 was observed between NHOF, parental NHEK, and NHEK/ Δ Np63 α and NHEK/Si-p63. These data suggest that p63 may regulate the epithelial phenotype in keratinocytes by direct regulation of GRHL2 and miR-200 family genes, although miR-141 may be bound and regulated by other factors downstream of p63.

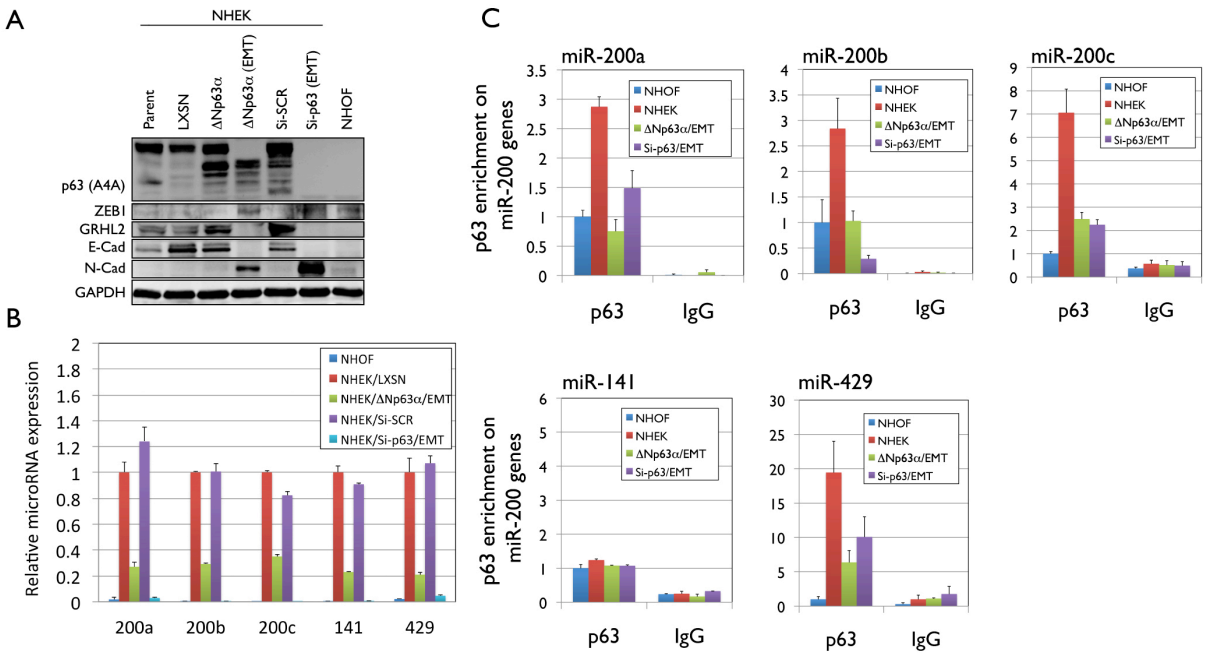

Figure 3-6. Modulation of p63 results in the loss of GRHL2 and miR-200 family expression.

(**A**) NHEK ectopically expressing ΔNp63α and transiently transfected with p63 siRNA were harvested before and after the onset of EMT. Non-transduced/transfected NHEK were used as an epithelial cell control, and NHOF were used as a mesenchyme control. Whole cell lysates were collected, and Western blot was performed for p63, ZEB1, GRHL2, E-Cad, and N-Cad. GAPDH was used as a loading control. (**B**) Change in expression of miR-200a, miR-200b, miR-200c, miR-141, and miR-429 was assessed by qRT-PCR using QuantiMir cDNA. (**C**) ChIP assay and ChIP-qPCR was performed to examine binding of p63 to the miR-200a, miR-200b, miR-200c, miR-141, and miR-429 promoter regions in NHOF, parental NHEK, NHEK/ΔNp63α and NHEK/Si-p63 cells showing EMT phenotype.

3.4 Modulation of GRHL2 alters p63 expression and EMT induction

In order to investigate the regulatory relationship between p63 and GRHL2 in mediating EMT, we induced EMT in SCC4 and HaCaT epithelial cell lines by exposure to TGF-β. In time-dependent manner after TGF-β treatment, protein expression of p63 and GRHL2 were reduced and the expression of FN, N-Cad, ZEB-1, and Snail were enhanced in SCC4 compared to the untreated cells (**Figure 3-7A**). Similarly, HaCaT cells showed reduced expression of GRHL2, p63, and E-Cad and enhanced expression of FN and ZEB-1 upon TGF-β treatment in time-dependent manner (**Figure 3-7B**). These data further confirm the regulatory relationship between p63 and GRHL2 in EMT.

Since GRHL2 is a transcription regulator for diverse gene targets, including those in the epidermal differentiation complex (EDC) (Chen *et al.,* 2012), we tested whether p63 itself would be under the regulation of GRHL2. GRHL2 was ectopically expressed in NHOF and NHOK by using retroviral vectors. Overexpression of GRHL2 resulted in a weak but notable upregulation of p63 and E-Cad in NHOF and very strong upregulation in NHOK (**Figure 3-7C**). Also, GRHL2 overexpression in SCC9, which lack endogenous GRHL2 gene expression, led to visible p63 band and enhanced mRNA expression. Knockdown of GRHL2 in SCC4, which express high endogenous GRHL2, almost completely abolished p63 expression (**Figure 3-7C, E**). Furthermore, *in situ* staining for GRHL2, p63, and β-catenin revealed protein expression only in SCC9 cells transduced with GRHL2, and not in the control cells (**Figure 3-7D**). Notably, there was heterogeneity in the level of p63 staining in the SCC9 cells expressing exogenous GRHL2, presumably due to the varied level of GRHL2 expression in cells.

Because our prior data indicated that p63 was necessary for GRHL2 expression (**Figure 3-3C**), the above data indicate reciprocity in the regulation between p63 and GRHL2 in

determining the epithelial phenotype. We explored this possibility by performing a Dual-Luciferase reporter assay. Knockdown of GRHL2 in SCC4 cells resulted in diminished p63 promoter activity, whereas GRHL2 overexpression in SCC9 cells resulted in enhanced p63 promoter activity (**Figure 3-7F)**. Interestingly, knockdown of p63 in SCC4 cells also led to a notable reduction of GRHL2 promoter activity. Therefore, GRHL2 and p63 mutually regulate their promoter activity through a reciprocal feedback loop.

To examine whether GRHL2 directly binds to the promoter region of p63, ChIP assay was performed with SCC4 and NHEK cells. In both cell types, GRHL2 pull-down co-immunoprecipitated the p63 promoter fragment near the TSS. Also, GRHL2 enrichment on the p63 promoter was altered according to the level of GRHL2 protein, i.e., GRHL2 knockdown in SCC4 or overexpression in NHEK (**Figure 3-8A, B**). As positive control, we included GRHL2 binding to the promoter region of the hTERT gene, which is a known transcriptional target of GRHL2 (Kang *et al.,* 2009). ChIP revealed concordant GRHL2 binding signal to the hTERT promoter according to the GRHL2 protein level (**Figure 3-8C**). ChIP-qPCR quantitatively showed the altered GRHL2 binding to the p63 promoter in concordance to the GRHL2 protein levels in SCC4 and NHEK (**Figure 3-8D,E**). Furthermore, ChIP-qPCR analysis revealed reduced enrichment of trimethylated histone 3 at lysine 4 (H3K4Me3) indicative of active chromatin on the p63 promoter when GRHL2 was knocked down in SCC4 (**Figure 3-8F**), in keeping with the loss of p63 expression in SCC4 with GRHL2 silencing. On the contrary, the repressive mark (H3K27Me3) was slightly elevated with GRHL2 knockdown. Since p63 modulation showed regulatory effects on GRHL2 expression, these data indicate a reciprocal regulation between GRHL2 and p63 to establish the epithelial phenotype.

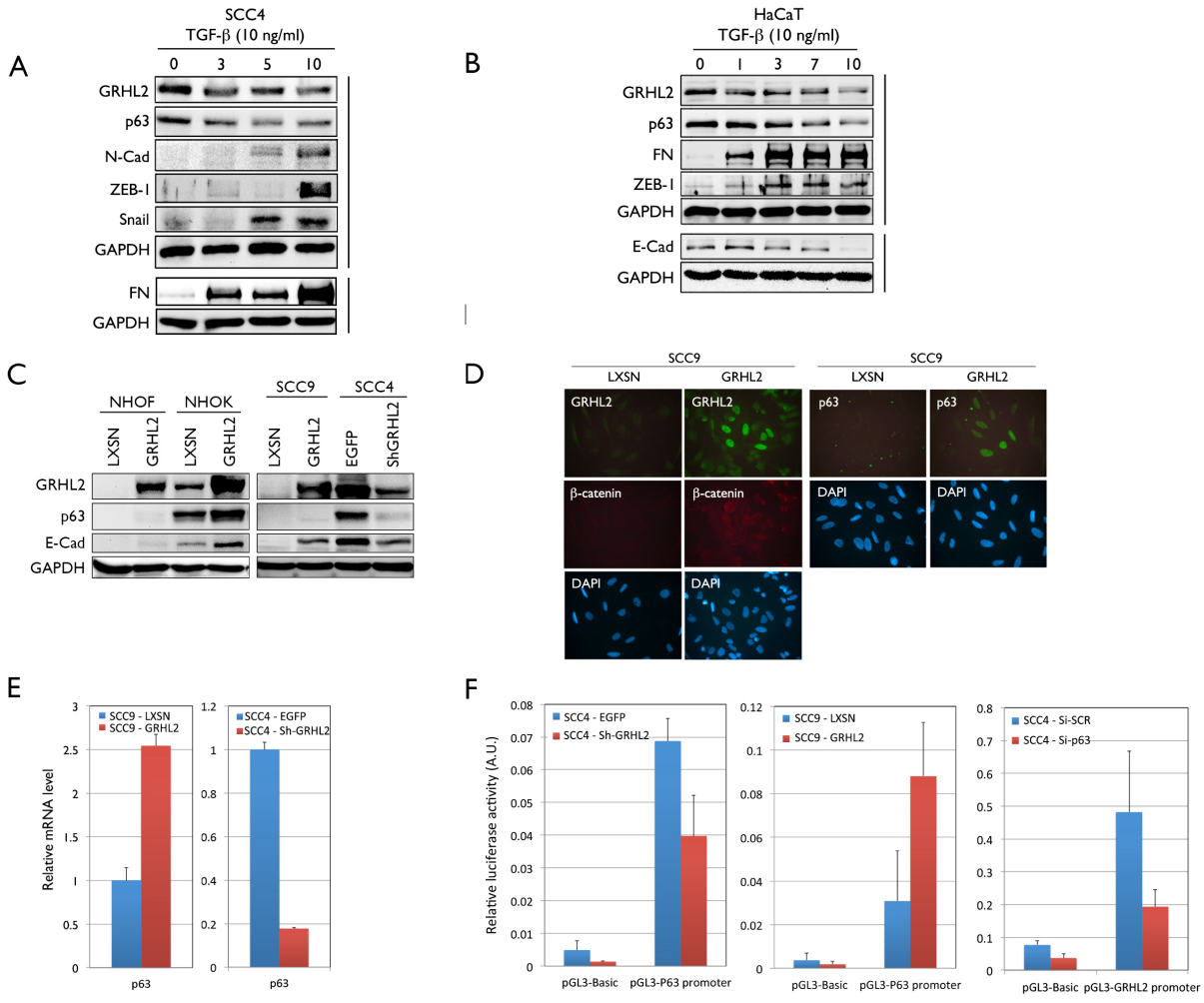

Figure 3-7. Modulation of GRHL2 alters p63 expression and EMT phenotype in human keratinocytes and epithelial cancer cell lines.

(**A**) SCC4 cells were treated with 10 ng/ml TGF-β for 0, 3, 5, and 10 days and harvested. Whole cell lysates were collected, and Western blotting was performed for p63, GRHL2, FN, N-Cad, ZEB1, and Snail. GAPDH was used as a loading control. (**B**) HaCaT cells were treated with 10 ng/ml TGF-β for 0, 1, 3, 7, and 10 days and harvested. Whole cell lysates were collected, and Western blotting was performed for GRHL2, p63, FN, ZEB-1, and E-Cad. GAPDH was used as a loading control. (**C**) GRHL2 was overexpressed in NHOF, NHOK, and SCC9, and knocked down in SCC4 cells using shRNA. Whole cell lysates were collected, and Western blot was performed for GRHL2, p63, and E-Cad. GAPDH was used as a loading control. (**D**) Change in p63, GRHL2, and β-catenin expression was determined in SCC9 overexpressing GRHL2 by immunofluorescence staining. (**E**) Change in mRNA expression of p63 was assessed in SCC9 overexpressing GRHL2 and SCC4 after GRHL2 knockdown by qRT-PCR. (**F**) GRHL2 and p63 were independently knocked down in SCC4 and GRHL2 was overexpressed in SCC9, and dual luciferase reporter assay was performed to assess the promoter activity.

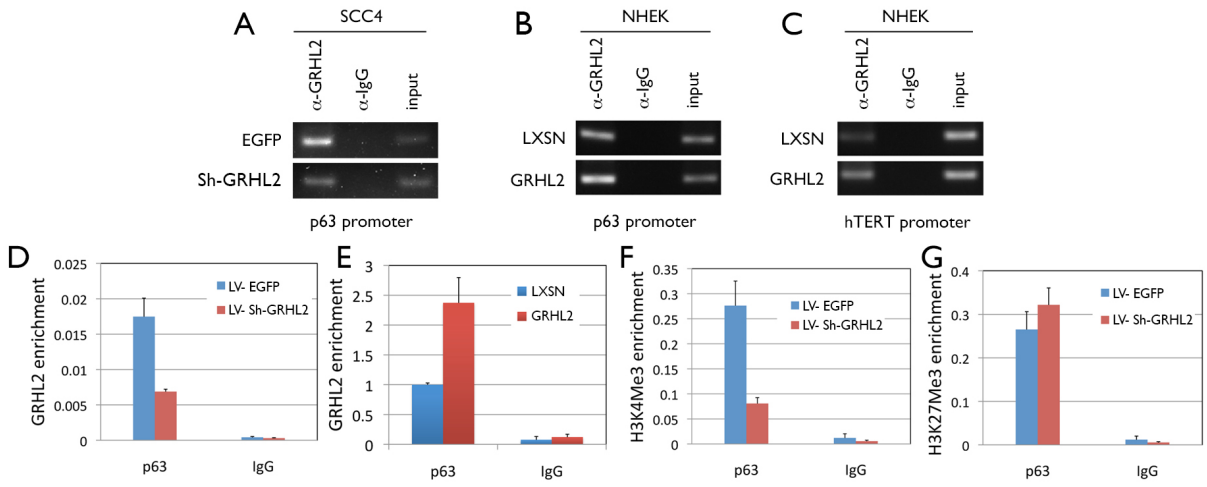

Figure 3-8. GRHL2 directly binds to and activates p63 promoter in human keratinocytes and epithelial cancer cell lines.

(**A**) ChIP assay was performed to examine binding of GRHL2 to p63 promoter in SCC4 infected with Sh-GRHL2 and (**B**) in NHEK overexpressing GRHL2. (**C**) ChIP assay was performed to examine binding of GRHL2 to the hTERT promoter in NHEK with or without GRHL2 overexpression. Pull down using α-IgG was used as a negative control. (**D**) ChIP-qPCR was performed to quantify enrichment of GRHL2 on the p63 promoter in SCC4 with GRHL2 knockdown and (**E**) in NHEK overexpressing GRHL2. (**F**) Enrichment of H3K4Me3 and (**G**) H3K27Me3 on the p63 promoter in SCC4 with GRHL2 knockdown was also assessed by ChIP-qPCR.

3.5 GRHL2 is necessary for epithelial barrier integrity

Transforming growth factor beta (TGF-β) is known to initiate EMT in epithelial cells, and its expression is upregulated in these cells in response to inflammation or injury of epithelial tissues in the human oral cavity (Steinsvoll *et al.*, 1999; Gurkan *et al.,* 2006; Xu *et al*., 2009; Mize *et al*., 2015). We demonstrated that GRHL2 expression is downregulated in NKH cultured with TGF-β, and that knockdown of GRHL2 leads to downregulation of p63, loss of E-Cadherin and cell-cell adhesion, and facilitation of EMT (**Figure 3-7C-F**). In order to assess the functional role of GRHL2 in maintaining epithelial barrier function, we generated GRHL2 conditional knockout (KO) mice. We assessed tissue specificity of GRHL2 knockout by collecting tissue from skin, tongue, gingiva, stomach, and small intestine and evaluated GRHL2 expression by qRT-PCR. We found that GRHL2 expression was downregulated in skin, tongue, and gingiva, but not significantly in stomach and small intestine in GRHL2 KO mice (**Figure 3-9A**). We examined the effect of GRHL2 knockout on the epithelial barrier in oral tissues by exposing wildtype (Wt) and GRHL2 KO mice to to *P.g.* bacteria by oral inoculation or ligature placement around 2nd molars. We found that tongues of GRHL2 KO mice showed significant toluidine blue staining and altered epithelial barrier phenotype than Wt mice (**Figure 3-9B**). GRHL2 KO mice also showed enhanced endogenous *P.g.* bacterial load in blood in the absence of oral *P.g.* inoculation (**Figure 3-9C**) or ligature placement (**Figure 3-9D**). Upon *P.g.* inoculation or ligature placement, GRHL2 KO mice showed significantly higher *P.g.* in the blood compared to Wt mice (**Figure 3-9C,D).** These results indicate that GRHL2 plays a critical role in the maintenance of epithelial plasticity and barrier function, and that loss of GRHL2 may result in increased *P.g.* bacterial load in the bloodstream.

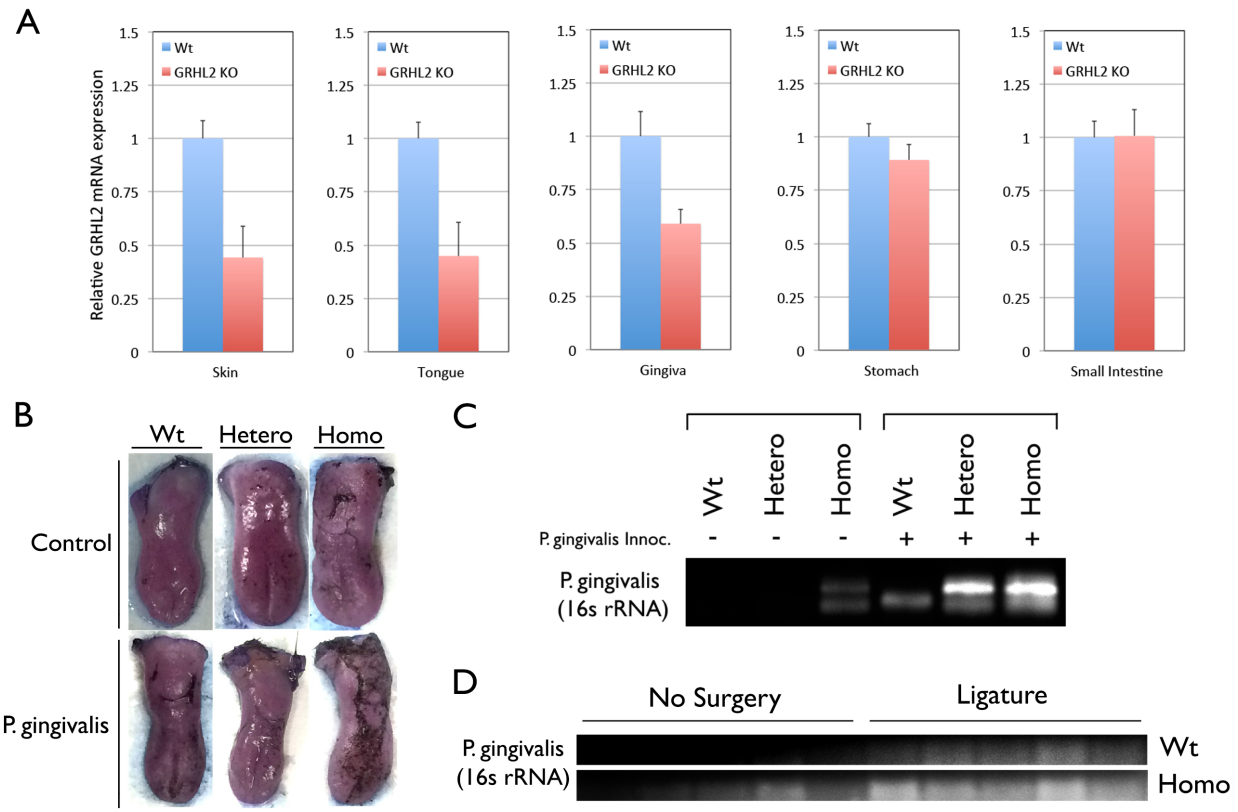

Figure 3-9. GRHL2 knockout results in altered epithelial barrier phenotype and enhanced *P.g.* bacterial load in the bloodstream.

(**A**) Tissue from skin, tongue, gingiva, stomach, and small intestine of Wt and GRHL2 conditional knockout (KO) mice were collected and tissue specific knockout of GRHL2 was assessed by qRT-PCR. (**B**) Wt and KO mice were administered *P.g.* bacteria by oral inoculation every 48 hours for a duration of 6 weeks prior to being sacrificed. Tongues of harvested mice were collected and stained with 1% toluidine blue to assess epithelial barrier damage. (**C**) Whole blood was collected by cardiac puncture from Wt and KO mice administered *P.g.* bacteria by oral inoculation, or (**D**) mice with ligatures placed around second molars for a duration of 3 weeks. Genomic DNA was extracted, and semi-quantitative PCR was performed to assess bacterial load of P.g. in whole blood.

3.6 Discussion

Our laboratory previously showed that overexpression of the ΔNp63α isoform conferred EMT phenotype in NHEK in TGF-β dependent manner (Oh *et al.,* 2011). The current study further showed that ΔNp63β or ΔNp63γ do not fully transform NHEK to mesenchymal state, although there was morphological transition by ΔNp63β expression in NHEK. One of the speculations from our prior study was that the ΔNp63α isoforms abolished the expression of the high molecular weight (~75 kDa; band marked with an asterisk in **Figures 3-1B, C**) p63 protein with unknown identity, which invariably occurred during EMT (Oh *et al.,* 2011). As an alternative approach, in the current study we knocked down all p63 isoforms using pan-p63 siRNA. This transient knockdown of p63 isoforms led to EMT phenotype after 10 days post-transfection. Acquisition of the EMT phenotype in the NHEK/ΔNp63α and NHEK/Si-p63 cells was assessed by altered morphology and expression of the EMT markers, *e.g.* loss of E-Cad, K14, β-catenin expression and enhanced FN, and ZEB1 expression. Whereas NHEK/ΔNp63α required serial subculture and several passages to induce molecular and phenotypic EMT-associated changes, NHEK/Si-p63 acquired these altered phenotype quite readily within 10 days after the gene knockdown (**Figures 3-1C and 3-3A**).

In our previous paper, we showed that the NHEK/ΔNp63α cells with EMT phenotype acquired stemness characteristics and expressed high levels of the reprogramming factors, *e.g.,* Lin28 and Nanog (Oh *et al.,* 2011). Likewise, the NHEK/Si-p63 showed stem characteristics, *e.g.*, transdifferentiation ability into osteogenic and adipocytic lineages (data not shown). We also found that NHEK/Si-p63 expressed cell surface markers CD44, CD73, CD90, and CD105, which are characteristically expressed in mesenchymal stem cell (MSC) population (**Figure 3-4**) (Pittenger *et al.,* 1999; Dominici *et al.,* 2006). Therefore, our studies demonstrate that EMT in

NHEK is associated with acquisition of stem characteristics, whether it is triggered by overexpression of ΔNp63α or knockdown of all p63 isoforms. We coined the term "induced mesenchymal stem cells" (iMSCs) to describe these epithelial cells that have acquired multipotency through EMT to distinguish them from endogenous MSCs or induced pluripotent stem cells (iPSCs), which acquire embryonic stem cell characteristics after stable infection of the reprogramming factors (Takahashi & Yamanaka, 2006). These iMSCs may be derived from cultured primary epithelial cells from skin via transient transfection of p63 siRNA, and may have tissue-engineering potential for cases requiring autologous cell transplantation approach.

The current study reveals GRHL2 as the regulatory partner of p63, which is critical for epithelial cell identity and embryonic morphogenesis (Barbareschi *et al.,* 2001; Laurikkala *et al.,* 2006). GRHL2 is a transcription factor responsible for regulating epithelial proliferation (Chen *et al.,* 2012), and is known to play an important role in inducing many epithelial cancers and has been found to regulate EMT (Xiang *et al.,* 2012; Kang *et al.,* 2009). The current study showed that EMT in NHEK/ΔNp63α and NHEK/Si-p63 accompanied downregulation of GRHL2 and E-Cad, and upregulation of ZEB1 and N-Cad expression (**Figure 3-6A**). GRHL2 has also been shown to suppress EMT in breast cancer cells by suppressing ZEB1 signaling, and a reciprocal feedback loop has been found between GRHL2 and ZEB1 in regulating EMT (Cieply *et al.,* 2012; Cieply *et al.,* 2013). Furthermore, GRHL2 has been found to inhibit ZEB1 expression and EMT by activating miR-200b and miR-200c (Cieply *et al.,* 2013). We found that NHEK/ΔNp63α and NHEK/Si-p63 resulted in downregulation of miR-200 family gene expression, including miR-200a, miR-200b, miR-200c, miR-141, and miR-429 (**Figure 3-6B**), and that p63 binds directly to the promoter of miR-200 family genes (**Figure 3-6C**). It is important to note that p63 did not bind to the promoter of miR-141, and that miR-141 may be

bound and regulated by a downstream target of p63. Thus, p63 modulation may alter miR-200 family gene activation and induce EMT by facilitating upregulation of ZEB1 expression. These findings indicate a novel role for p63 in GRHL2-mediated regulation of EMT. In addition, GRHL2 was found to be required and necessary for the expression of p63. In NHOF, NHOK and SCC9 cells, GRHL2 overexpression led to notable increase in the p63 expression level. Also, GRHL2 knockdown in SCC4 abolished the expression of p63, suggesting p63 regulation by GRHL2. This was confirmed by ChIP analyses showing direct GRHL2 binding on the p63 gene promoter and concordant alteration of the histone mark at the gene promoter. We also demonstrated through dual luciferase reporter assay that GRHL2 is required for p63 promoter activity, and *vice versa*. Hence, we propose a model in which p63 and GRHL2 regulate each other's expression, through direct promoter binding, and this reciprocal regulatory loop between GRHL2 and p63 is critical for maintaining the epithelial phenotype through transcriptional regulation of their target genes (**Figure 3-10**).

The current study also demonstrated that TGF-β-dependent EMT leads to both downregulation of GRHL2 and p63 expression. TGF-β initiates EMT in human keratinocytes to facilitate wound healing (Xu *et al*., 2009), and is also highly expressed when epithelial tissues encounter injury or inflammation in the oral cavity (Jagels & Hugli, 2000; Nozawa *et al.,* 2009; Jun & Lau, 2011). The current study showed that knockout of GRHL2 was sufficient to alter epithelial barrier phenotype, and that this altered phenotype led to increased *Porphyromonas gingivalis* (*P.g.*) bacterial load in the bloodstream in mice (**Figure 3-9B,C,D**). These findings suggest that during infection in epithelial tissue, TGF-β-mediated downregulation of GRHL2 in epithelial cells results in phenotypic changes that alter the epithelial barrier and facilitate persistent infection. Collectively, our findings provide a framework to study the molecular

mechanisms that regulate epithelial plasticity, a key player in physiologic and disease processes, including cancer metastasis, epithelial wound healing, infection, and tissue injury response to environmental insults.

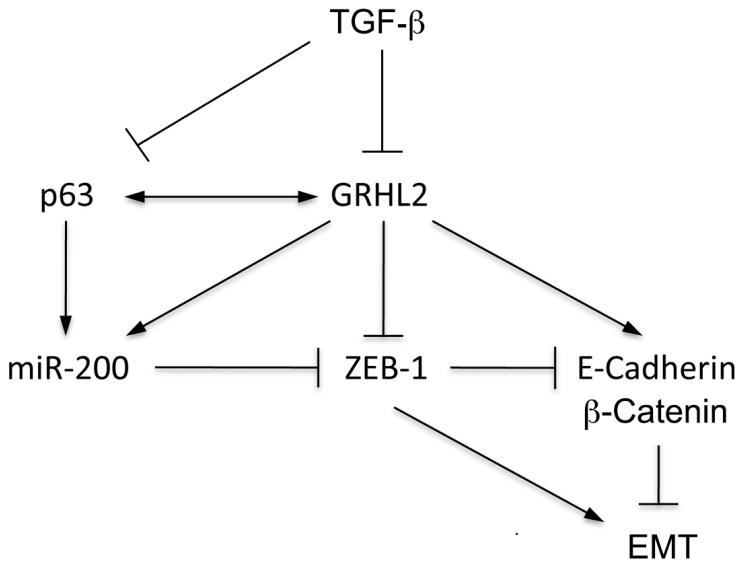

Figure 3-10. Role of p63 and GRHL2 in epithelial plasticity.

Current data establish a reciprocal regulation between p63 and GRHL2 through direct promoter binding. GRHL2 and p63 expression is negatively regulated by TGF-β. Both p63 and GRHL2 are required for the expression of miR-200 family genes, which then suppress EMT through negative regulation of ZEB1. In this model, GRHL2 appears to be intricately involved with many different factors that determine epithelial phenotype.

4 EPIGENETIC REGULATION OF INFLAMMATORY RESPONSE BY KDM3C

4.1 Histone lysine demethylase KDM3C is induced by P.g. LPS

We previously demonstrated that knockout of GRHL2 lead to altered epithelial barrier phenotype and increased *P.g.* bacterial load in the bloodstream in mice (**Figure 3-9**). *P.g.* is a gram-negative bacteria known to secrete lipoglycan endotoxins known as lipopolysaccharides (*P.g.* LPS) that activate pro-inflammatory cytokine induction and secretion (Kabanov & Prokhorenko, 2010). An association between dynamic demethylation of histone marks and cytokine transcriptional activation has been previously made (Saccani & Natoli, 2002), however the role of histone lysine demethylases in epigenetic regulation of inflammatory response is unknown. In order to investigate the effect of *P.g.* LPS on differential expression of histone lysine demethylases, human DPSCs and THP-1 cells were cultured with *P.g.* LPS for 24 hours. We performed qRT-PCR screening to assess differential mRNA expression of several KDMs, which showed distinct KDM expression profiles for both DPSC and THP-1 cells. *P.g.* LPS culture resulted in upregulation of KDM2B, KDM3A, KDM3B, and KDM5A expression in DPSC and KDM4D and KDM6A expression in THP-1 cells. Among the KDMs screened, KDM3C was shown to be most strongly induced in both cell types (**Figure 4-1A,C**). Further, *P.g.* LPS exposure also resulted in time-dependent induction of KDM3C protein expression in both DPSC and THP-1, and KDM3C expression pattern was consistent with that of IL-6 protein expression (**Figure 4-1B,D**). Although KDM3C expression peaked at 1 hour and then again at 24 hours post-*P.g.* LPS exposure in DPSC, in THP-1, KDM3C expression increased steadily for 24 hours post-*P.g.* LPS exposure. Thus, additional *in vitro* experiments were performed using 24 hour culture with *P.g.* LPS.

In order to determine whether *P.g.* LPS exposure also induces KDM3C expression *in vivo,* we injected *P.g.* LPS between first and second molars in C57BL/6 mice and collected peripheral blood mononuclear cells (PBMCs) from whole blood after 24 hours (**Figure 4-1E**). These PBMCs demonstrated enhanced KDM3C and IL-6 mRNA expression when compared to the control group (**Figure 4-1F**). Collectively, these data demonstrate that *P.g.* LPS upregulates KDM3C expression *in vitro* and *in vivo*, and that KDM3C may play an important role in mediating pro-inflammatory cytokine expression.

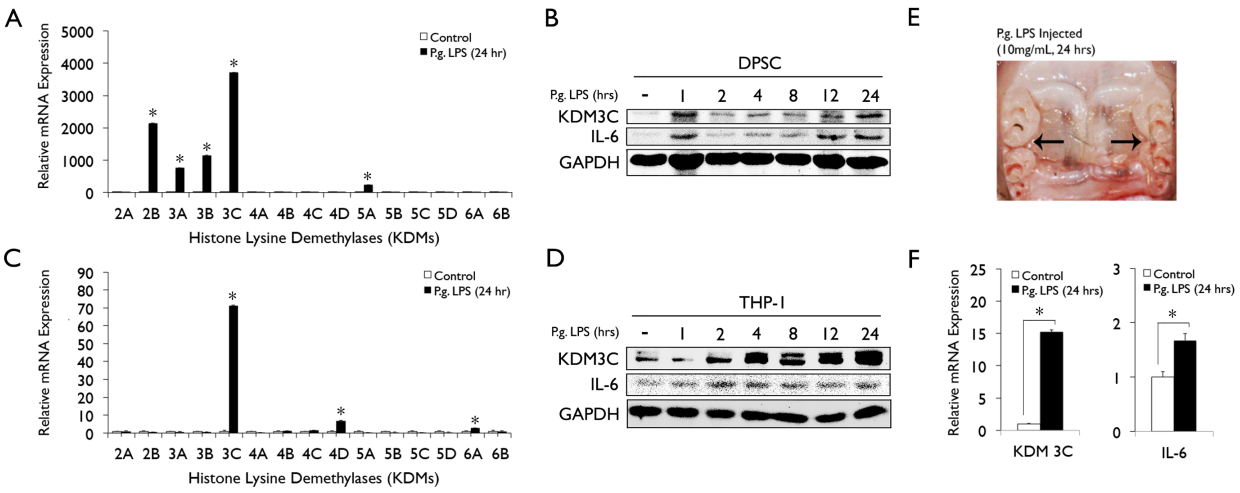

Figure 4-1. *P.g.* LPS strongly induces KDM3C expression in DPSC, THP-1 cells, and peripheral blood mononuclear cells.

(A) DPSC were exposed to 1 ug/ml *P.g.* LPS for 24 hours, harvested and screened for differential mRNA expression of KDMs by qRT-PCR. **(B)** Change in KDM3C and IL-6 protein expression upon time-dependent *P.g.* LPS exposure in DPSC was determined by Western blotting. GAPDH was used as a loading control. **(C)** THP-1 cells were also harvested and screened for differential mRNA expression of KDMs and **(D)** KDM3C protein expression. **(E)** C57BL/6 mice were injected between first and second molars with 10 mg/ml *P.g.* LPS, and **(F)** whole blood was collected by cardiac puncture 24 hours post-injection. Peripheral blood mononuclear cells (PBMCs) were isolated and change in KDM3C and IL-6 mRNA expression was assessed by qRT-PCR.

4.2 KDM3C knockdown abrogates pro-inflammatory cytokine induction by P.g. LPS

KDM3C has been shown to activate gene transcription by demethylating mono- and di-methylated H3K9 in several developmental and diseases processes (Kim *et al.,* 2010; Wang *et al.,* 2014; Sroczynska *et al.,* 2014). In order to determine whether KDM3C plays a functional role in the induction of pro-inflammatory cytokines by *P.g.* LPS, KDM3C was knocked down in DPSC by transient transfection of Si-RNA targeting KDM3C (Si-KDM3C) or scrambled sequence (Si-SCR). We successfully knocked down KDM3C in DPSC, and found that Si-KDM3C/DPSC showed suppressed induction of IL-6 mRNA and protein expression by *P.g.* LPS compared to Si-SCR/DPSC (**Figure 4-2A, B**), suggesting that KDM3C plays an important functional role in regulating IL-6 induction by *P.g.* LPS.

In order to investigate the functional role of KDM3C in pro-inflammatory cytokine induction *in vivo*, we intravenously administered *in vivo*-grade Si-KDM3C, followed by intravenous *P.g.* LPS administration in C57BL/6 mice (**Figure 4-3A)**. We found that *in vivo* knockdown of KDM3C led to suppressed induction of IL-6 mRNA by *P.g.* LPS in peripheral blood mononuclear cells **(Figure 4-3B)**. Since both bacterial endotoxins and *in vivo* Si-RNA are known to be cleared by the liver (Scott *et al.,* 2009; Shao *et al.,* 2012; Zhang *et al.,* 2014), we also assessed the impact of KDM3C knockdown on IL-6 induction by *P.g.* LPS in liver. We found that *P.g.* LPS induction of both IL-6 mRNA and protein expression was suppressed in livers of Si-KDM3C mice (**Figure 4-3C, D).** Lastly, we examined the impact KDM3C knockdown on pro-inflammatory cytokine secretion into whole blood serum by ELISA. We found that protein secretion of many distinct pro-inflammatory cytokines, including IL-6, was suppressed upon *in vivo* KDM3C knockdown **(Figure 4-3E,F,G).** Collectively, these data indicate that KDM3C

plays a functional role in *P.g.* LPS-mediated inflammatory signal transduction, and is critical for induction of many distinct pro-inflammatory cytokines.

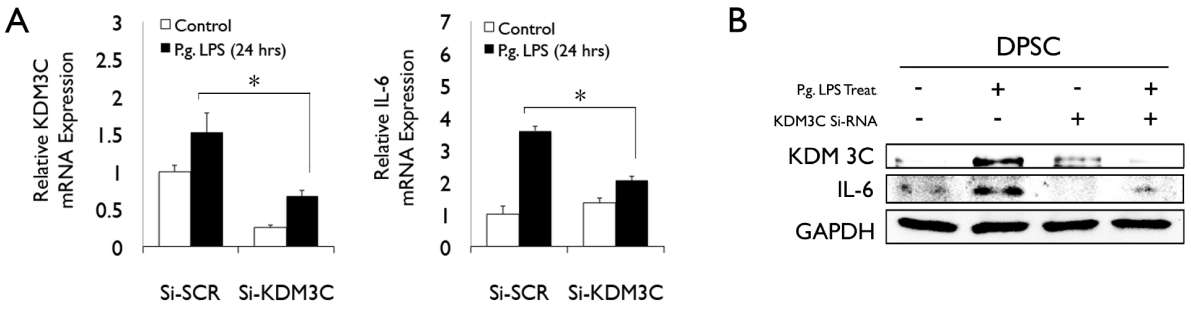

Figure 4-2. Transient knockdown of KDM3C suppresses *P.g.* LPS-dependent cytokine induction.

(A) KDM3C was knocked down by transient transfection using Si-RNA targeting KDM3C (Si-KDM3C) or scrambled sequence (Si-SCR) in DPSC, and transfected cells were cultured with *P.g.* LPS for 24 hours and harvested. mRNA expression of KDM3C and IL-6 were assessed by qRT-PCR, and **(B)** protein expression of KDM3C and IL-6 were assessed by Western blotting. GAPDH was used as a loading control.

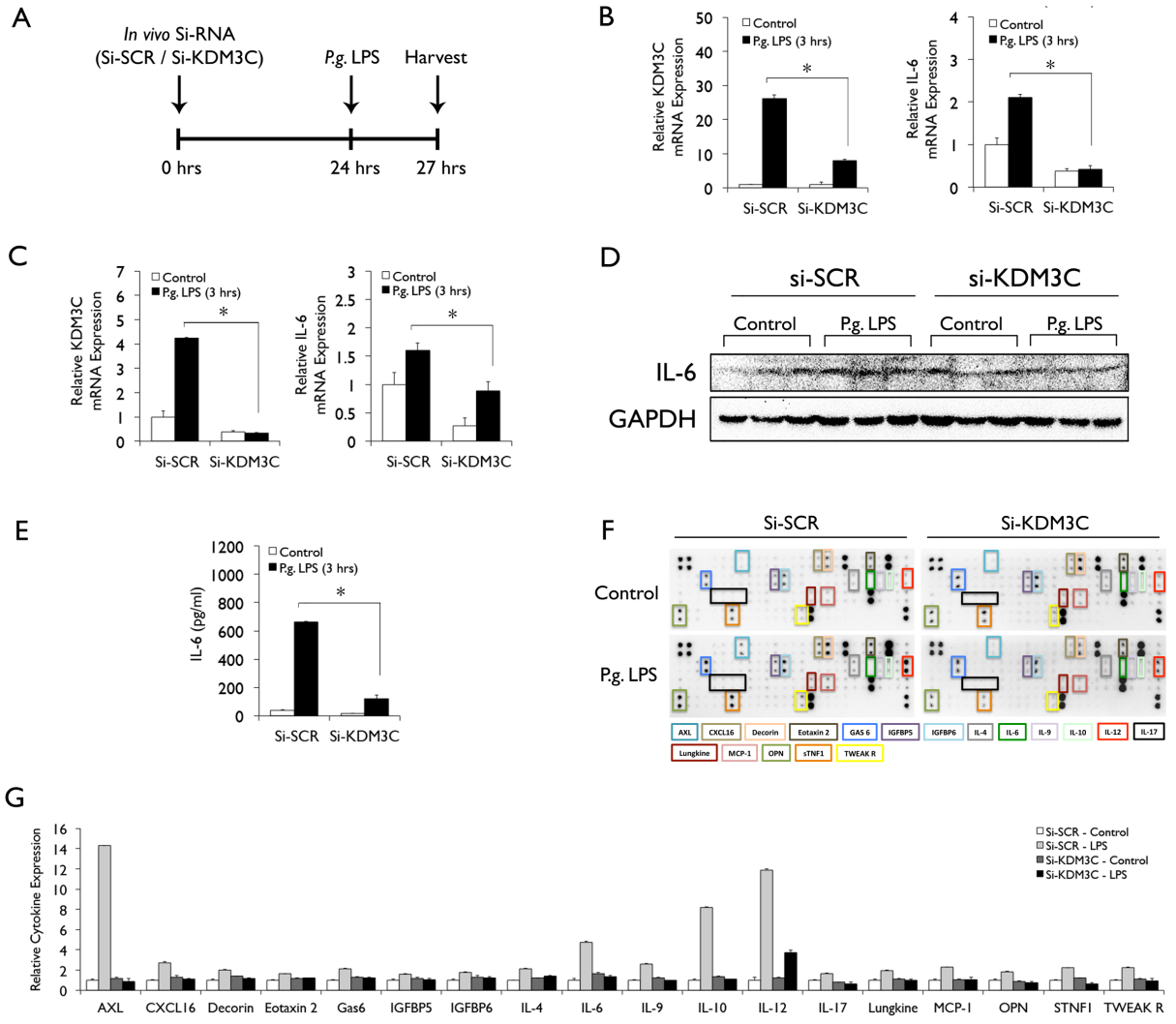

Figure 4-3. *In vivo* knockdown of KDM3C suppresses pro-inflammatory cytokine induction by *P.g.* LPS.

(A) C57BL/6 mice were intravenously injected with *in vivo* specific Si-KDM3C or Si-SCR, and 24 hours later intravenously injected with *P.g.* LPS. These mice were sacrificed 3 hours post-LPS injection, and whole blood, PBMCs, and liver tissue were collected. **(B)** Differential mRNA expression of KDM3C and IL-6 was assessed by means of qRT-PCR in PBMCs and **(C)** liver tissue of Si-SCR and Si-KDM3C mice injected with *P.g.* LPS. **(D)** Change in IL-6 protein expression in liver tissue of Si-SCR and Si-KDM3C mice was assessed by Western blotting. GAPDH was used as a loading control. **(E)** ELISA was performed to assess IL-6 secretion in whole blood serum, and **(F)** cytokine antibody array was used to assess secretion of a wide range of pro-inflammatory cytokines in whole blood serum. **(G)** Cytokine array data was quantified using ImageJ software.

4.3 *P.g.* LPS alters KDM3C & G9a binding to IL-6 promoter and H3K9me2 demethylation

Having demonstrated that KDM3C plays a functional role in regulating *P.g.* LPS-dependent inflammatory cytokine induction, we investigated whether KDM3C epigenetically regulates IL-6 by binding to the IL-6 promoter. We performed a chromatin immunoprecipitation (ChIP) assay, examining KDM3C binding to several sites, including regions both upstream and spanning the transcription start site (**Figure 4-4A).** Our data showed that in both DPSC and THP-1 cells, enrichment of KDM3C on the IL-6 promoter increased upon *P.g.* LPS exposure (**Figure 4-4B**).

KDM3C is known to demethylate histone 3 at lysine 9 (H3K9) that is mono- and di-methylated (H3K9me1, H3K9me2) (Kim *et al.,* 2010), and H3K9 is initially mono- and di-methylated by histone methyltransferase G9a, resulting in transcriptional silencing (Tachibana *et al.,* 2005; El-Gazzar *et al.,* 2008). We were interested in whether G9a was enriched on the same region of the IL-6 promoter as KDM3C, and whether G9a methylated H3K9 that would later be demethylated by KDM3C upon *P.g.* LPS exposure. We found that G9a was enriched on the IL-6 promoter at the same site as KDM3C, and that enrichment of G9a was lost upon culture with *P.g.* LPS in both DPSC and THP-1 **(Figure 4-4C**). Lastly, we examined the methylation status of H3K9 bound to the IL-6 promoter. We found that enrichment of H3K9me2 on the IL-6 promoter was lost in both DPSC and THP-1 upon exposure to *P.g.* LPS (**Figure 4-4D**). H3K9me1 enrichment was strongly enhanced in THP-1 cells, and only slightly enhanced in DPSC. Collectively, this data indicates that KDM3C and G9a regulate IL-6 expression by directly binding to and altering the methylation of H3K9, and that *P.g.* LPS exposure leads to loss of G9a and increase in KDM3C enrichment and demethylation of H3K9.

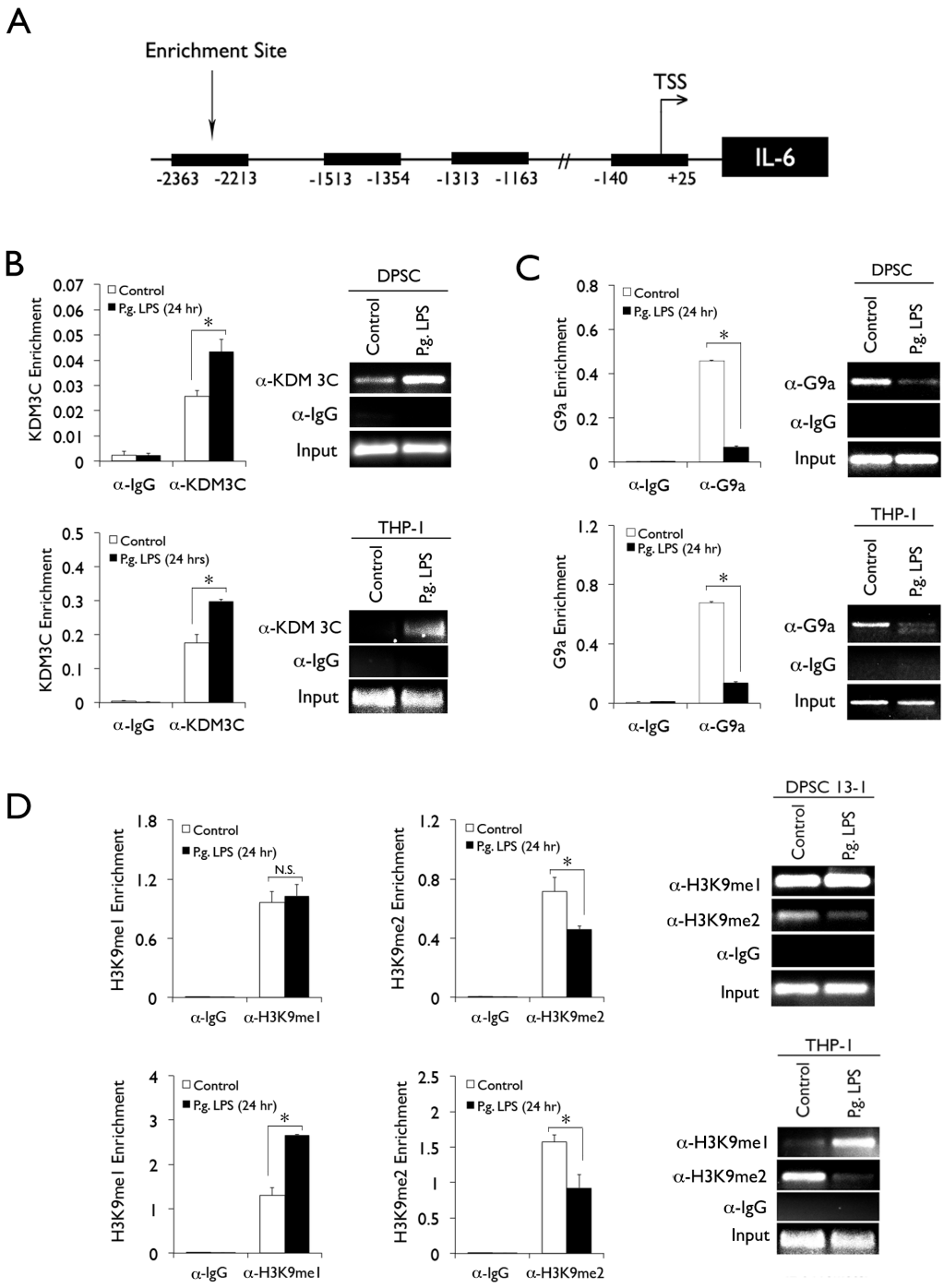

Figure 4-4. *P.g.* LPS alters KDM3C and G9a enrichment on IL-6 promoter and H3K9me2 demethylation.

(A) Chromatin immmunoprecipitation (ChIP) assay was performed to assess binding to several regions upstream and spanning the transcription start site of the IL-6 promoter. **(B)** Enrichment of KDM3C, **(C)** G9a and **(D)** H3K9me1 and H3K9me2 on the IL-6 promoter was assessed by both ChIP qPCR and conventional PCR in DPSC and THP-1 cells cultured with *P.g.* LPS for 24 hours.

4.4 Modulation of histone methyltransferase G9a alters IL-6 induction by P.g. LPS

Histone methyltransferase G9a has been shown to mono-/di-methylate H3K9 (Tachibana *et al.,* 2005; El-Gazzar *et al.,* 2008), recruiting heterochromatin protein 1 (HP1) to bind to and stabilize methylated H3K9. G9a also recruits DNA methyltransferase 3a/b (DNMT3a/b) to methylate DNA CpG islands upstream of the transcription start site (TSS) and silence gene expression (El-Gazzar *et al.,* 2008). In order to investigate the impact of *P.g.* LPS on G9a complex formation and histone methylation in DPSC and THP-1, we assessed differential protein expression of G9a, HP-1, and DNMT3a/b, as well as H3K9me1 and H3K9me2, upon *P.g.* LPS culture. We found that in both DPSC and THP-1, protein expression of G9a, HP-1, DNMT3a/b, and H3K9me2 was downregulated upon exposure to *P.g.* LPS **(Figure 4-5A, B).** Protein expression of H3K9me1 remained unchanged in DPSC, and was downregulated in THP-1 cells. Collectively, these data were consistent with our previous ChIP analysis, and indicated that in the absence of *P.g.* LPS, G9a and complex proteins HP-1 and DNMT3a/b serve to maintain H3K9 in a dimethylated state.

In order to assess whether G9a plays a functional role in the transcriptional repression of IL-6, we cultured DPSC and THP-1 cells with G9a-specific small molecule inhibitor BIX-01294 (Kubicek *et al.,* 2007; Chang *et al.,* 2009). Cells cultured with BIX-01294 showed significant increase in IL-6 secretion, comparable to that of *P.g.* LPS cultured DPSC and THP-1 **(Figure 4-5C).** We also ectopically expressed G9a in DPSC using retroviral vectors. Whereas *P.g.* LPS culture normally resulted in loss of G9a and enhanced IL-6 and TNF-α expression, overexpression of G9a suppressed IL-6 and TNF-α induction by *P.g.* LPS **(Figure 4-5D).** Collectively, this data indicates that in the absence of inflammatory stimuli, G9a silences pro-inflammatory cytokine expression by methylating H3K9me1/me2, and that modulation of G9a is sufficient to alter pro-inflammatory cytokine induction.

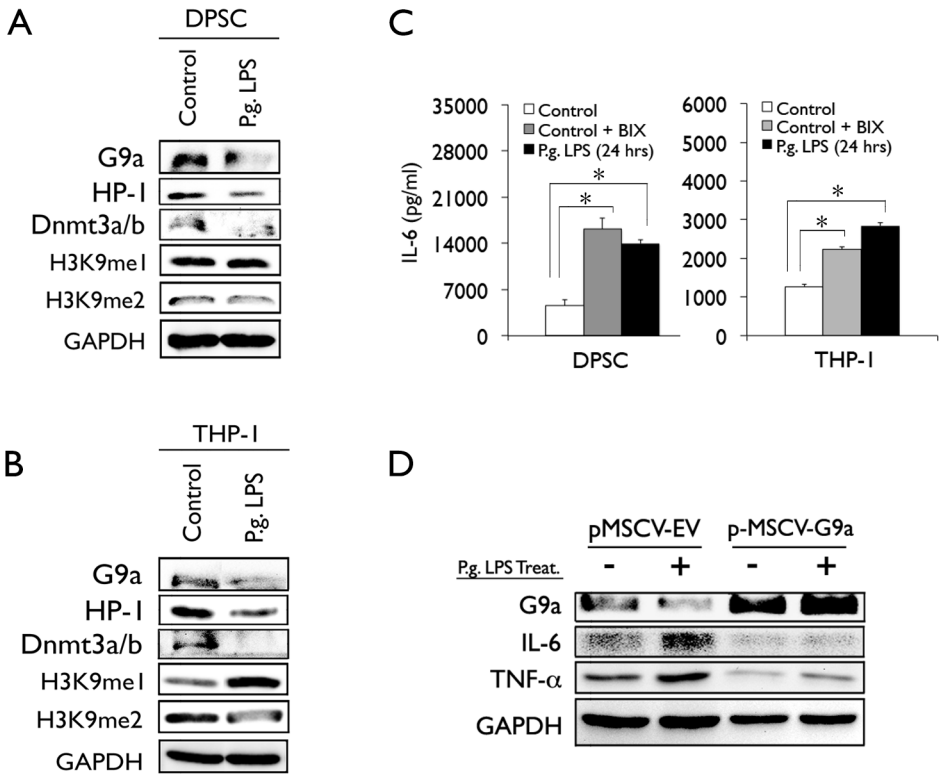

Figure 4-5. G9a modulation affects pro-inflammatory cytokine induction.

(A) Protein expression of histone methyltransferase G9a, G9a complex proteins HP-1 and DNMT3a/b, and H3K9me1/me2 were assessed by Western blotting in DPSC and **(B)** THP-1, with GAPDH being used as a loading control. **(C)** IL-6 protein secretion in untreated, BIX-01294 treated, and *P.g.* LPS treated DPSC and THP-1 was assessed by ELISA. **(D)** DPSC stably infected with pMSCV empty vector (pMSCV-EV) and pMSCV containing G9a overexpressing plasmid (pMSCV-G9a) were cultured with *P.g.* LPS, and protein expression of G9a, IL-6, and TNF-α was assessed by Western blotting. GAPDH was used as a loading control.

4.5 KDM3C epigenetically regulates several distinct pro-inflammatory signaling pathways

We previously demonstrated that KDM3C plays a functional role in pro-inflammatory cytokine induction by *P.g*. LPS. In order to determine changes in global binding sites of KDM3C between untreated and *P.g*. LPS cultured THP-1 cells, we performed chromatin immunoprecipitation followed by high throughput sequencing (ChIP-Seq). We found that KDM3C bound to 57 unique genes that belonged to signaling pathways involved in macrophage activation in THP-1 cells that were not cultured with *P.g.* LPS. In *P.g.* LPS cultured THP-1 cells, KDM3C bound to 89 unique inflammatory genes involved in several inflammatory signaling pathways, with IL-6, IL-33, MAPK14, STAT3, and PIK3R1 being involved in several of these pathways **(Figure 4-6A,B).**

We sought to validate our ChIP-Seq data by means of ChIP-qPCR using the same DNA libraries used for sequencing. We found KDM3C enrichment on the promoter regions identified by ChIP-Seq of pro-inflammatory cytokines IL-6 and IL-33 and signaling proteins MAPK14, STAT3, and PIK3R1 were upregulated upon *P.g.* LPS culture **(Figure 4-6C).** Using ingenuity pathway analysis (IPA) software, we were also able to determine the conserved DNA binding motif for KDM3C **(Figure 4-6D).** Collectively, this data indicates that KDM3C promotes macrophage activation in the absence of inflammatory stimuli and epigenetically regulates pro-inflammatory signaling and inflammatory response.

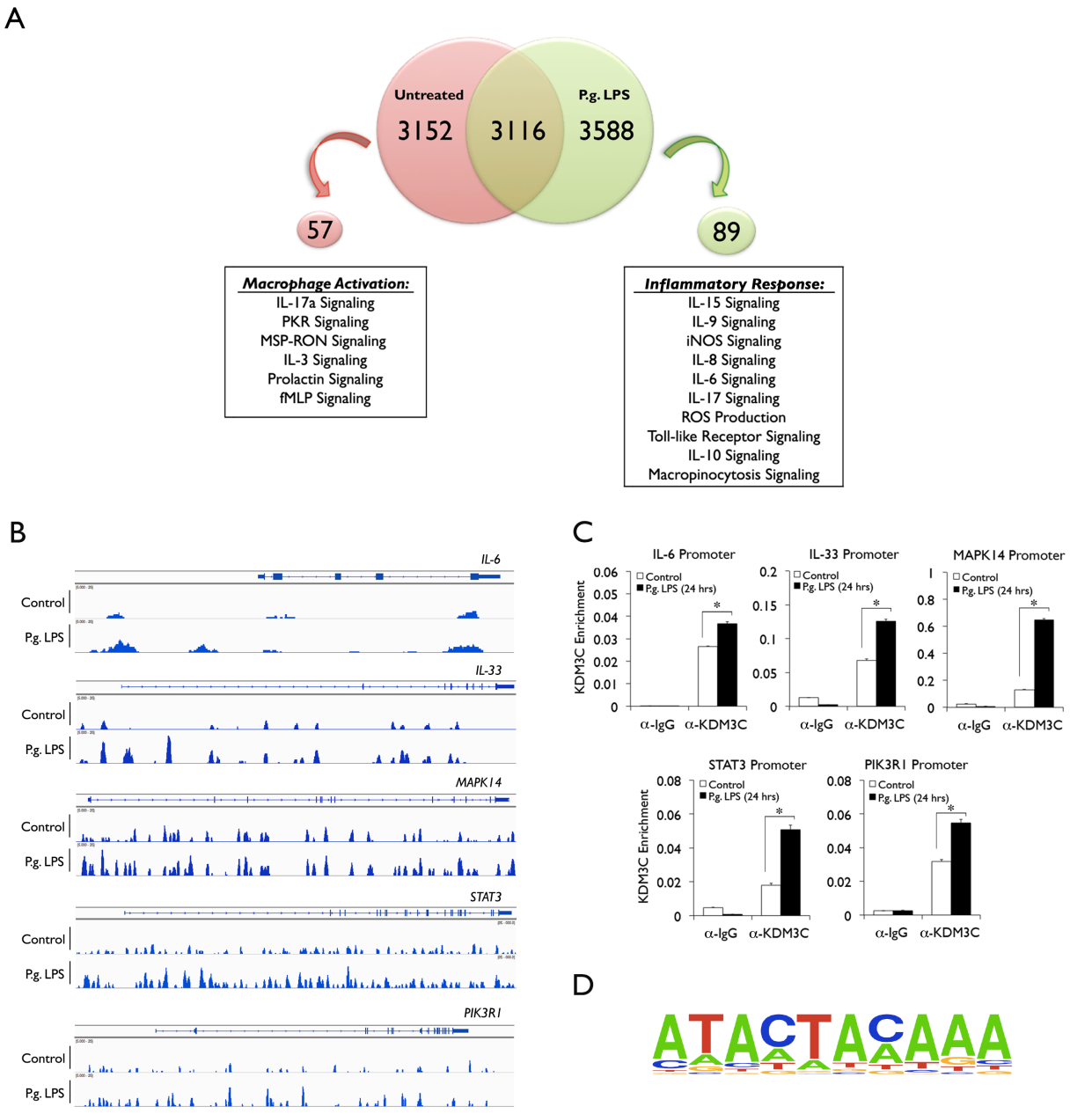

Figure 4-6. KDM3C epigenetically regulates several pro-inflammatory signaling pathways and inflammatory response.

(A) Global binding sites of KDM3C in untreated and *P.g.* LPS treated THP-1 cells were determined by chromatin immunoprecipitation followed by high throughput sequencing (ChIP-Seq). Ingenuity Pathway Analysis (IPA) software was used to identify KDM3C binding targets unique to untreated THP-1, *P.g.* LPS treated THP-1, and sites common between both. **(B)** KDM3C binding to ChIP-Seq identified promoter regions on IL-6, IL-33, MAPK14, STAT3 and PIK3R1 was assessed and (**C**) validated by ChIP-qPCR using original ChIP libraries used for ChIP-Seq experiments. **(D)** Ingenuity Pathway Analysis (IPA) software was used to identify the conserved DNA binding motif for KDM3C.

4.6 KDM3C knockout inhibits P.g. LPS-dependent inflammatory response

We previously demonstrated that KDM3C bound to genes belonging to several inflammatory signaling pathways upon *P.g*. LPS exposure in THP-1 cells. In order to determine whether KDM3C plays a functional role in regulating transcription of these inflammatory signaling genes, we cultured bone marrow macrophages (BMMs) isolated from wild type and KDM3C knockout mice with *P.g*. LPS *ex vivo* in a time-dependent manner. We found BMMs cultured with *P.g* LPS exhibited upregulation of KDM3C mRNA expression in a time-dependent manner, and that its expression was consistent with that of IL-6, IL-33, and STAT3, and that MAPK14 and PIK3R1 24 hours post-*P.g*. LPS. We also found that in BMMs from KDM3C knockout mice, KDM3C mRNA expression was completely abrogated and *P.g*. LPS induction of IL-6, IL-33, MAPK14, STAT3, and PIK3R1 was suppressed (**Figure 4-7**). These data indicate that KDM3C does indeed play a functional role in regulating transcriptional activation of the inflammatory signaling genes identified by our ChIP-Seq analysis.

In order to further investigate whether KDM3C plays a functional role in regulating systemic inflammatory response, we intravenously administered *P.g*. LPS in wild type and KDM3C knockout mice. Similar to our *ex vivo* findings in BMMs, we found *P.g*. LPS administration enhanced KDM3C, IL-6, IL-33, MAPK14, STAT3, and PIK3R1 mRNA expression in liver tissue of wild type mice, and that knockout of KDM3C inhibited induction of these genes (**Figure 4-8A**).

We also assessed the impact of intravenous *P.g*. LPS injection on pro-inflammatory cytokine secretion into blood serum by performing ELISA and cytokine antibody array analyses. We found that in KDM3C knockout mice, *P.g*. LPS-dependent blood serum secretion of 40 distinct pro-inflammatory cytokines, including IL-6, was suppressed. (**Figure 4-8B,C,D**). We also found

that secretion of two distinct inflammatory proteins, epidermal growth factor (EGF) and MIG, increased in KDM3C knockout mice. Collectively, this data indicates that KDM3C plays a critical functional role in epigenetically regulating systemic inflammatory response.

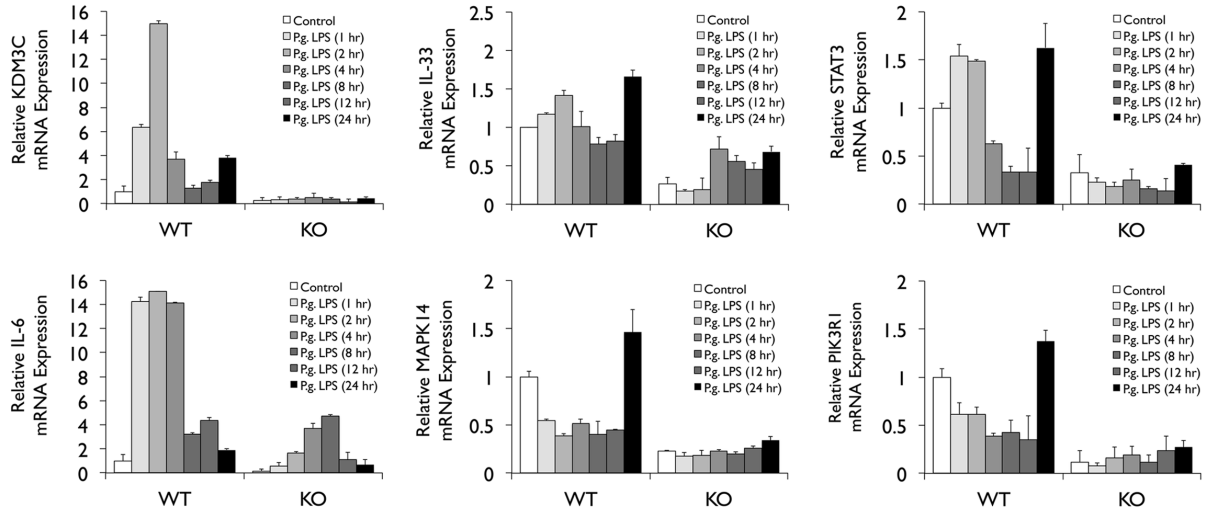

Figure 4-7. KDM3C knockout inhibits induction of inflammatory signaling genes.

Bone marrow monocytes were isolated from wild type (WT) and KDM3C knockout (KO) mice and cultured in 40 ng/ml M-CSF for 5 days to induce differentiation into bone marrow macrophages. Bone marrow macrophages from these mice were cultured with *P.g.* LPS for 1, 2, 4, 8, 12, and 24 hours *ex vivo* and qRT-PCR was performed to assess mRNA expression of KDM3C, IL-6, IL-33, MAPK14, STAT3, and PIK3R1.

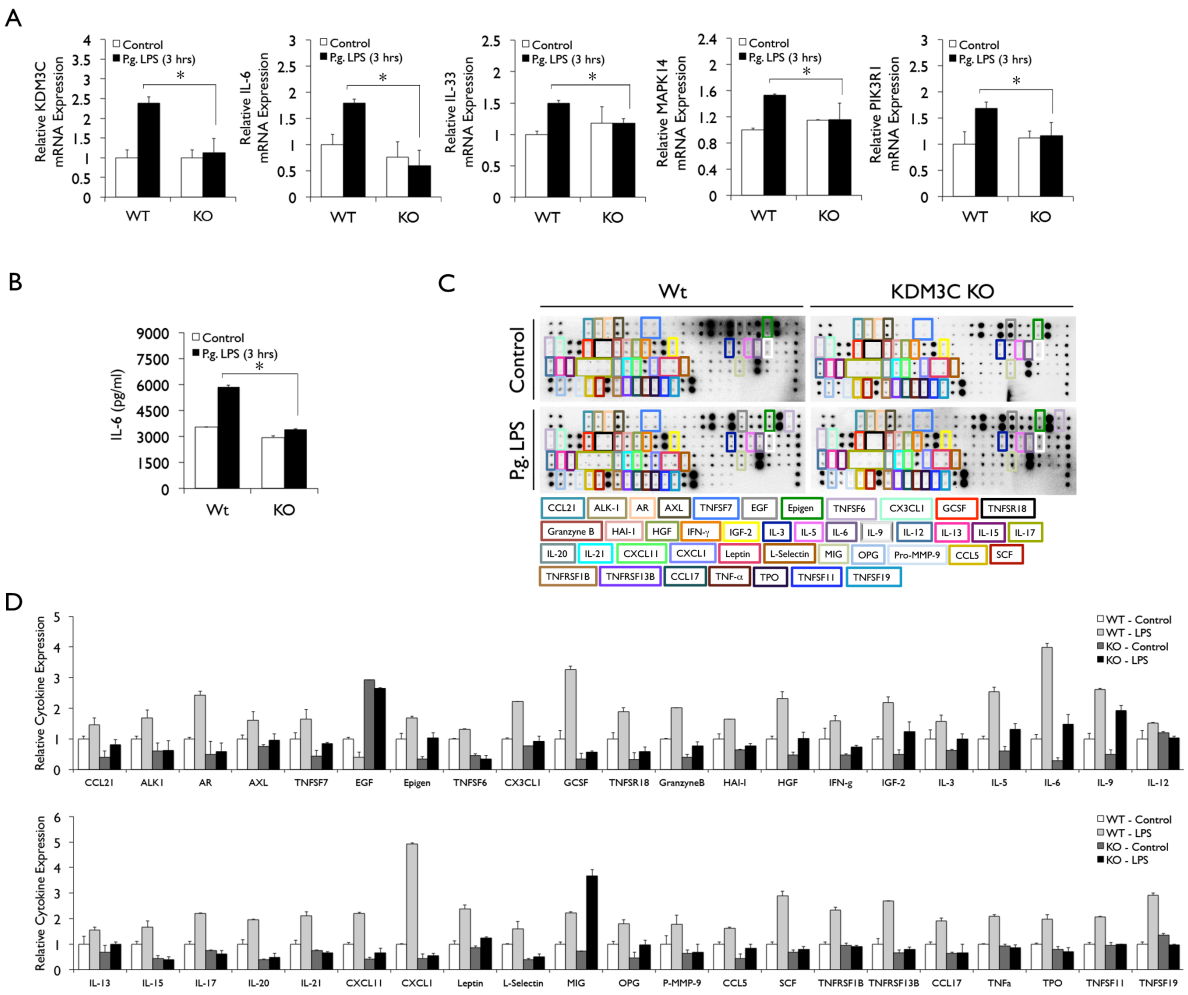

Figure 4-8. KDM3C knockout inhibits pan-inflammatory cytokine induction.

(A) WT and KO mice were intravenously injected with 250 mg/kg *P.g.* LPS and sacrificed 3 hours post-LPS injection. Differential mRNA expression of IL-6, IL-33, MAPK14, STAT3 and PIK3R1 was assessed in liver tissue by qRT-PCR. **(B)** ELISA was performed to assess IL-6 secretion in whole blood serum, and **(C)** cytokine antibody array was performed to assess pan-inflammatory cytokine secretion in whole blood serum. **(D)** Cytokine array data was quantified using ImageJ software.

4.7 Discussion

Although KDM3C has been heavily implicated in several developmental and disease processes, including tumor suppression (Wolfe *et al.,* 2007), steroidogenesis (Kim *et al.,* 2010), and repression of neural differentiation of human embryonic stem cells (Wang *et al.,* 2014), its role in inflammation has not been previously investigated. Our study demonstrates a novel role for KDM3C as a key epigenetic regulator of pro-inflammatory cytokine expression in response to *P.g.* LPS. However, although we demonstrated that KDM3C was strongly upregulated in DPSC, THP-1, PBMCs and mouse bone marrow macrophages in response to *P.g.* LPS, we also demonstrated that *P.g.* LPS-dependent KDM expression profiles are cell-type specific and that other KDMs may also regulate pro-inflammatory cytokine expression in a cell-specific manner. While screening for differential mRNA expression of KDMs in DPSC and THP-1, we observed upregulation of KDM2B, KDM3A, KDM3B, and KDM5A in DPSC and KDM4D and KDM6A in THP-1, in addition to strong KDM3C upregulation found in both cell types (**Figure 4-1A**). It is important to note that although KDM3C demethylates H3K9me1/me2 (Kim *et al.,* 2010) to transcriptionally activate gene expression, these additional KDMs upregulated in DPSC and THP-1 possess distinct demethylation patterns. In particular, KDM2B demethylates H3K6me1/me2 and H3K4me3 (Tsukada *et al.,* 2006; Frescas *et al.,* 2007), KDM3A and KDM3B demethylate H3K9me1/me2 similar to KDM3C (Yamane *et al.,* 2006; Brauchle *et al.,* 2013), KDM5A demethylates H3K4me2/me3 (Christensen *et al.,* 2007; Klose *et al.,* 2007; Nishio *et al.,* 2014), KDM4D demethylates H3K9me2/me3 and H3K36me2/me3 (Whetstine *et al.,* 2006; Iwamori *et al.,* 2011), and KDM6A demethylates H3K27me2me3 (Agger *et al.,* 2007; Lan *et al.,* 2007). Thus, whether these KDMs cooperatively regulate pro-inflammatory cytokine expression with KDM3C or whether they are responsible for the transcriptional activation or

repression of pro-inflammatory cytokines not regulated KDM3C is not known and will be further investigated.

In this study, we demonstrate that exposure to *P.g.* LPS is sufficient to induce both KDM3C and pro-inflammatory cytokine induction in several cell types (**Figure 4-1A-F, Figure 4-7**). Although generally lipopolysaccharides (LPS) are known bind to TLR4 to activate MyD88, MAPK, and NF-kB signaling pathways (He *et al.,* 2013), *P.g.* LPS has been shown to bind to both TLR2 and TLR4 (Darveau *et al.,* 2004). Although we have been able to demonstrate reproducibly that *P.g.* LPS leads to transcriptional activation of KDM3C, it is not evident whether this activation involves TLR2 or TLR4 activation, or which signaling pathway is responsible for KDM3C induction. Thus, extensive pathway analysis studies will be necessary to fully understand and characterize how *P.g.* LPS induces KDM3C expression.

Inasmuch as KDM3C serves as a transcriptional activator by demethylating H3K9me1/me2, it was important for us to identify the methyltransferase responsible for methylating H3K9me1/me2 and transcriptionally silencing those pro-inflammatory genes regulated by KDM3C. We were able to demonstrate that both G9a and KDM3C bind to the same region on the IL-6 promoter, and that the *P.g.* LPS-mediated downregulation of G9a and upregulation of KDM3C enrichment on this region correlated with demethylation of H3K9me2 and transcriptional activation of IL-6 (**Figure 4-4A-D**). We also demonstrated that G9a played a functional role in silencing IL-6 expression in DPSC and THP-1, and that modulation of G9a impacted IL-6 expression (**Figure 4-5C,D**). However, it is not clear what, if any, interaction exists between G9a and KDM3C. It is possible that KDM3C transcriptional activation results in activation of downstream genes that are responsible for the downregulation of G9a or removal of G9a from the IL-6 promoter region. Further, G9a may transcriptionally silence KDM3C in the

absence of *P.g.* LPS. It will be important to further investigate the potential interaction between G9a and KDM3C and its impact of pro-inflammatory cytokine regulation.

Another important question that remains is the state of DNA methylation upon KDM3C-dependent demethylation of H3K9. G9a is known to both methylate H3K9 and to recruit DNA methyltransferase 3a/b (DNMT3a/b) to methylate CpG island repeats on the promoter region, ultimately resulting in halted transcription and transcriptional silencing (El Gazzar *et al.,* 2008). Although we were able to demonstrate that exposure to *P.g.* LPS resulted in enhanced enrichment of KDM3C, loss of enrichment of G9a, and demethylation of H3K9 bound to the IL-6 promoter, it will be important to further investigate whether CpG islands are methylated by DNMT3a/b, whether these sites are demethylated upon loss of G9a enrichment, and exactly what leads to the demethylation of these sites in order to facilitate transcriptional activation of IL-6.

By performing a ChIP-Seq analysis, we were able to identify several genes belonging to inflammatory signaling pathways that are both bound by and functionally regulated by KDM3C. We also identified several of these genes that were conserved among multiple interleukin-signaling pathways, including IL-6, IL-33, STAT3, MAPK14, and PIK3R1 (**Figure 4-6A-D**). We found that among bone marrow macrophages isolated from WT and KDM3C KO mice, time-dependent induction of KDM3C and IL-6, IL-33, and STAT3 mRNA expression followed a similar pattern, with these genes being induced after 1-2 hours and again after 24 hours post-*ex vivo P.g.* LPS culture (**Figure 4-7**). However, we found that unlike IL-6, IL-33, and STAT3, the mRNA expression of MAPK14 and PIK3R1 only peaked 24 hours post-*P.g.* LPS expression, suggesting that KDM3C may not be regulating transcriptional activation of these genes immediately upon *P.g.* LPS stimulation. It is possible that transcriptional activation of these genes may require cooperative demethylase activity by other KDMs expressed upon prolonged

P.g. LPS exposure, as described previously.

We utilized two distinct mouse models in our study to examine the functional role KDM3C plays in regulating pro-inflammatory cytokine induction *in vivo.* Whereas one model utilized intravenous *in vivo* Si-RNA administration to transiently knockdown KDM3C, our other model utilized a non-conditional, non-transient knockout, in which exons 24 to 57 of the KDM3C gene were replaced with an IRES-neo cassette (Kuroki *et al.,* 2013). It is interesting to note that although several key inflammatory cytokines, such as IL-6, IL-9, IL-12, and IL-17, were downregulated in both the KDM3C knockdown and knockout model, these mice exhibited distinct cytokine profiles (**Figure 4-3F,G; Figure 4-8C,D**). It is possible that upon complete deletion of the KDM3C gene from birth, other mechanisms may compensate and result in distinct cytokine expression profiles between these mice models. We also noticed that *P.g.* LPS-dependent secretion of 40 distinct inflammatory cytokines was suppressed in KDM3C knockout mice, and that two secreted proteins in particular, epidermal growth factor (EGF) and MIG, were upregulated in KDM3C KO mice (**Figure 4-8C, D**). It is possible that KDM3C transcriptionally activates downstream genes that serve as inhibitors of EGF and MIG, and that KDM3C intricate regulates inflammatory response in response to *P.g.* LPS. Although we anticipate that KDM3C KO mice will exhibit anti-inflammatory phenotype and minimal inflammatory lesion development, the potential deregulation of pro-inflammatory cytokine induction in these mice may result in aberrant inflammatory response, as demonstrated elsewhere (Balto *et al.,* 2001). It will be important to establish a conditional knockout mouse model to be able to closely study the effect of transient KDM3C knockout on both inflammatory cytokine expression and inflammatory phenotype *in vivo.*

Collectively, the findings of this study provide insight into the functional role that KDM3C

plays in *P.g.* LPS-mediated inflammation, as well as its role in reversing G9a-mediated pro-inflammatory cytokine gene silencing during inflammation. We propose a model in which G9a binds to the promoter regions of pro-inflammatory cytokines and di-methylates H3K9 to silence cytokine transcription in the absence of inflammatory stimuli, and that G9a enrichment is lost in the presence of *P.g.* LPS, allowing KDM3C to demethylate H3K9me2 and transcriptionally activate pro-inflammatory cytokines and drive inflammatory response (**Figure 4-9**). These findings provide insight into the epigenetic mechanisms by which KDM3C regulates pro-inflammatory cytokine induction, indicating its potential as a novel anti-inflammatory therapeutic target in the management and treatment of inflammatory oral diseases.

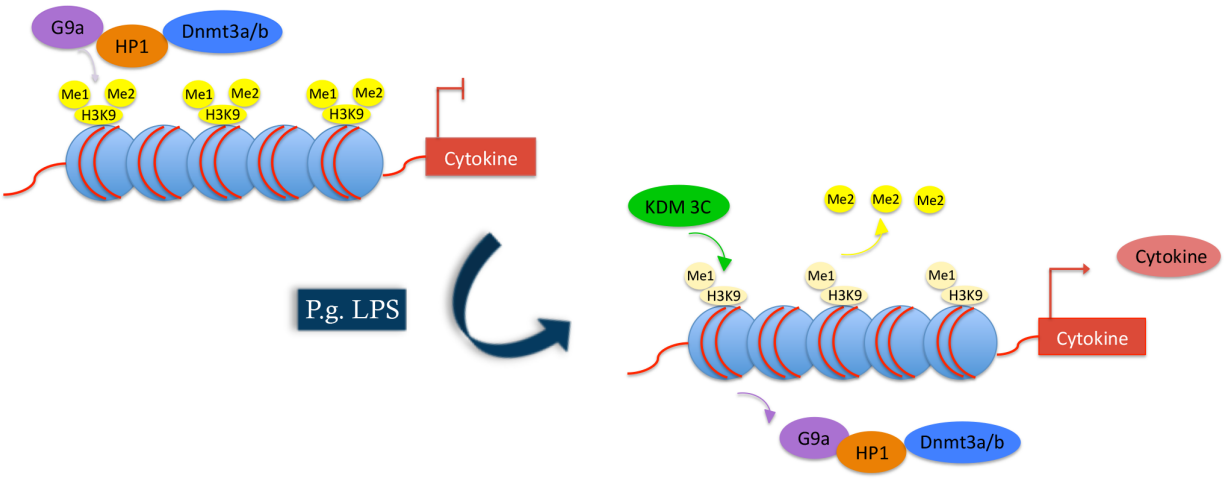

Figure 4-9. Role of KDM3C and G9a in epigenetic regulation of *P.g.* LPS-dependent pro-inflammatory cytokine transcription.

Current data establish complementary roles for KDM3C and G9a in the maintenance of H3K9 methylation and transcriptional activation of inflammatory cytokines. G9a and complex proteins HP-1 and DNMT3a/b are necessary to mono-/di-methylate H3K9 and transcriptionally silence cytokine transcription in the absence of inflammatory stimuli. In the presence of *P.g.* LPS, G9a complex is no longer bound, allowing KDM3C to demethylate H3K9me2 and facilitate transcriptional activation of pro-inflammatory cytokines necessary for inflammatory response.

5 SUMMARY AND CONCLUSION

Epithelial barrier function plays an important role as the first line of defense against infection, and as such, epithelial plasticity and integrity are important areas of investigation in the study of inflammation in the oral cavity. In the course of this dissertation, the mechanisms regulating epithelial barrier function and the epigenetic mechanisms by which inflammatory response is elicited and regulated were investigated and addressed.

In Chapter 3, we explored the molecular mechanisms of TGF-β-dependent EMT and investigated the effects of p63 and Grainyhead-like 2 (GRHL2) modulation on epithelial plasticity. We reported that GRHL2 and p63 engage in a reciprocal feedback loop and that their abrogation leads to EMT phenotype and altered epithelial barrier phenotype. Here we highlight several notable findings that contribute to our understanding of EMT and epithelial plasticity:

1. TGF-β leads to downregulation of GRHL2 and p63, and facilitation of EMT molecular phenotype *e.g.* downregulation of K14, β-catenin, and E-Cadherin and upregulation of FN and ZEB-1.
2. Knockdown of p63 leads to adoption of EMT phenotype in NHK, including fibroblast-like morphology, stress fiber formation, and EMT molecular patterns. Knockdown of p63 also results in downregulation of and loss of enrichment on miR-200 family genes, which are known inhibitors of EMT.
3. GRHL2 and p63 participate in reciprocal feedback loop and mutually regulate their promoter activity.
4. Knockout of GRHL2 results in altered epithelial barrier phenotype and increased *P.g.* bacterial load in bloodstream of conditional knockout mice orally fed *P.g.* or in which ligatures were placed.

In Chapter 4, we investigated the role of histone lysine demethylases in the epigenetic regulation of *P.g.* LPS induced inflammation and reported that KDM3C played an important functional role in regulating cytokine induction. Here, we highlight important findings made that aid in our understanding of epigenetic regulation of inflammatory response:

1. KDM3C is strongly upregulated in DPSC, THP-1, PBMCs and bone marrow macrophages cultured with *P.g.* LPS.
2. KDM3C binds to the promoter regions of several inflammatory signaling molecules and cytokines, and facilitates demethylation of H3K9me2.
3. G9a di-methylates H3K9, and overexpression of G9a prevents *P.g.* LPS dependent cytokine induction.
4. Abrogation of KDM3C by Si-RNA or in KDM3C KO mice suppresses inflammatory response and induction of inflammatory signaling molecules, including pro-inflammatory cytokines, by *P.g.* LPS.

In summary, our findings support a model in which injury or inflammation of epithelial tissues in the oral cavity result in upregulated expression of TGF-β in epithelial cells, downregulation of GRHL2 and p63, and altered epithelial barrier phenotype. This altered phenotype results in compromised resistance against *P.g.* bacteria, resulting in the upregulation of KDM3C, demethylation of H3K9me2 and transcriptional activation of inflammatory signaling molecules and cytokines, triggering and maintaining an inflammatory response.

BIBLIOGRAPHY

Agger K, Cloos PA, Christensen J, Pasini D, Rose S, Rappsilber J, Issaeva I, Canaani E, Salcini AE, Helin K (2007). UTX and JMJD3 are histone H3K27 demethylases involved in HOX gene regulation and development. *Nature*, **449**:731–734.

Akira S, Uematsu S, Takeuchi O (2006). Pathogen recognition and innate immunity. *Cell,* **124:**783-801.

Alam H, Sehgal L, Kundu ST, Dalal SN, Vaidya MM (2011). Novel function of keratins 5 and 14 in proliferation and differentiation of stratified epithelial cells. *Mol Biol Cell,* **22:**4068-4078.

American Dental Association, Survey Center (2007). 2005–06 Survey of Dental Services Rendered. *Am Dent Assoc,* Chicago.

Ansieau S, Bastid J, Doreau A, Morel AP, Bouchet BP, Thomas C, Fauvet F, Puisieux I, Doglioni C, Piccinin S (2008). Induction of EMT by twist proteins as a collateral effect of tumor-promoting inactivation of premature senescence. *Cancer Cell*, **14**:79–89.

Bai B, Zhang Q, Liu X, Miao C, Shangguan S, Bao Y, Guo J, Wang L, Zhang T, Li H (2014). Different epigenetic alterations are associated with abnormal IGF2/Igf2 upregulation in neural tube defects. *PLoS One,* **9**:e113308.

Balto K, Sasaki H, Stashenko P (2001). Interleukin-6 Deficiency Increases Inflammatory Bone Destruction. *Infect Immun,* **69:**744-750.

Banyard J and Bielenberg DR (2015). The role of EMT and MET in cancer dissemination. *Connect Tissue Res,* **56:**403-413.

Barbareschi M, Pecciarini L, Cangi MG, Marci E, Rizzo A, Viale G, Doglioni C (2001). p63, a p53 homologue, is a selective nuclear marker of myoepithelial cells of the human breast. *Am J Surg Pathol,* **25:**1054-1060.

Barrallo-Gimeno A and Nieto MA (2005). The Snail genes as inducers of cell movement and survival: implications in development and cancer. *Development,* **132:**3151-3161.

Barski A, Cuddapah S, Cui K, Roh TY, Wang Z, Wei G, Chepelev I, Zhao K (2007). High-resolution profiling of histone methylations in the human genome. *Cell,* **4:**823-837.

Batlle E, Sancho E, Franci C, Dominguez D, Monfar M, Baulida J, Garcia De Herreros A (2000). The transcription factor snail is a repressor of E-cadherin gene expression in epithelial tumour cells. *Nat Cell Biol,* **2:**84-89.

Bement WM, Forscher P, Mooseker MS (1993). A novel cytoskeletal structure involved in purse string wound closure and cell polarity maintenance. *J Cell Biol,* **121**:565–578.

Bestor T, Laudano A, Mattaliano R, Ingram V (1988). Cloning and sequencing of a cDNA encoding DNA methyltransferase of mouse cells: The carboxyl-terminal domain of the mammalian enzymes is related to bacterial restriction methyltranferase. *J Mol Biol,* **203:**971-983.

Buhlin K, Gustafsson A, Pockley AG, Frostegard J, Klinge B (2003). Risk factors for cardiovascular disease in patients with periodontitis. *Eur Heart J,* **24:**2099-107.

Bjorkman M, Ostling P, Harma V, Virtanen J, Mpindi JP, Rantala J, Mirtti T, Vesterinen T, Lundin M, Sankila A, Rannikko A, Kaivanto E, Kohonen P, Kallioniemi O, Nees M (2011). Systematic knockdown of epigenetic enzymes identifies a novel histone demethylase PHF8 overexpressed in prostate cancer with an impact on cell proliferation, migration and invasion. *Oncogene*, **31:**3444-3456.

Boulle F, van den Hove DL, Jakob SB, Rutten BP, Hamon M, van Os J, Lesch KP, Lanfumey L, Steinbusch HW, Kenis G (2012). Epigenetic regulation of the BDNF gene: implications for psychiatric disorders. *Mol Psychiatry,* **17:**584-596.

Brauchle M, Yao Z, Arora R, Thigale S, Clay I, Inverardi B, Fletcher J, Taslimi P, Acker MG, Gerritis B, Voshol J, Bauer A, Schubeler D, Bouwmeester T, Ruffner H (2013).
Protein complex interactor analysis and differential activity of KDM3 subfamily members towar ds H3K9methylation. *PLoS One,* **8:**e60549.

Buer J and Balling R (2003). Mice, microbes, and models of infection. *Nat Rev Genet,* **4:**195-205.

Cao R, Wang L, Wang H, Xia L, Erdjument-Bromage H, Tempst P, Jones RS, Zhang Y (2002). *Science,* **298:** 1039-1043.

Carver EA, Jiang R, Lan Y, Oram KF, Gridley T (2001). The mouse snail gene encodes a key regulator of the epithelial-mesenchymal transition. *Mol Cell Biol,* **21:**8184-8188.

Cetinkaya B, Guzeldemir E, Ogus E, Bulut S (2013). Proinflammatory and anti-inflammatory cytokines in gingival crevicular fluid and serum of patients with rheumatoid arthritis and patients with chronic periodontitis. *J Periodontol,* **84:**84-93.

Chang L and Karin M (2001). Mammalian MAP kinase signaling cascades. *Nature*, **410:**37-40.

Chang Y, Zhang X, Horton JR, Upadhyay AK, Spannhoff A, Liu J, James PS, Bedford MT, Cheng X (2009). Structural basis for G9a-like protein lysine methyltransferase inhibition by BIX-01294. *Nat Struct Mol Biol,* **16:**312-317.

Chen L, Arbieva ZH, Guo S, Marucha PT, Mustoe TA, DiPietro LA (2010a). Positional differences in the wound transcriptome of skin and oral mucosa. *BMC Genomics*, **11:**471.

Chen JD, Lapiere JC, Sauder DN, Peavey C, Woodley DT (1995). Interleukin-1 alpha stimulates keratinocyte migration through an epidermal growth factor/transforming growth factor-alpha-independent pathway. *J Invest Dermatol, **104**:729-733.*

Chen W, Dong Q, Shin KH, Kim RH, Oh JE, Park NH, Kang MK (2010b). Grainyhead-like enhances the human telomerase reverse transcriptase gene expression by inhibiting DNA methylation at the 5-CpG island in normal human keratinocytes. *J Biol Chem*, **285:**40852–40863.

Chen W, Xiao Liu Z, Oh JE, Shin KH, Kim RH, Jiang M, Park NH, Kang MK (2012). Grainyhead-like 2 (GRHL2) inhibits keratinocyte differentiation through epigenetic mechanism. *Cell Death Dis,* **3:**e450.

Christensen J, Agger K, Cloos PA, Pasini D, Rose S, Sennels L, Rappsilber J, Hansen KH, Salcini AE, Helin K (2007). RBP2 belongs to a family of demethylases, specific for tri- and dimethylated lysine 4 on histone 3. *Cell*, **128:**1063-1076.

Cieply B, Farris J, Denvir J, Ford HL, Frisch SM (2013). Epithelial-mesenchymal transition and tumor suppression are controlled by a reciprocal feedback loop between ZEB1 and Grainyhead-like-2. *Cancer Res*, **73:**6299-6309.

Cieply B, Riley P, Pifer PM, Widmeyer J, Addison JB, Ivanov AV, Denvir J, Frisch SM (2012). Suppression of the epithelial-mesenchymal transition by Grainyhead-like-2. *Cancer Res,* **72:**2440–2453.

Colombo AV, da Silva CM, Haffajee A, Colombo AP (2007). Identification of intracellular oral species within human crevicular epithelial cells from subjects with chronic periodontitis by fluorescence in situ hybridization. *J Periodontal Res,* **42:236-243.**

Copeland RA, Olhava EJ, Scott MP (2010). Targeting epigenetic enzymes for drug discovery. *Curr Opin Chem Biol,* **14:**505-510.

Dahlen G (2000). Microbiology and treatment of dental abscesses and periodontal-endodontic lesions. *Periodontol*, **28:**206-39.

Darveau RP, Pham TT, Lemley K, Reife RA, Bainbridge BW, Coats SR, Howald WN, Way SS, Haijar AM (2004). Porphyromonas gingivalis lipopolysaccharide contains multiple lipid A species that functionally interact with both toll-like receptors 2 and 4. *Infect Immun,* **72:**5041-5051.

De Santa F, Totaro MG, Prosperini E, Notarbartolo S, Testa G, Natoli G (2007). The histone H3 lysine-27 demethylase Jmjd3 links inflammation to inhibition of polycomb-mediated gene silencing. *Cell,* **130:**1083-1094.

Dominici M, Le Blanc K, Mueller I, Slaper-Cortenbach I, Marini F, Krause D, Deans R, Keating A, Prockop DJ, Horwitz E (2006). Minimal criteria for defining multipotent mesenchymal stromal cells. The International Society for Cellular Therapy position statement. *Cytotherapy,* **8:**315-317.

Eke PI, Dye BA, Wei L, Thornton-Evans GO, Genco RJ, Beck J, Douglass G, Page R (2012). Prevalence of periodontitis in adults in the United States: 2009 and 2010. *J Dent Res,* **10:**914-920.

El Gazzar M, Yoza BK, Chen X, Hu J, Hawkins GA, McCall CE (2008). G9a and HP1 couple histone and DNA methylation to TNFalpha transcription silencing during endotoxin tolerance. *J Biol Chem*, **283:**32198-208. PMC2583293.

Faria-Almeida R, Navarro A, Bascones A (2006). Clinical and metabolic changes after conventional treatment of type 2 diabetic patients with chronic periodontitis. *J Periodontol*, **77:**591-8.

Fitchett JE and Hay ED (1989). Medial edge epithelium transforms to mesenchyme after embryonic palatal shelves fuse. *Dev Biol,* **131:**455-474.

Fodor BD, Kubicek S, Yonezawa M, O'Sullivan RJ, Sengupta R, Perez-Burgos L, Opravil S, Mechtler K, Schotta G, Jenuwein T (2006). Jmjd2b antagonizes H3K9 trimethylation at pericentric heterochromatin in mammalian cells. *Genes Dev*, **20:**1557-1562.

Frescas D, Guardavaccaro D, Bassermann F, Koyama-Nasu R, Pagano M (2007). JHDM1B/FBXL10 is a nucleolar protein that represses transcription of ribosomal RNA genes. *Nature,* **450**:309-313.

Fujii R, Muramatsu T, Yamaguchi Y, Asai T, Aida N, Suehara M, Morinaga K, Furusawa M (2014). An endodontic-periodontal lesion with primary periodontal disease: a case report on its bacterial profile. *Bull Tokyo Dent Coll*, **55:**33-7.

Gallucci RM, Simeonova PP, Matheson JM, Kommineni C, Guriel JL, Sugawara T, Luster MI (2000). Impaired cutaneous wound healing in interleukin-6-deficient and immunosuppressed mice. *FASEB,* **14:**2525-2531.

Gandarillas A and Watt FM (1997). c-Myc promotes differentiation of human epidermal stem cells. *Genes Dev,* **21:**2869-2882.

Giannelli G, Falk-Marzillier J, Schiraldi O, Stetler-Stevenson W, aQuaranta V (1997). Induction of cell migration by Matrix Metalloprotease-2 cleavage of Laminin-5. *Science,* **277**:225-228.

Grellner W, Georg T, Wilske J (2000). Quantitative analysis of proinflammatory cytokines (IL-1beta, IL-6, TNF-alpha) in human skin wounds. *Forensic Sci Int*, **113:**251-264.

Grille SJ, Bellacosa A, Upson J, Klein-Szanto AJ, van Roy F, Lee- Kwon W, Donowitz M, Tsichlis PN, and Larue L (2003). The protein kinase Akt induces epithelial mesenchymal transition and promotes en- hanced motility and invasiveness of squamous cell carcinoma lines. *Cancer Res*, **63:**2172–2178.

Groeger S, Doman E, Chakraborty T, Mevle J (2010). Effects of Porphyromonas gingivalis infection on human gingival epithelial barrier function in vitro. *Eur J Oral Sci*, **118:**582-589.

Gurkan A, Emingil G, Cinarcik S, Berdeli A (2006). Gingival crevicular fluid transforming growth factor-beta1 in several forms of periodontal disease. *Arch Oral Biol,* **51:**906-912.

Hay ED (1995). An overview of epithelio-mesenchymal transformation. *Acta Anat*, **154**:8–20.

Hay ED and Griffith CM (1992). Epithelial-mesenchymal transformation during palatal fusion: carboxyfluorescein traces cells at light and electron microscopic levels. *Development,* **116:**1087-1099.

Hay ED and Zuk A (1995). Transformations between epithelium and mesenchyme: normal, pathological, and experimentally induced. *Am J Kidney Dis,* **26:**678 – 690.

Hayami S, Yoshimatsu M, Veerakumarasivam A, Unoki M, Iwai Y, Tsunoda T, Field HI, Kelly JK, Neal DE, Yamaue H, Ponder BA, Nakamura Y, Hamamoto R (2010). Overexpression of the JmjC histone demethylase KDM5B in human carcinogenesis: involvement in the proliferation of cancer cells through the E2F/RB pathway. *Mol Cancer,* **9:**59.

Hazan RB, Kang L, Whooley BP, Borgen PI (1997). N-cadherin promotes adhesion between invasive breast cancer cells and the stroma. *Cell Adhes Commun,* **4:**399-411.

He J, Nguyen AT, Zhang Y (2011). KDM2b/JHDM1b, an H3K36me2-specific demethylase, is required for initiation and maintenance of acute myeloid leukemia. *Blood*, **117**:3869–3880.

He W, Qu T, Yu Q, Wang Z, Lv H, Zhang J, Zhao X, Wang P (2013). LPS induces IL-8 expression through TLR4, MyD88, NF-kappaB and MAPK pathways in human dental pulp stem cells. *Int Endod J,* **46:**128-136.

Heitz-Mayfield LJ, Trombelli L, Heitz F, Needleman I, Moles D (2002). A systematic review of the effect of surgical debridement vs non-surgical debridement for the treatment of chronic periodontitis. *J Clin Periodontol,* **3:**92-102.

Hubner G, Brauchle M, Smola H, Madlener M, Fassler R, Werner S (1996). Differential regulation of pro-inflammatory cytokines during wound healing in normal and glucocorticoid treated mice. *Cytokine*, **8:**548-856.

Hubner MR and Spector DL (2011). Role of H3K27 demethylases Jmjd3 and UTX in transcriptional regulation. *Spring Harb Symp Quant Biol,* **75:**43-49.

Iwamori N, Zhao M, Meistrich ML, Matzuk MM (2011). The testis-enriched histone demethylase, KDM4D, regulates methylation of histone H3 lysine 9 duringspermatogenesis in the mouse but is dispensable for fertility. *Biol Reprod,* **84:**1225-1234.

Jagels MA and Hugli TE (2000). Mixed effects of TGF-beta on human airway epithelial-cell chemokine responses. *Immunopharmacology*, **48:**17-26.

Jepsen K, Solum D, Zhou T, McEvilly RJ, Kim HJ, Glass CK, Hermanson O, Rosenfeld MG (2007). SMRT-mediated repression of an H3K27 demethylase in progression from neural stem cell to neuron. *Nature,* **450:**415-419.

Johnson JD, Chen R, Lenton PA, Zhang G, Hinrichs JE, Rudney JD (2008). Persistence of Extracrevicular Bacterial Reservoirs After Treatment of Aggressive Periodontitis. *J Periodontol,* **79:**2305-2312.

Jones PA and Takai D (2001). The role of DNA methylation in mammalian epigenetics. *Science*, **293:**1068-1070.

Jun JI and Lau LF (2011). Taking aim at the extracellular matrix: CCN proteins as emerging therapeutic targets. *Nat Rev Drug Discov,* **10:**945-963.

Kabanov DS and Prokhorenko IR (2010). Structural analysis of lipopolysaccharides from Gram-negative bacteria. *Biochemistry (Mosc),* **75:**383-404.

Kalluri R and Weinberg RA (2009). The basics of epithelial-mesenchymal transition. *J Clin Invest,* **119:**1420-1428.

Kang MK, Bibb C, Baluda MA, Rey O, Park NH (2000). In vitro replication and differentiation of normal human oral keratinocytes. *Exp Cell Res*, **258**:288-297.

Kang X, Chen W, Kim RH, Kang MK, Park NH (2009). Regulation of the hTERT promoter activity by MSH2, the hnRNPs K and D, and GRHL2 in human oral squamous cell carcinoma cells. *Oncogene,* **28:**565-574.

Kang MK, Guo W, Park NH (1998). Replicative senescence of normal human oral keratinocytes is associated with the loss of telomerase activity without shortening of telomeres. *Cell Growth Differ,* **9**:85-95.

Kang MK, Kameta A, Shin KH, Baluda MA, Park NH (2004). Senescence occurs with hTERT repression and limited telomere shortening in human oral keratinocytes cultured with feeder cells. *J Cell Physiol,* **199:**364-370.

Kang MK and Park NH (2007). Extension of cell life span using exogenous telomerase. *Methods Mol Biol*, **371**:151-165.

Kawai T and Akira S (2010). The role of pattern-recognition receptors in innate immunity: update on Toll-like receptors. *Nat Immunol,* **11:**373-384.

Kim SM, Kim JY, Choe NW, Cho IH, Kim JR, Kim DW, Seol JE, Lee SE, Kook H, Nam KI, Kook H, Bhak YY, Seo SB (2010). Regulation of mouse steroidogenesis by WHISTLE and JMJD1C through histone methylation balance. *Nucleic Acids Res,* **38**:6389-6403.

Kinney JS, Ramseier CA, Giannobile WV (2007). Oral fluid-based biomarkers of alveolar bone

loss in periodontitis. *Ann N Y Acad Sci*, **1098:**230-251.

Klose RJ, Yan Q, Tothova Z, Yamane K, Erdjument-Bromage H, Tempst P, Gilililand DG, Zhang Y, Kaelin WG (2007). The retinoblastoma binding protein RBP2 is an H3K4 demethylase. *Cell*, **128:**889-900.

Korpal M, Lee ES, Hu G, Kang Y (2008). The miR-200 family inhibits epithelial-mesenchymal transition and cancer cell migration by direct targeting of E-cadherin transcriptional repressors ZEB1 and ZEB2. *J Biol Chem*, **283:**14910-14914.

Kubicek S, O'Sullivan RJ, August EM, Hickey ER, Zhang Q, Teodoro ML, Rea S, Mechtler K, Kowalski JA, Homon CA, Kelly TA, Jenuwein T (2007). Reversal of H3K9me2 by a small-molecule inhibitor for the G9a histone methyltransferase. *Mol Cell,* **25:**473-481.

Kuroki S, Akiyoshi M, Tokura M, Miyachi H, Nakai Y, Kimura H, Shinkai Y, Tachibana M (2013). JMJD1C, a JmjC domain-containing protein, is required for long-term maintenance of male germ cells in mice. *Biol Reprod*, **89:**93.

Krogan NJ, Kim M, Tong A, Golshani A, Cagney G, Canadien V, Richards DP, Beattie BK, Emili A, Boone C, Shilatifard A, Buratowski S, Greenblatt J (2003). Methylation of histone H3 by Set2 in Saccharomyces cerevisiae is linked to transcriptional elongation by RNA polymerase II. *Mol Cell Biol,* **23:** 4207-4218.

Lan F, Bayliss PE, Rinn JL, Whetstine JR, Wang JK, Chen SZ, Iwase S, Alpatov R, Issaeva I, Canaani E, Roberts TM, Chang HY, Shi Y (2007). A histone H3 lysine 27 demethylase regulates animal posterior development. *Nature*, **449**:689–694.

Laurikkala J, Mikkola ML, James M, Tummers M, Mills AA Thesleff I (2006). p63 regulates multiple signaling pathways required for ectodermal organogenesis and differentiation. *Development,* **133:**1553-1563.

Leask A and Abraham DJ (2006). All in the CCN family: essential matricellular signaling modulators emerge from the bunker. *J Cell Sci,* **119:**4803-4810.

Liechty HW, Adzick NS, Crombleholme TM (2000). Diminished interleukin 6 (IL-6) production during scarless human fetal wound repair. *Cytokine*, **12:**671-676.

Liu Y, El-Naggar S, Darling DS, Higashi Y, Dean DC (2008). Zeb1 links epithelial-mesenchymal transition and cellular senescence. *Development*, **135:**579-588.

Maeshima N and Fernandez RC (2013). Recognition of lipid A variants by the TLR4-MD-2 receptor complex. *Front Cell Infect Microbiol,* **3:** 3.

Mak K, Manji A, Gallant-Behm C, Wiebe C, Hart DA, Larjava H, Hakkinen L (2009). Scarless healing of oral mucosa is characterized by faster resolution of inflammation and control of myofibroblast action compared to skin wounds in the red Duroc pig model. *J Dermatol Sci*,

56:168-180.

McAleer JP and Vella AT (2008). Understanding how lipopolysaccharide impacts CD4 T cell immunity. *Crit Rev Immunol,* **28:**281-299.

Mize TW, Sundararaj KP, Leite RS, Huang Y (2015). Increased and correlated expression of connective tissue growth factor and transforming growth factor beta 1 in surgically removed periodontal tissues with chronic periodontitis. *J Periodontal Res,* **50**:315-319.

Moll R, Franke WW, Schiller DL, Geiger B, Krepler R (1982). The catalog of human cytokeratins: patterns of expression in normal epithelia, tumors and cultured cells. *Cell,* **31**:11–24.

Morel AP, Hinkal GW, Thomas C, Fauvet F, Courtois-Cox S, Wierinckx A, Devouassoux-Shisheboran M, Treilleux I, Tissier A, Gras B (2012). EMT inducers catalyze malignant transformation of mammary epithelial cells and drive tumorigenesis towards claudin-low tumors in transgenic mice. *PLoS Genet*, **8**:e1002723.

Moreno-Bueno G, Peinado H, Molina P, Olmeda D, Cubillo E, Santos V, Palacios J, Portillo F, and Cano A (2009). The morphological and molecular features of the epithelial-to-mesenchymal transition. *Nat Protoc*, **4:**1591–1613.

Nair PN (2004). Pathogenesis of apical periodontitis and the causes of endodontic failures. *Crit Rev Oral Biol Med*, **15:**348-381.

Netea MG, van der Graaf C, Van der Meer JW, Kullberg BJ (2004). Toll-like receptors and the host defense against microbial pathogens: bringing specificity to the innate-immune system. *J Leukoc Biol,* **75:**749-755

Ngo VN, Young RM, Schmitz R, Ihavar S, Xiao W, Lim KH, Kohlhammer H, Xu W, Yang Y, Zhao H, Shaffer AL, Romesser P, Wright G, Powell J, Rosenwald A, Muller-Hermelink HK, Ott G, Gascoyne RD, Connors JM, RImsza LM, Campo E, Jaffe ES, Delabie J, Smeland EB, Fisher RI, Braziel RM, Tubbs R, Cook JR, Weisenburger DD, Chan WC, Staudt LM (2011). Oncogenically active MYD88 mutations in human lymphoma. *Nature*, **470:**115-119.

Nieman MT, Prudoff RS, Johnson KR, Wheelock MJ (1999). N-cadherin promotes motility in human breast cancer cells regardless of their E-cadherin expression. *J Cell Biol*, **147***:*631-634.

Nieto MA (2002). The snail superfamily of zinc-finger transcription factors. *Nat Rev Mol Cell Biol,* **3:**155-166.

Nishio H, Hayashi Y, Moritoki Y, Kamisawa H, Mizuno K, Kojima Y, Kohri K (2014). Distinctive changes in histone H3K4 modification mediated via Kdm5a expression in spermatogonial stem cells of cryptorchid testes. *J Urol,* **191:**1564-1572.

Nishioka K, Rice JC, Sarma K, Erdjument-Bromage H, Werner J, Wang Y, Chuikov S,

Valenzuela P, Tempst P, Steward R, Lis JT, Allis CD, Reinberg D (2002). PR-Set7 is a nucleosome-specific methyltransferase that modifies lysine 20 of histone H4 and is associated with silent chromatin. *Mol Cell,* **9:** 1201-1213.

Nozawa K, Fujishiro M, Kawasaki M, Kaneko H, Iwabuchi K, Yanagida M, Suzuki F, Miyazawa K, Takasaki Y, Ogawa H, Takamori K, Sekigawa I (2009). Connective tissue growth factor promotes articular damage by increased osteoclastogenesis in patients with rheumatoid arthritis. *Arthritis Res Ther,* **11:**R174.

Oh JE, Kim RH, Shin KH, Park NH, Kang MK (2011). DeltaNp63-alpha triggers epithelial-mesenchymal transition and confers stem cell properties in normal human keratinocytes. *J Biol Chem,* **286:**38757–38767.

Ohnishi K, Semi K, Yamamoto T, Shmizu M, Tanaka A, Mitsunaga K, Okita K, Osafune K, Arioka Y, Maeda T, Soejima H, Moriwaki H, Yamanaka S, Woltjen K, Yamada Y (2014). Premature termination of reprogramming in vivo leads to cancer development through altered epigenetic regulation. *Cell,* **156:**633-677.

Okano M, Xie S, Li E (1998). Cloning and characterization of a family of novel mammalian DNA (cytosine-5) methyltransferases. *Nat Genet,* **19:**219-220.

Park J and Schwarzbauer JE (2014). Mammary epithelial cell interactions with fibronectin stimulate epithelial-mesenchymal transition. *Oncogene,* **33:**1649-1657.

Peeken J, Seeger TS, Wehrle J, Schanne Dh, Gothwal M, Grunder A, Pahl HL (2013). Overexpression Of The Histone Demethylase JMJD1C In Polycythemia Vera Contributes To NF-E2 Overexpression Via Epigenetic Dysregulation and An Auto-Regulatory Loop. *Blood*, **122:**1602.

Peterson CL and Laniel MA (2004). Histones and histone modifications. *Curr Biol,* **14:**R546-551.

Pittenger MF, Mackay AM, Beck SC, Jaiswal RK, Douglas R, Mosca JD, Moorman MA, Simonetti DW, Craig S, Marshak DR (1999). Multilineage potential of adult human mesenchymal stem cells. *Science,* **284:**143-147.

Postigo AA, Dean DC (2000). Differential expression and function of members of the zfh-1 family of zinc finger/homeodomain repressors. *Proc Natl Acad Sci USA,* **97:**6391-6396.

Preshaw PM, Alba AL, Herrera D, Jepsen S, Konstantinidis A, Makrilakis K, Taylor R (2012). Periodontitis and diabetes: a two-way relationship. *Diabetologia*, **55:**21-31.

Rossol M, Heine H, Meusch U, Quandt D, Klein C, Sweet MJ, Hauschildt S (2011). LPS-induced cytokine production in human monocytes and macrophages. *Crit Rev Immunol,* **31:**379-446.7

Rudney JD, Chen R, Sedgewich GJ (2005). Actinobacillus actinomycetemcomitans, Porphyromonas gingivalis, and Tannerella forsythensis are components of a polymicrobial intracellular flora within human buccal cells. *J Dent Res,* **84:**59-63.

Saccani S and Natoli G (2002). Dynamic changes in histone H3 Lys 9 methylation occurring at tightly regulated inducible inflammatory genes. *Genes Dev,* **16:**2219-2224.

Sawado T, Halow J, Im H, Ragoczy T, Bresnick EH, Bender MA, Groudine M (2008). H3 K79 dimethylation marks developmental activation of the beta-globin gene but is reduced upon LCR-mediated high-level transcription. *Blood,* **112:** 406-414.

Schrementi ME, Ferreira AM, Zender C, DiPietro LA (2008). Site-specific production of TGF-beta in oral mucosal and cutaneous wounds. *Wound Repair Regen,* **16**:80-86.

Scott MJ, Liu S, Shapiro RA, Vodovotz Y, Billiar TR (2009). Endotoxin uptake in mouse liver is blocked by endotoxin pretreatment through a suppressor of cytokine signaling-1-dependent mechanism. *Hepatology*, **49:**1695-1708.

Shao B, Munford RS, Kitchens R, Varley AW (2012). Hepatic uptake and deacylation of the LPS in bloodborne LPS-lipoprotein complexes. *Innate Immun,* **18:**825-833.

Soo K, O'Rouke MP, Khoo PL, Steiner KA, Wong N, Behringer RR, Tam PP (2002). Twist function is required for the morphogenesis of the cephalic neural tube and the differentiation of the cranial neural crest cells in the mouse embryo. *Dev Biol,* **247:**251-270.

Sroczynska P, Cruickshank VA, Bukowski JP, Miyagi S, Bagger FO, Walfridsson J, Schuster MB, Porse B, Helin K (2014). shRNA screening identifies JMJD1C as being required for leukemia maintenance. *Blood*, **123:**1870-1882.

Szpaderska AM, Walsh CG, Steinberg MJ, DiPietro LA (2005). Distinct patterns of angiogenesis in oral and skin wounds. *J Dent Res*, **84**:309-314.

Steinsvoll S, Halstensen TS, Schenck K (1999). Extensive expression of TGF-beta1 in chronically inflamed periodontal tissue. *J Clin Periodontol,* **26**:366-373.

Szpaderska AM, Zuckerman JD, DiPietro LA (2003). Differential injury responses in oral mucosal and cutaneous wounds. *J Dent Res*, **82**:621-626.

Tachibana M, Sugimoto K, Fukushima T, Shinkai Y (2001). Set domain-containing protein, G9a, is a novel lysine-preferring mammalian histone methyltransferase with hyperactivity and specific selectivity to lysines 9 and 27 of histone H3. *J Biol Chem,* **276:** 25309-25317.

Tachibana M, Ueda J, Fukuda M, Takeda N, Ohta T, Iwanari H, Sakihama T, Kodama T, Hamakubo T, Shinkai Y (2005). Histone methyltransferases G9a and GLP form heteromeric complexes and are both crucial for methylation of euchromatin at H3-K9. *Genes Dev*, **19:**815-26.

Takahashi K and Yamanaka S (2006). Induction of pluripotent stem cells from mouse embryonic and adult fibroblast cultures by defined factors. *Cell,* **126:**663-676.

Teng YT, Nguyen H, Gao X, Kong YY, Gorczynski RM, Singh B, Ellen RP, Penninger JM (2000). Functional human T-cell immunity and osteoprotegerin ligand control alveolar bone destruction in periodontal infection. *J Clin Invest*, **106:**R59-67.

Tian X, Liu Z, Niu B, Zhang J, Tan TK, Lee SR, Zhao Y, Harris DC, Zheng G (2011). E-cadherin/b-catenin complex and the epithelial barrier. *J Biomed Biotechnol,* **2011:**567305.

Todaro GJ, Lazar GK, Green H (1965). The initiation of cell division in a contact-inhibited mammalian cell line. *J Cell Physiol,* **66**:325–333.

Truong AB, Kretz M, Ridky TW, Kimmel R, Khavari PA (2006). p63 regulates proliferation and differentiation of developmentally manture keratinocytes. *Genes Dev,* **20:**3185-3197.

Tsai JH and Yang J (2013). Epithelial-mesenchymal plasticity in carcinoma metastasis. *Genes Dev,* **27:**2192-2206.

Tsukada Y, Fang J, Erdjument-Bromage H, Warren ME, Borchers CH, Tempst P, Zhang Y (2006). Histone demethylation by a family of JmjC domain-containing proteins. *Nature*, **439:**811-816.

Tunkel J, Heinecke A, Flemming TF (2002). A systematic review of efficacy of machine-driven and manual subgingival debridement in the treatment of chronic periodontitis. *J Clin Periodontol*, **3:**72-81.

Uematsu S, Jang MH, Chevrier N, Guo Z, Kumagi Y, Yamamoto M, Kato H, Sougawa N, Matsui H, Kuwata H, Hemmi H, Coban C, Kawai T, Ishii KJ, Takeuchi O, Miyasaka M, Takeda K, Akira S (2006). Detection of pathogenic intestinal bacteria by Toll-like receptor 5 on intestinal CD11c+ lamina propia cells. *Nat Immunol,* **7:**868-874.

van Haaften G, Dalgliesh GL, Davies H, Chen L, Bignell G, Greenman C, Edkins S, Hardy C, O'Meara S, Teague J, Butler A, Hinton J, Latimer C, Andrews J, Barthorpe S, Beare D, Buck G, Campbell PJ, Cole J, Forbes S, Jia M, Jones D, Kok CY, Leroy C, Lin ML, McBride DJ, Maddison M, Maquire S, McLay K, Menzies A, Mironenko T, Mulderrig L, Mudie L, Pleasance E, Shepherd R, Smith R, Stebbings L, Stephens P, Tang G, Tarpey PS, Turner R, Turrell K, Varian J, West S, Widaa S, Wray P, Collins VP, Ichimura K, Law S, Wong J, Yuen ST, Leung SY, Tonon G, DePinho RA, Tai YT, Anderson KC, Kahnoski RJ, Massie A, Khoo SK, Teh BT, Stratton MR, Futreal PA (2009). Somatic mutations of the histone H3K27 demethylase gene UTX in human cancer. *Nat Genet,* **41:**521-523.

van Roy F and Berx G (2008). The cell-cell adhesion molecule E-cadherin. *Cell Mol Life Sci,* **65:**3756-3788.

Varma S, Cao Y, Tagne JB, Lakshminarayanan M, Li J, Friedman TB, Morell RJ, Warburton D, Kotton DN, Ramirez MI (2012). The transcription factors Grainyhead-like 2 and NK2-homeobox 1 form a regulatory loop that coordinates lung epithelial cell morphogenesis and differentiation. *J Biol Chem,* **287:**27282-27295.

Wang H, Cao R, Xia L, Erdjument-Bromage H, Borchers C, Tempst P, Zhang Y (2001). Purification and functional characterization of a histone H3-lysine 4-specific methyltransferase. *Mol Cell,* **8:** 1207-1217.

Wang J, Park JW, Drissi H, Wang X, Xu RH (2014). Epigenetic regulation of miR-302 by JMJD1C inhibits neural differentiation of human embryonic stem cells. *J Biol Chem,* **289**:2384-2395.

Wellner U, Schubert J, Burk UC, Schmalhofer O, Zhu F, Sonntag A, Waldvogel B, Vannier C, Darling D, zur Hausen A, Brunton VG, Morton J, Sansom O, Schuler J, Stemmler MP, Herzberger C, Hopt U, Keck T, Brabletz S, Brabletz T (2009). The EMT-activator ZEB1 promotes tumorigenicity by repressing stemness-inhibiting microRNAs. *Nat Cell Biol,* **11:**1487–1495.

Werner S and Grose R (2003). Regulation of wound healing by growth factors and cytokines. *Physiol Rev*, **83:**835-870.

Werner S, Peters KG, Longaker MT, Fuller-Pace F, Banda MJ, Williams LT (1992). Large induction of keratinocyte growth factorexpression in the dermis during wound healing. *Proc Natl Acad Sci USA,* **89:**6896-6900.

Whetstine JR, Nottke A, Lan F, Huarte M, Smolikov S, Chen Z, Spooner E, Li E, Zhang G, Colaiacovo M, Shi Y (2006). Reversal of histone lysine trimethylation by the JMJD2 family of histone demethylases. *Cell*, **125:**467-481.

Whitfield C, Perry MB, MacLean LL, Yu SH (1992). Structural analysis of the O-antigen side chain polysaccharides in the lipopolysaccharides of Klebsiella serotypes O2(2a), O2(2a,2b), and O2(2a,2c). *J Bacteriol,* **174:**4913-4919.

Wilson M (1995). Biological activities of lipopolysaccharides from oral bacteria and their relevance to the pathogenesis of chronic periodontitis. *Sci Prog*, **78:**19-34.

Wolf SS, Patchev VK, Obendorf M (2007). A novel variant of the putative demethylase gene, s-JMJD1C, is a co-activator of the AR. *Arch Biochem Biophys,* **460**:56-66.

Xiang X, Deng Z, Zhuang X, Ju S, Mu J, Jiang H, Zhang L, Yan J, Miller D, Zhang HG (2012). Grhl2 determines the epithelial phenotype of breast cancers and promotes tumor progression. *PLoS ONE,* **7:**e50781.

Xu J, Lamouille S, Derynck R (2009). TGF-β-induced epithelial to mesenchymal transition. *Cell Res,* **19:**156-172.

Yamane K, Toumazou C, Tsukada Y, Erdjument-Bromage H, Tempst P, Wong J, Zhang Y (2006). JHDM2A, a JmjC-containing H3K9 demethylase, facilitates transcription activation by androgen receptor. *Cell,* **125:**483-495.

Yan C, Grimm WA, Garner WL, Qin L, Travis T, Tan N, Han YP (2010). Epithelial to mesenchymal transition in human skin wound healing is induced by tumor necrosis factor-alpha through bone morphogenic protein-2. *Am J Pathol,* **176:**2247-2258.

Yang ZQ, Imoto I, Fukuda Y, Pimkhaokham A, Shimada Y, Imamura M, Sugano S, Nakamura Y, Inazawa J (2000). Identification of a novel gene, GASC1, within an amplicon at 9p23-24 frequently detected in esophageal cancer cell lines. *Cancer Res,* **60:**4735-4739.

Yang J and Weinberg RA (2008). Epithelial-mesenchymal transition: at the crossroads of development and tumor metastasis. *Dev Cell,* **14:**818-829.

Yao D, Dai C, Peng S (2011). Mechanism of the mesenchymal-epithelial transition and its relationship with metastatic tumor formation. *Mol Cancer Res,* **9:**1608-1620.

Ye L, Fan Z, Yu B, Chang J, Al Hezaimi K, Zhou X, Park NH, Wang CY (2012). Histone demethylases KDM4B and KDM6B promtes osteogenic differentiation of human MSCs. *Cell Stem Cell,* **11:**50-61.

Zehnder M, Gold S, Hasselgren G (2002). Pathologic interactions in pulpal and periodontal tissues. *J Clin Periodontol,* **29:**663-671.

Zhang X, Xie X, Heckmann BL, Saarinen AM, Czyzyk TA, Liu J (2014). Targeted Disruption of G_0/G_1 Switch Gene 2 Enhances Adipose Lipolysis, Alters Hepatic Energy Balance, and Alleviates High-Fat Diet–Induced Liver Steatosis. *Diabetes*, **63:**934-946.